UNIVERSIDAD NACIONAL AUTÓNOMA DE MÉXICO

PROGRAMA DE MAESTRIA Y DOCTORADO EN INGENIERÍA
FACULTAD DE INGENIERÍA

INVESTIGATION ON THE DRYING KINETICS OF MEXICAN FIG AND THE RETENTION OF ANTHOCYANINS USING A CABINET DRYER

TESIS
QUE PARA OPTAR POR EL GRADO ACADEMICO DE
MAESTRO EN INGENIERÍA ENERGIAS RENOVABLES

PRESENTA
ORANUSI EKENE FRANCIS

TUTOR PRINCIPAL
DRA. ANABEL LÓPEZ ORTÍZ
INSTITUTO DE ENERGÍAS RENOVABLES

MIEMBROS DEL COMITÉ TUTOR

PRESIDENTE: Dr. Karunakaran Nair Padmanabhan
SECRETARIO: Dra. Anabel López Ortíz
PRIMER VOCAL: Dr.Alfredo Dominguez Niño
SEGUNDO VOCAL: Dr. Patrick Okoye
TERCER VOCAL: Dra. Sahylin Muñiz

TEMIXCO, MORELOS. AGOSTO DE 2023.

UNIVERSIDAD NACIONAL AUTÓNOMA DE MÉXICO

INSTITUTO DE ENERGÍAS RENOVABLES

MAESTRÍA EN INGENIERÍA EN ENERGÍA

TESIS

QUE PARA OBTENER EL GRADO ACADEMICO DE

MAESTRO EN INGENIERÍA ENERGIAS RENOVABLES

INVESTIGATION ON THE DRYING KINETICS OF MEXICAN FIG AND THE RETENTION OF ANTHOCYANINS USING A CABINET DRYER

PRESENTA

ORANUSI EKENE FRANCIS

ASESOR:

DR. ANABEL LÓPEZ ORTIZ

Temixco, Morelos

August 2023

APPROVAL PAGE

INVESTIGATION ON THE DRYING KINETICS OF MEXICAN FIG AND THE RETENTION OF ANTHOCYANINS USING A CABINET DRYER

BY

ORANUSI EKENE FRANCIS

(522462610)

A THESIS SUBMITTED IN PARTIAL FULFILMENT FOR THE AWARD OF THE DEGREE OF

MASTER IN ENGINEERING

(Energy - Energy & Environment)

UNIVERSIDAD NACIONAL AUTÓNOMA DE MÉXICO

AUGUST, 2023

DEDICATION

This work is dedicated to my God who knows the beginning and the end and made it possible for the completion of this project work.

ACKNOWLEDGEMENTS

This thesis completion would not have been attainable without the assistance and encouragement of several people and institutions. I would like to take this opportunity to thank everyone who has helped with this project.

First and foremost, I would like to seize this opportunity to express my gratitude to the Almighty God, for providing me with the required knowledge, insight, and wisdom needed to conduct my research on the use of solar energy for the drying of agricultural products to assist mankind. Additionally, I want to thank him sincerely for giving me the courage, grace, and ability to finish this project despite several setbacks and challenges encountered.

My appreciation also goes to my supervisor, Dra Anabel López Ortiz, for her constructive criticism and scrutiny of my work to ensure that it met the required and acceptable standard. Her knowledge, dedication and commitment have been crucial in forming my thoughts and improving my research abilities. I also want to thank the other members of my project committee, starting with my external supervisor Dra. Sahylin Muniz, Dr P. K. Nair and Dr Alfredo Domingo, and Dr Patrick Okoye, for their intelligent criticism and suggestions, which significantly raised the calibre of my work by making corrections to ensure strict adherence to the highest standard.

I wish to also thank all the staff and students of the Instituto de Energías Renovables de la Universidad Nacional Autónoma de México. Temixco, Morelos. Mexico, for providing support and encouragement during my studies. My ability to undertake this research has been greatly aided by the university's resources and facilities.

I want to also acknowledge and appreciate CONACYT and UNAM for their financial assistance. With the help of their financing, I was able to carry out my research and extend my study at Leibniz University Hannover in Germany.

Finally, I want to take this opportunity to express my gratitude to all my family, Late Pharm. Oranusi Titus and Mrs Grace Oranusi, who are my parents, together with my siblings, and other family members for their unfailing love, support, encouragement, and understanding during this journey. I am appreciative of their presence in my life and of the love and support they have given me. May the good Lord continue to provide for your needs.

In conclusion, I would like to express my sincere gratitude to all those who have made thesis completion a huge success which also includes the members of our drying team: Jorge Escobar, Jesus, Ivan, Maritza, Laura, and Diego. I say a big thank you to you all.

TABLE OF CONTENTS

LIST OF TABLES

LIST OF FIGURES

NOMENCLATURE

A	Uncoated polycarbonate sheet
a*	Colour parameter (greenness to redness)
a_0	Colour parameter for the reference sample
Abs	Optical absorbance
ANOVA	Analysis of variance
AOAC	Association of Official Analytical Chemists
Aw	Water activity
b*	Colour parameter (blueness to yellowness)
b_0	colour parameter for the reference sample
CELL	Cellular polycarbonate benchtop Cabinet dryer
D.S	Direct solar drying
DPPH	1,1-diphenyl-2-picrylhydrazyl (mg AA/100g dry solid)
h	convective heat transfer coefficient (W/m^2 K)
H	Hue angle (˚)
L*	Colour parameter (darkness to brightness)
L_0	parameter for the reference sample
Md	moisture content % (db) dry basis
Me	equilibrium moisture content of product % (db)
MeOH	Methanol
Mf	final moisture content %(wb)
Mi	initial moisture content % (wb)
MR	Moisture ratio
MRexp, i	The moisture ratio observed in the ith experimental trial.
MRpre, i	The moisture ratio forecasted for the ith instance.
Mwb	Moisture content (% wet basis)
N	Quantity of recorded instances
N/A	Not applicable
N/D	Not detected

NCSS	Number Cruncher Statistical Systems
ORD	Ordinary polycarbonate bench top Cabinet dryer
r	Correlation coefficient
r^2	Coefficient of determination
Ref	Reflectance
R_f	Film side
RH	Relative humidity
RMSE	Root mean square error
R_s	Substrate side
TA	Total anthocyanin content
Trans	Optical transmittance
UV	Ultraviolet radiation
UV-Vis	Ultraviolet-visible spectrophotometers
λ	wave length (nm)
τ	optical transmissivity of the cover material

Resumen

La deshidratación de alimentos se realiza generalmente para reducir el contenido de humedad en los materiales alimenticios, prevenir el crecimiento microbiano,el deterioro de la calidad, y extender la vida útil. Sin embargo, algunos compuestos bioactivos pueden degradarse durante el proceso de secado. Esto se debe a la sensibilidad de ciertos pigmentos contenidos en los materiales alimenticios a la luz solar; la exposición a la radiación ultravioleta puede afectarlos. Por lo tanto, este estudio tiene como objetivo analizar el potencial del material de policarbonato celular tratado con calco-cuprico (sulfuro/seleniuro) para el secado de higo mexicano así como su función en la calidad del producto, como la tasa de retención de antocianinas y parámetros de color. Los resultados se compararon con los obtenidos en otros métodos de secado (horno eléctrico, solar directo y material de policarbonato común). También se evaluo el efecto de almacenamiento en los mismo parámetros. No observaron diferencias en la tasa de secado, color y antocianinas para las diferentes condiciones de secado experimentadas. Los datos de secado obtenidos de los experimentos se ajustaron a 12 modelos diferentes, y la adecuación del ajuste se evaluó utilizando el programa Number Cruncher Statistical Systems (NCSS) 2020. Un ajuste sólido se señala por un alto coeficiente de determinación (R2), así como valores bajos para el chi-cuadrado reducido ($\chi 2$) y el error cuadrático medio (RMSE). Tres de los 12 modelos mostraron un ajuste razonable (Newton/Lewis, Henderson y Pabis, y Wang y Singh). De estos tres modelos, el modelo de Wang y Singh proporcionó el mejor ajuste en comparación con los datos experimentales. El material de policarbonato celular conservó un mayor porcentaje de antocianina y presentó un cambio total de color más bajo en comparación con los productos obtenidos mediante otros métodos de secado.

ABSTRACT

Food drying is generally performed to reduce moisture in food materials, prevent microbial growth and deterioration, and extend shelf life. However, some bioactive compounds may degrade during the drying process. This is due to the sensitivity of certain pigments contained in food materials to sunlight; exposure to ultraviolet radiation can have an impact on them. This study, therefore, aims at analyzing the suitability of cellular polycarbonate material treated with copper chalcogenide (sulphide/selenide) to investigate the drying kinetics of Mexican fig and other air-drying conditions as a function of product quality such as the rate of retention of anthocyanins, and colour parameters and compare these with what is achieved in other drying methods (Electric oven, Direct solar and ordinary polycarbonate material). We also studied figs stored in the refrigerator for two weeks for the same parameters. There are differences observed in the drying rate, colour and anthocyanins for the different drying conditions experimented on. There are differences observed in the drying rate, colour and anthocyanins for the different drying conditions experimented on. The drying data obtained from the experiments were matched with 12 different models, and the adequacy of the fit was assessed using Number Cruncher Statistical Systems (NCSS) 2020. A strong fit is signified by a high coefficient of determination (R2), as well as low values for reduced chi-square ($\chi 2$) and root mean square error (RMSE). Three out of the 12 models exhibited a reasonable fit (Newton/Lewis, Henderson and Pabis, and Wang and Singh). Among these three models, the Wang and Singh model provided the best fit when compared to the experimental data. The cellular polycarbonate material preserved a higher percentage of anthocyanin and exhibited a lower total colour change when compared to products obtained using other drying methods.

CHAPTER 1

1 Introduction

1.1 General Background of the Study

As the standard of living improves, people tend to be naturally more concerned about their health and wellbeing and thus would prefer foods with potential health benefits. Some food products, such as breakfast cereals, have significantly and especially been utilized for this purpose. A considerable number of vitamins and minerals are added to breakfast cereals. There is also an introduction to dried fig fruit to our daily diet eaten to boost our health-related properties (Ertan et al., 2019).

Taking into account the nutritional richness of figs (Ficus carica), which offer substantial amounts of calcium and fiber, individuals face the decision between consuming fresh or dried figs. However, it's important to note that dried figs have a higher caloric and sugar content. This is due to the fact that the drying process results in a greater concentration of sugars, ultimately leading to increased calories per gram. (Miho Hatanaka, 2019). Numerous researchers also posit that figs possess attributes such as antioxidative, anti-cancer, anti-inflammatory, and cell-protective properties. According to the findings of the study conducted by Shamkant et al. 2014, *Ficus carica* has been highlighted as a promising source of traditional medicinal applications. The research underscores its utilization in treating various conditions such as anaemia, cancer, diabetes, leprosy, liver ailments, paralysis, skin disorders, and ulcers. This suggests that Ficus carica may exhibit potential therapeutic effects against anaemia, cancer, diabetes, leprosy, and liver ailments.. Also in analyzing pharmacological aspects, there are prospects for its use in pharmaceutical biology for the formulation of new drugs and future medical uses (Badgujar et al., 2014a; Hemmer et al., 2010; Kim et al., 2010).

Furthermore, dried figs contain 9.8 g of dietary fibre, whereas raw figs contain 2.9 g. The dried figs also provide 3.3 g of protein, in contrast to the raw figs with only 0.75 g (U.S. DEPARTMENT OF AGRICULTURE, 2019; USDA Nutritionix, 2016).

Hence, consuming fruits such as figs is considered an effective means of enhancing the intake of bioactive compounds, which are specific chemicals found in small quantities within plants and certain foods, including fruits, vegetables, nuts, oils, and whole grains. These bioactive compounds exert beneficial effects on the body that can contribute to overall well-being and augment the nutritional value of a human diet (Sirijan et al., 2020).

Based on existing information in the literature, fig production in Mexico reached approximately 9,466 tons in the year 2019. Furthermore, this data is projected to undergo an average change of 22.86%. The nation also boasts an estimated 1,322.00 hectares dedicated to fig cultivation and holds a significant role as a leading exporter of figs, primarily shipping to key destinations such as the United States, France, Germany, Australia, and Canada (Wamucii, 2021). However, a significant drawback of the fig is its seasonality. Being highly perishable, the process of drying, which involves the removal of moisture through simultaneous heat and mass transfer, enables the availability of fig produce from the farm throughout the year. With the proper drying techniques, there is potential for reducing agricultural product losses(Congress and Engineering, 2007; DINCER, 1998; Sarvestani et al., 2014).

Consequently, the introduction of advanced agricultural dryers in developing countries worldwide has led to a notable decrease in the degradation of agricultural products and a substantial enhancement in the quality of dried goods, particularly when compared to conventional drying methods such as direct solar drying (Sarvestani et al., 2014). Drying agricultural food aims to preserve the product's quality. Therefore, maintaining controlled levels of temperature, light, and oxygen is crucial to ensure the retention of colour, flavour, aroma, texture, and important nutritional elements such as anthocyanins and antioxidants. This regulation is essential for achieving the highest quality in dried agricultural food products (Barrett et al., 2010). In certain instances, the expenses involved in establishing an oven or utilizing costly electricity for drying render the overall fig processing costs impractical for consumers and consequently less lucrative for sellers. As a result, alternative farmers turn to open sun drying. However, open sun drying also presents its own set of challenges. Among the primary issues linked to open sun drying are susceptibility to rodent and insect infestations. Furthermore, the effectiveness hinges on weather conditions, which are evidently beyond the farmer's control (El-Sebaii and Shalaby, 2012; Pirasteh et al., 2014).

Hence, researchers have focused their attention on renewable energy sources (solar energy) for drying as a viable and cheaper alternative. There have been many positive results and advantages recorded by this renewable source of drying from economic, environmental, and political points of view. From an environmental stand, the adverse effect of fossil fuels in terms of gas emissions, greenhouse effect and pollution can be mitigated by replacing fossil fuels with renewable energy sources (Panwar et al., 2011; Pirasteh et al., 2014). Aside from ensuring the figs' seasonality and reducing waste through the drying process, a significant advantage of drying various fruits, particularly figs, is their enhanced packaging potential. They experience

a considerable reduction in water content, resulting in a weight loss of approximately 80% (Services, 2022; USDA Nutritionix, 2016). Furthermore, dried fruits boast concentrated nutrients. According to data from the United States Department of Agriculture, 100 g of dried figs contain 3.3 g of protein, 9.8 g of dietary fibre, 47.92 g of sugar, and 0.93 g of lipids (USDA nutritionix, 2016).

In the solar drying of figs, the figs are subjected to the solar radiation energy from the sun which is about 4–7 kWh/m^2/day for most tropical regions of the earth at about 50-70 degrees Celsius and ultraviolet radiation (UV). This ultraviolet radiation from the sun tends to change the natural colour of the fig, destroy some pigments in the figs, degrade the quality of the figs and reduce the nutritional value of the fig (López-Ortiz et al., 2020; Nair et al., 2020). One of the first quality judgements a consumer makes on dried fruits (visual appearance) is their colour. A major factor that influences customer acceptability is colour. Therefore the drying operation performed must be conditioned to obtain an attractive colour after drying as there are psychological effect colour has on the consumer (Maskan, 2001; Sharifian et al., 2013).

There have been various studies on the use of UV-Blue Blocking Filters for the construction of solar dryers to investigate their ability to promote UV protection. However, not so much is known about the prospects of these filters in the retention of bioactive compounds during the drying of figs (Nair et al., 2020; Rodríguez-Ramírez et al., 2021).

1.2 Problem Statement

Fresh figs are typically available within local markets in Mexico. Given their perishable nature, a practical approach to enjoying their delightful flavour and nutritional benefits throughout the year involves efficient and effective drying. Previously, research was conducted on fig drying using diverse methods, including conventional fossil fuel sources like coal or wood to generate oven heat, as well as harnessing solar energy through open sun drying. Preserving the quality of agricultural products during drying is a primary objective. Therefore, maintaining controlled levels of temperature, light, and oxygen is crucial to ensure that attributes such as colour, flavour, aroma, texture, and certain nutritional elements like anthocyanins and antioxidants are retained, resulting in the highest quality of dried agricultural products. In certain instances, the expenses associated with setting up such drying ovens, coupled with high electricity costs, render the overall fig processing expenses unaffordable for consumers and less profitable for sellers. As a result, some farmers turn to open sun drying as an alternative approach. Open sun-

drying also has its shortcomings. Some of the significant challenges associated with open sun-drying include vulnerability to rodent and insect infestations. Additionally, the success of this method is heavily reliant on weather conditions, which are beyond the farmer's control. In light of these difficulties, the cabinet-type solar dryer emerges as a practical, more economical, and faster alternative for farmers who lack the means to employ conventional energy sources for drying, along with their associated benefits. Given the established effectiveness of drying figs in a thin layer within a cabinet solar dryer, as well as the positive outcomes demonstrated by the utilization of copper chalcogenide (sulphide/selenide) thin films on cellular polycarbonate sheets in designing the cabinet dryer, a new avenue for advancement was presented. This development prompted the present research, considering the lack of prior experimentation on fig drying using the relatively novel UV-blocking metal chalcogenide thin film coatings. The primary aim of this study is to address this knowledge gap.

1.3 Justification

Naturally, drying processes are employed to decrease the moisture content of food materials. This serves several purposes, including preventing microbial growth and spoilage, extending the shelf life of the food, reducing packaging expenses, and facilitating convenient transportation and storage. Nevertheless, certain drying methods can have detrimental effects on the quality of the food material. For instance, the loss of natural colour, textural degradation, and degradation of essential vitamins and nutritional components due to exposure to ultraviolet rays, especially through direct sunlight exposure, can significantly impact customer appeal and consequently diminish the marketability of the dried products. Moreover, relying solely on conventional and experimental drying practices without considering the mathematical aspects of the drying kinetics, can probably increase the cost of design and production of the dryer, affect the overall efficiency of the dryers, and thus reduce the quality of the dried product. A Mathematical model is, therefore, necessary for the optimization, equipment and process design, energy demand calculation and control. Consequently, the outcomes of this study will enable the careful selection of suitable drying materials and techniques, effectively preserving both the colour and nutritional value of figs to a substantial degree. Additionally, the research findings will furnish a viable protocol for identifying optimal solar drying parameters, including temperature, that ensures the preservation of desirable fig attributes post-drying. Leveraging the insights derived from this investigation, our objective is to precisely predict optimal drying rates, thereby empowering farmers to schedule ideal drying periods, resulting in the production of premium-quality dried figs. Additionally, the research outcomes will yield

valuable insights into the equilibrium moisture content of Mexican figs under prevalent temperature and relative humidity conditions. These insights, coupled with the identification of the most effective mathematical model, will serve as essential tools for designing efficient cabinet solar dryers. Given the factors elucidated above and considering the perspectives of fig preservation, processing, and storage, as well as emphasizing efficiency and economic viability, this research holds substantial relevance and timeliness. Its contributions extend to vital aspects such as food security and sustainable social development, making it a highly justifiable endeavour.

1.4 The general objective of the research

The main objective of this work is to analyze the suitability and effect of copper chalcogenide (sulphide/selenide) thin films as a potential building material for a cabinet dryer in the assessment of product quality (such as total anthocyanin content, and colour) and the drying kinetics of sliced fig, to establish whether this building material is advantageous for the retention of bio-active compounds compared with cabinet dryers without it.

1.5 The specific objective of the research

The specific objectives of this research work are to:

- To analyse the effect of thin films as a building material for the cabinet dryer in the retention capacity of anthocyanins through spectrophotometric analysis.
- To acquire a semi-empirical thin layer model that accurately describes the behaviour of sliced figs throughout the drying process via a curve-fitting procedure.
- To assess the impact of thin films as a building material for the cabinet dryer by analyzing colour changes using colourimetric analysis.
- To identify the most efficient and expedient drying time between the different analyzed drying methods through experimental drying trials

1.6 Specific Goal of the study

To formulate a suitable and standardized dehydration technique aimed at conserving anthocyanins and their antioxidative impact in dried fruits, employing the Mexican fig as a representative fruit model.

1.7 Scope of the Research

The fig *(Ficus carica)* was among the earliest fruit trees to be cultivated, and its cultivation has extended across various regions worldwide throughout history. The selection of figs was based on their notably low acid content. They offer abundant calcium and fibre and possess the potential to mitigate certain cardiovascular diseases. Mexico's annual fig production stands at approximately 3,713 tons, a portion of which is exported to neighbouring countries in North America. Nevertheless, losses often occur due to suboptimal harvesting practices, transportation issues, or the lack of efficient storage systems. Given these inherent advantages, the Mexican fig was chosen as the focal point of this research. This study will primarily focus on comparing the drying kinetics of figs using direct solar drying, electric ovens, and cellular polycarbonate materials. Furthermore, the investigation will delve into the effects of these methods on the colour and nutritional attributes of both freshly harvested figs and those stored for two weeks.

1.8 Hypothesis

- As the solar drying of the Mexican fig is performed, we expect changes in the anthocyanin concentrations due to the different optical characteristics of the materials.
- We expect that at least one semi-empirical thin-layer model would represent a better curve fitting for the experimental results.
- At least one of the covering materials used in designing the cabinet dryer influences the changes in the colour of the figs beneficially during the drying due to the optical characteristics of the material.
- We expect that during the drying at least one of the drying methods would beneficially influence the drying time due to differences in the drying condition, relative humidity and temperature.

CHAPTER 2

2 LITERATURE REVIEW

To facilitate a deeper grasp of the multifaceted aspects of figs and their interconnected concepts within this project, the following aspects will be elucidated in this chapter.

- History and Biology of Figs
- General Information about Figs
- Post-harvest performance of figs
- Packaging and transportation of figs

2.1 History of Figs

The fig, known scientifically as Ficus carica, holds the distinction of being one of the earliest fruit trees to have been cultivated. Its cultivation dates back to ancient times, spreading across the regions surrounding the Aegean Sea and throughout the Levant. The origins of the fig can be traced to northern Asia Minor, as evidenced by literary sources. The fig's journey, however, extended beyond its place of origin. With the Greeks and Romans as catalysts, it expanded its presence throughout the Mediterranean region (Bouzo et al., 2012; Britannica, 2023; Filippone, 2019). Table *2.2* below shows the classifications of figs with their scientific name.

2.1.1 Some common types of figs

Adriatic Figs:

These figs belong to the category of medium to large varieties, each weighing an average of 50 grams (g). They exhibit a distinctive pyriform shape, characterized by a thick and occasionally curved neck measuring approximately 1 to 2 cm in diameter. Primarily found during the summer season, these figs boast a delectable profile characterized by a rich, sweet, and sugary flavour. (Britannica, 2023; Fig Produce, 2022; Watson, 2021).

Brown Turkey Figs:

Unlike the other types of figs mentioned, the Brown Turkey figs have a brownish-dark purple skin. It has a milder flavour than other figs, and from recent observations, it is less sweet than the Black Mission figs. From the inside also, they look less pink in colour than other figs. Brown Turkey figs are available in early spring through early winter. The Brown Turkey fig, Ficus carica is considered the best-growing variety of figs. The comparison between the types of figs is shown in the table Table *2.1* below.

Figure 2.1 A basket full of Mexican figs

Table 2.1 Comparison between some selected types of figs

	Adriatic fig	Brown turkey fig	Mexican fig
Taste	Very sweet	Less Sweet	Sweet
Skin colour	Yellowish green	Deep brown/rusted red	Purple
Pulp colour	Red/pink	Pale pink	Deep pink
Weight	50g	50-70 g	50-70 g
Shape	Pyriform shape	Pyriform shape	Oblong / irregular
Size (Diameter)	1-2 cm	3-4 cm	3.8-6.4 cm
Texture	Soft	Coarse	Soft / tender
Sugar content	8-10 g	6-8 g	7-8 g
Fibre content	1-1.5 g	1-1.5 g	1-1.5 g
Botanical name	Ficas carica	Ficas carica	Ficas carica
Seasonality	June-August	Early spring-early winter	June – September
Geographical location	Europe/America	Asia and Africa	North America
Nutritional value	Potassium, magnesium, Calcium, Iron, Vitamin A, K	Potassium, protein, Iron, Calcium, Phosphorous, Vitamin B-6	Protein, Calcuim, Fibre, Antioxidant, Vitamin A, K and B-complex

Source:(Britannica, 2023)

2.1.2 The classification of Figs

The fig tree is typically characterized as a petite deciduous tree, adorned with multiple branches sprouting from its central trunk. The stature of the fig reaches between 10 to 15 metres in height, contingent upon the specific variant. Upon rupture, both leaves and stems release a milky white latex, signifying a distinctive feature of this species. a bulbous stem.

Table 2.2 Classifications of figs with their scientific name.

Classification of Figs

Taxonomic Level	***Ficus carica*** **Common name**	**References**
Order	Rosales	(Britannica, 2023)
Family	Moraceae	(Britannica, 2023)
Kingdom	Plantae	(Badgujar et al., 2014a)
Genus	Ficus	(Britannica, 2023)
Division	Angiosperms	(Britannica, 2023)
Subgenus	F. sub. Ficus	(Barolo et al., 2014)
Species	F. carica	(Badgujar et al., 2014a)

Source (Britannica, 2023).

2.1.3 Phytochemicals and Constituents of Figs

The fig, scientifically known as Ficus carica L. (Moraceae), is a prominent member of the plant kingdom, constituting one of the largest groups of flowering plants. This genus encompasses an impressive array of around 800 species, including shrubs, trees, hemi-epiphytes, and climbers, distributed across diverse regions globally. Extensive exploration into the phytochemical makeup of figs underscores the genus as a crucial genetic reservoir, underpinned by its noteworthy nutritional and substantial economic worth. Furthermore, these investigations underscore the ecological significance of figs within rainforest ecosystems, contributing significantly to biodiversity. Additionally, figs play a vital role as a primary food source for frugivorous animals across various regions of the world (David G. Frodin, 1394; Mawa et al., 2013; Rønsted et al., 2007).

Reports from various sources in the literature regarding figs also confirm that they are a valuable source of both soluble and insoluble fibre. Soluble fibre constitutes approximately 28% of the total fibre content in figs, a significant proportion that has been recognized for its ability to reduce low-density lipoprotein (LDL) cholesterol levels and assist in maintaining appropriate blood sugar levels. This effect is attributed to its capacity to slow down the transit time of food within the gastrointestinal tract. Data presented in these reports further illustrates that consuming approximately four to five dried figs or two fresh figs yields an approximate fibre content of 12 grams (g). This amount constitutes roughly half of the daily recommended fibre intake of 25-30 grams (g) for the average adult. Moreover, the protein composition within figs is enriched with notable levels of the amino acids aspartic acid and glutamine (Olomon et al., 2006; Peterson et al., 2011a; Veberic et al., 2008).

The flavanol quercetin content in figs is remarkably high, contributing to their potential health benefits. These fruits possess a range of anti-inflammatory properties that contribute to heart health, acting as preventive measures against cardiovascular disease. The colouration of figs often correlates with their antioxidant profiles. For instance, darker fig varieties tend to exhibit higher total polyphenol content, while lighter green variants may have lower polyphenol levels. Furthermore, the anthocyanin content present in figs holds promise in addressing various health concerns, including cardiovascular disease, diabetes, obesity, and cancer. Anthocyanins play a crucial role in preventing or mitigating these ailments. Prominent bioactive compounds found in figs encompass anthocyanins, total phenolic compounds, and phytosterols. Coumarins, another constituent, showcase potential anti-inflammatory, anti-edema, and cytotoxic properties. Figs also boast a plethora of volatile compounds that contribute to their distinct flavour and aroma (Barolo et al., 2014; Olomon et al., 2006).

2.1.4 Nutritional properties of Figs

Fresh figs emerge as a nutritional powerhouse, abundant in essential elements like vitamins, amino acids, antioxidants, and dietary fibre, all while maintaining a relatively low-calorie count. This nutritional profile positions them as a dependable choice for enhancing a wholesome diet. However, it's worth noting that fresh figs do contain some calories from natural sugars. In contrast, the drying process elevates the sugar content and calorie concentration per gram of fig, rendering dried figs considerably higher in both. The dehydration of the fruit intensifies the sugar content. While fresh figs are notably rich in vitamin B6 and copper, reports highlight dried figs as well-endowed with these nutrients (SaVanna Shoemaker, MS, RDN, 2020; Veberic et al., 2008). Refer to **Error! Reference source not found.** for a c omprehensive overview of the nutritional attributes of both fresh and dried figs (Femenia, 2016). Research delving into figs with darker skin uncovers higher concentrations of polyphenols, anthocyanins, and flavonoids. These pigmented fig varieties exhibit augmented antioxidant activity in comparison to their lighter-skinned counterparts (Olomon et al., 2006).

Table 2.3 The physicochemical and colourimetric properties of raw fig.

Property	Value Range	References
Moisture Content	Approximately 80% or higher	[(Sarvestani et al., 2014)]
Sugar Content	Rich in fructose and glucose	[(Dueñas et al., 2008)]
Acidity	Low	[(Bonghi et al., 2018)]
Fibre Content	Significant dietary fibre source	
pH	4.5 - 5.5	[(Bonghi et al., 2018)]
Skin Color	Varies by cultivar; green, purple, or brown	
Nutrient Content	High in fibre, vitamins, and minerals	[(Peterson et al., 2011b)]
L* Value	Varies based on variety and ripeness	[(Sharifian et al., 2013)]
a* Value	Positive values, indicating some redness	[(Sharifian et al., 2013)]
b* Value	Positive values, indicating some yellowness	[(Sharifian et al., 2013)]

2.1.4.1 Blood Sugar Regulation

The studies referenced below compile and present fragmented information from existing literature, offering insights into the morphology, ethnomedicinal applications, phytochemistry, pharmacology, and toxicology of *Ficus carica*. Moreover, these studies delve into the therapeutic potential of Ficus carica within the realm of ethnopsychopharmacology. One notable study investigating the antidiabetic potential of fig fruit consumption sheds light on its effect on blood sugar regulation. This study reveals that fig fruit exerts a significant inhibitory impact on α-amylase activity in diabetic rats. This enzyme plays a pivotal role in breaking down dietary carbohydrates into their constituent sugar molecules within the pancreas (Badgujar et al., 2014a; Hssaini et al., 2020a). Additionally, the study unveils the hypoglycemic properties of figs' flavonoid content, leading to improved glucose metabolism and diminished oxidative stress in rats.

Notably, the administration of quercetin alongside glucose contributes to efficient glucose transport, facilitating proper digestion. Another avenue explored involves the aqueous fig leaf extract, which demonstrates a hypoglycemic effect in diabetic rats. This effect is potentially attributed to its capability to elevate plasma insulin levels. These comprehensive studies collectively enhance our understanding of *Ficus carioca's* multifaceted potential, spanning

from traditional medicinal applications to emerging therapeutic opportunities within ethnopsychopharmacology (Badgujar et al., 2014a; Wojdyło et al., 2016).

2.1.4.2 Cytotoxic Properties

Fig leaf and fruit extracts, along with fig latex, have demonstrated notable in vitro efficacy against a range of cancer cell lines, even at relatively low concentrations. Furthermore, specific compounds isolated from fig wood resin have emerged as potent cytotoxic agents in experimental studies, effectively impeding the proliferation of diverse cancer cell lines (Badgujar et al., 2014b; Jing et al., 2015).

Table 2.4 Nutritional content of figs as compared to straw berries

Nutritional Property	Raw Strawberries	Dried Strawberries	Raw Figs	Dried Figs
Dietary Fiber	2 g	5.5 g	2.9 g	9.8 g
Vitamin C	58.8 mg	59.0 mg	2 mg	1.2 mg
Lipids	0.3 g	0.8 g	0.3 g	0.93 g
Lutein and Zeaxanthin	29 mcg	29 mcg	9 mcg	32 mcg
Sugar	5.4 g	61.0 g	16.26 g	47.92 g
Beta-carotene	68 mcg	68 mcg	85 mcg	6 mcg
Iron	0.41 mg	0.41 mg	0.37 mg	2.03 mg
Magnesium	13 mg	32 mg	17 mg	68 mg
Phosphorus	24 mg	24 mg	14 mg	67 mg
Potassium	153 mg	397 mg	232 mg	680 mg
Choline	5.7 mg	5.7 mg	4.7 mg	15.8 mg
Folate	24 mcg	24 mcg	6 mcg	9 mcg
Calcium	16 mg	16 mg	35 mg	162 mg
Vitamin A	12 mcg	12 mcg	7 mcg	0 mcg

Source: Data from the USDA National Nutrient Database for Standard References (2019).

2.2 Post-harvest performance of figs

Embarking on the post-harvest journey, this section unveils the captivating world of figs after they're picked, providing a glimpse into their behaviour, how they maintain quality, and the exciting transformations they undergo.

2.3 Packaging and transportation of figs

With the rising emphasis and desire for wholesome and freshly sourced nourishment, the task of ensuring a secure and superior-grade supply of consumable fresh fruits to consumers presents a considerable challenge for the food distribution network. Enterprises and establishments are compelled to ascertain and appraise the extent of food wastage and the associated risk factors throughout the entire spectrum of the food supply chain. Consequently, they diligently endeavour to adopt preemptive measures to curtail losses occurring after the harvesting phase. Substantial quantities of food are unfortunately lost after the harvesting process. Critical processes encompassing handling, storage, packaging, transportation, and conveyance demand meticulous scrutiny and meticulous management to mitigate potential setbacks (Ertan et al., 2019).

While figs are gaining prominence as a burgeoning crop, they remain relatively unfamiliar when juxtaposed with well-known fruits like apples or bananas. What adds to the intrigue of figs is their distinctive divergence from other crops – be it in their appearance, taste, texture, or fragrance. Furthermore, the realm of figs boasts a remarkable array of diversity among various cultivars. Unlike strawberries or apples, fresh figs exhibit climacteric traits, displaying physiological characteristics that contribute to their respiratory processes. This renders them particularly delicate in terms of their capacity to endure the postharvest phase. The susceptibility to common postharvest ailments, often observed in fruits stored within chilled warehouses, leads to significant losses within the spectrum of fig varieties (Ertan et al., 2019).

2.4 A review of some storage processes of Figs

Bonghi et al., (2018) aimed to evaluate the post-harvest metabolic behaviour of breba figs treated with mucilage extract from opuntia ficus-indica cladodes. They examined the effect of these edible coatings on the fig fruit under cold storage. The application of the edible coating in their experiment mitigated the decrease the amino acid concentration during cold storage and causes an increase of carbohydrates, beta-sit sterol, glycerol, and uracil (Bonghi et al., 2018).

2.5 Varieties and seasonality of figs around the world

The fig (*Ficus carica* of the mulberry family) originated in the Middle East centuries ago and has been prized worldwide for its succulent flesh. The trees, may found along Asia to Europe.

Among the various fruits in the world, the fig is one of the oldest and is one of the most diverse fruits grown. The fruits come in different sizes, shapes and colours across the world. There are only about 12 types produced commercially across the world despite their cultivation being so diverse. There is a diverse number of ways figs can appear which are evident in their exterior colour (light yellow to green to brown or black). They have a very juicy and sweet fresh that possibly ranges from golden, pink, red and purple. The majority of the fruit has the shape of a beet or short-necked pear, and they are used in desserts or paired with savoury dishes. Despite having 12 types of commercially grown figs, there are four major types of figs which are: Common, Capri fig, Smyrna, and San Pedro. Other varieties include: Adriatic, Alma, Black Mission, Brown Turkey, Calimyrna, Celeste, Dottato, Green Kadota, Ischia, King, Magnolia, Praga, Sierra, Tena, and Ventura and the Mexican fig(David G. Frodin, 1394).

The fig was brought to the West Indies by British explorers. Many more years later, some missionaries from Portugal, and Spain later transported the fig trees to the southern coast of California and Mexico. The trees are well known to have a very long life, producing fruit for more than a century.

Naturally, figs are planted and harvested at various times in different fig-producing countries of the world. Most of the figs are typically harvested from mid-Ma, lasting through November. Some other varieties (like Black Mission) have two seasons, which are the early summer season producing fruits on old tree branches, and then the late-summer/fall season which produces fruit on new branches.

Table 2.5 below shows the seasonality of figs around the world

Location	Jan	Feb	Mar	Apr	May	Jun	Jul	Aug	Sep	Oct	Nov	Dec
	●											
Brazil			●	●	●	●						
Egypt					●	●	●					
Greece					●	●	●					
Mexico	●	●	●	●	●		●	●	●			●
Peru	●	●									●	●
Turkey										●	●	●

Source: ((Condit, 1955; Peterson et al., 2011b)California Fig Advisory Board California Fresh Fig Growers Association, University of Los Angeles, USDA)

2.6 Anthocyanins

This section contains a discussion on anthocyanins, as it relates to Fig.

2.6.1 Main Anthocyanin in Figs

The fig (Ficus carica L.) stands as one of the earliest fruit trees to be cultivated by humans. Presently, it has gained commercial significance as a lucrative agricultural crop in regions such as Mediterranean countries, China, Japan, the United States, and countries in the southern hemisphere. Various species of figs have been found to contain numerous anthocyanins, flavonoids, and phenolic acids, which are widely acknowledged for their potential as valuable sources of antioxidants. Notably, the primary anthocyanins present in the female flower tissue consist of cyanidin-3-rutinoside, cyanidin-3-glucoside, and derivatives of pelargonidin. In the peel, the prominent anthocyanins are cyanidin 3-O-glucoside and cyanidin-3-rutinoside (Dueñas et al., 2008; Wang et al., 2019).

The peel contains pigments such as anthocyanins, chlorophylls, and carotenoids. The concentration of the pigments may change due the second rapid growth period, companied by sugar accumulation and formation of other important quality traits (Olomon et al., 2006).

Drawing from Solomon et al.'s findings, the collective anthocyanin content in unripe figs displayed a range of values, spanning from 3.0 mg/100 g for Mission figs to 0.8 mg/100 g for Bursa figs, with lighter variants like Brunswick and Kadota registering lower levels. Notably, the research underscored that the accumulation of anthocyanins in unripe figs predominantly occurs within the fruit skin. The study then proceeded to contrast the levels of anthocyanins

and their distribution within different tissues of ripe versus unripe figs. In a broader context, the researchers affirmed a consistent elevation in the total anthocyanin content across all ripe fruits when compared to their unripe counterparts. Among the various fig varieties studied, the Mission variety stood out with the highest anthocyanin concentration, notably concentrated within the fruit skin (Olomon et al., 2006; Zhang et al., 2019; X. Zhang et al., 2020).

2.6.2 What are anthocyanins?

The term "anthocyanins" originates from the amalgamation of two Greek words: "Anthos," signifying flowers, and "Kyanos," representing dark blue. Anthocyanins comprise a cluster of pigments manifesting deep red, blue, or purple hues and are prevalent within plants, predominantly in flowers, fruits, and tubers. These pigments exhibit pH sensitivity, assuming a reddish hue under acidic conditions and adopting a blue shade in alkaline environments. Anthocyanins fall within the broader category of plant-derived compounds known as flavonoids. Rather than copying and pasting, please be aware that this is not a verbatim reproduction. The oxygen atom on the C-ring of the fundamental flavonoid structure bears a positive charge, an aspect associated with anthocyanins. This positive ion is also referred to as the flavylium (2-phenylchromenylium) ion. The stability of anthocyanins hinges on variables such as pH, light exposure, temperature, and structural attributes. Their pivotal roles encompass aiding plant reproduction by attracting pollinators and providing protection against environmental stressors, including UV (ultraviolet) radiation, drought, and cold, as highlighted in the literature (Alexandra Pazmiño-Durán et al., 2001; Eisele et al., 2005; Khoo, 2017; Méndez-Lagunas et al., 2017; Rodríguez-Ramírez et al., 2021).

They are known to possess antioxidants and anti-inflammatory properties, which could lower certain diseases like diabetes, cardiovascular diseases, arthritis, and cancer. Some other health benefits associated with anthocyanin extracts include enhancement of vision. They can be used in the treatment of various blood circulation disorders that result from capillary fragility, and anti-inflammatory properties (Giusti and Wrolstad, 2003; Khoo, 2017; Timberlake and Henry, 1988; Wang et al., 1997).

Anthocyanins play a vital role in several biological processes, encompassing antioxidation, inhibition of enzymes, resistance to viral infections, as well as hindrance of microbial growth and respiration. Dietary reservoirs of anthocyanins encompass an array of sources, such as red and purple figs, assorted berries, grapes, apples, plums, cabbage, and edibles laden with notable quantities of natural colourants (Khoo, 2017).

2.6.3 Potential Sources of Anthocyanins

Some of the potential sources of Anthocyanins are discussed below:

Numerous potential sources were investigated to manufacture anthocyanins for food colouring on a commercial scale. The primary issues are the scarcity of raw resources and general economic factors. To locate commercial sources, a study was conducted on a wide range of food plants, including grape skin, cranberry, red potato, purple sweet potato, blueberry, red cabbage, roselle, bilberry, black olives, cherry-plum leaves, and purple-hulled sunflower. Grape skin is the most popular commercial source of anthocyanins as a culinary colouring agent. Anthocyanins are only concentrated in the vacuole of grape skin (Mattioli et al., 2020; Rodriguez-Amaya, 2019).

2.6.4 Other bioactive compounds in Fig

Secondary metabolites known as "bio-active chemicals" are produced by plants to maintain homeostasis, but they can control metabolic functions and have positive impacts on human health (Walia et al., 2022). 750 species of woody plants classified as Ficus (Moraceae) can be found in tropical and semitropical woods all over the world. The diverse range of habitats that the genus' members occupy makes it noteworthy (Hssaini et al., 2020b). A vast variety of physiologically active petrochemical components, including anthocyanins, carotenoids, flavonoids, polyphenols, phenolic acids, triterpenoids, glycosides, polysaccharides, reducing agents, and vitamins C, K, and E, are abundant in figs which were reported to have viable effects in the treatment of Inflammation, Cancer etc (Nawaz et al., 2019). Bioactive substances like polyphenols, carotenoids, vitamins, and anthocyanins that are present in fruits and vegetables are gaining increased attention due to their potential health advantages. A diet high in fruits and vegetables may help delay the process of ageing and reduce the risk of some malignancies, cardiovascular disorders, and other chronic illnesses (Sharma et al., 2020).

2.6.4.1 Phenolic Compounds

Phenolic compounds can significantly contribute to the absorption and neutralization of free radicals, the protection of biological cells against hydrogen peroxide damage, and the protection of cells and organs against lipid peroxide damage to unsaturated fatty acids. Ficus species have a lot of phenolic compounds in them (Huarte et al., 2021).

The number of polyphenols in dry figs is one of the highest among commonly consumed fruits and vegetables. Most of the phytochemicals came from the skin of the fruit (Walia et al., 2022). The number of total polyphenols in fig extract is positively associated with the extract's colour.

In comparison to lighter-coloured variants, extract from darker-coloured cultivars has the highest polyphenol content (Abdel-Aty et al., n.d.).

2.6.4.2 Flavanoids

The chemicals known as flavonoids are found in a variety of edible plants, fruits, vegetables, and grains. They are a vital part of the human diet. Flavonoids are abundant in fig fruits (Walia et al., 2022). The presence of flavonoids, fruits, and leaves of Ficus species, which have biological properties like anti-carcinogenic, anti-inflammatory, and ant-atherosclerotic activity, contributes to the flowers' appealing colour (Ross and Kasum, 2002). The main flavonoids in figs are luteolin and quercetin. From the literature, it is found that the fig leaves' most prevalent flavonoid is luteolin.

Olomon et. al. reported that the fig fruit's skin contains most of the flavonoids. They further stated from their observations that darker kinds of figs have much more flavonoids than figs from other varieties. Thus, the skin is the main tissue that contributes to the concentration of flavonoids (Olomon et al., 2006; Walia et al., 2022; Yemis, 2012).

2.6.4.3 Antioxidant Activities

Reactive oxygen species generation is prevented by antioxidants. Fig extract's total polyphenols, anthocyanins, flavonoids, and antioxidant capacity are all positively correlated with the hue. Fig extracts of darker colour variants contained more phytochemicals than extracts of lighter colour versions.

Processed dried fruits have the same antioxidant properties as their fresh fruit counterparts which would depend on the unit of measuring (Walia et al., 2022).

Anthocyanins possess the characteristics of $C_6C_3C_6$ carbon skeletal structure of natural flavonoids The chemical structure of anthocyanin is derived from the flavylium ion, and the fundamental chemical formula is $C_{15}H_{11}O+$.

Anthocyanidin is commonly known as the flavonoid that disperses in water. The main structural unit of anthocyanins is 2-phenylchromenylium (flavylium), which are bonded to hydroxyl (-OH) and/or methoxy ($-OCH_3$) groups (Khoo, 2017; Sirijan et al., 2020). Anthocyanin is the glycosidic form of anthocyanidin. Glucose is the most common sugar residue attached to anthocyanins in positions 3 and 5(Lourdes et al., 2013; Peñaloza et al., 2022).. However, there are other different monosaccharides, disaccharides and trisaccharides which may serve as glycosyl moieties, some of which are galactose, xylose, rhamnose, and fructose. The configuration of sugar residues seems to exert a more substantial impact on

anthocyanin stability than the structure of the aglycone. Within organic constituents, the substituent groups on the flavylium B-ring commonly occur in conjunction with glucose, galactose, and rhamnose, yielding at least six distinct varieties: pelargonidin, cyanidin, delphinidin, malvidin, petunidin, and peonidin. Research findings suggest that the ortho-dihydroxy phenyl structure on the B-ring serves as the active site responsible for inhibiting tumour growth and metastasis.

The general molecular structure of anthocyanin is shown in Figure 2.2 below.

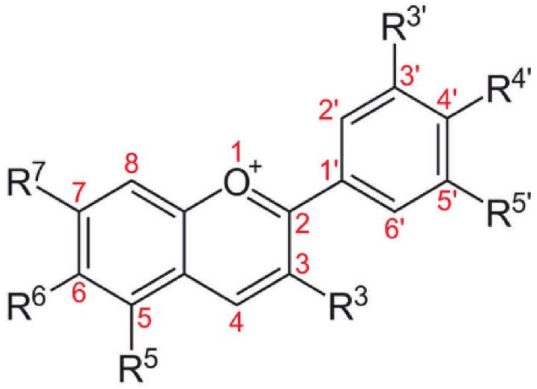

Figure 2.2 The general molecular structure of anthocyanin

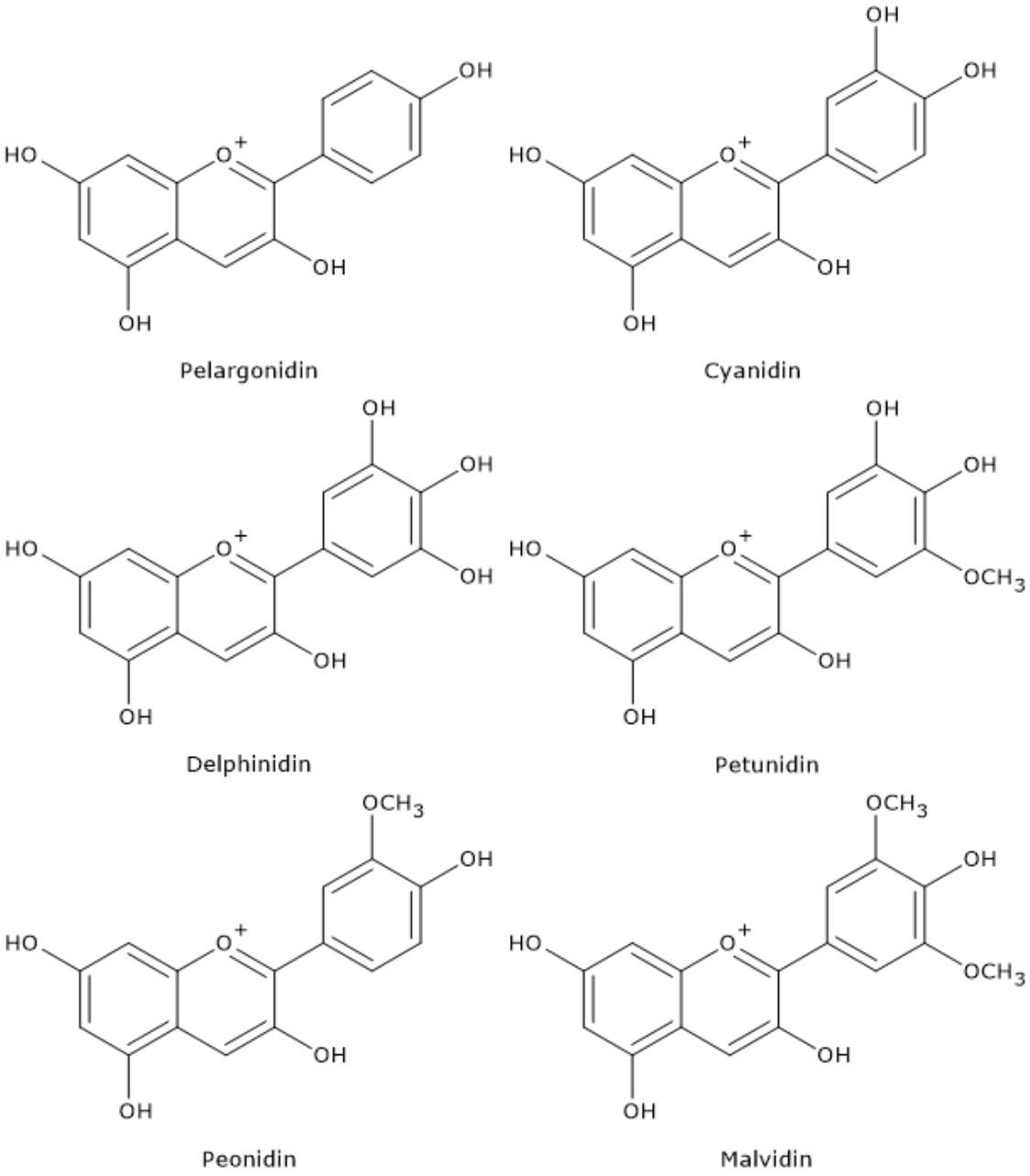

Figure 2.3 Structure of some of the naturally occurring anthocyanins.

2.6.5 The Optical Absorption Spectra of Anthocyanins

Anthocyanins are one of the pigments commonly used as a sensitizer. They are obtained from natural sources such as strawberries, figs, rosella flowers, etc. Rosella flowers, as an illustration, encompass an array of dynamic constituents, encompassing hydroxy citric acid, organic acids, hibiscus acid, anthocyanins, flavonoids, and polysaccharides. Following existing literature, there is documentation indicating that under certain acidic conditions, the colouration of both non- and monoarylated anthocyanins is primarily governed by substitutions occurring

in the B-ring of the aglycone (Da-Costa-Rocha et al., 2014; Giusti and Wrolstad, 2003; Yuniati et al., 2021).

The anthocyanins appear to be more coloured in an acid medium. For flavonoids, the absorption spectra are reported to be characterized by two separate bands. This band is determined by the B ring conjugation while the other one is characterized by the ultraviolet region (band II) and are determined by the A ring conjugation (Giusti and Wrolstad, 2003).

Yuniati et al, reported that based on UV-vis spectrophotometer analysis, the absorption spectra of anthocyanin extract were obtained with a peak at a wavelength of 516-517 nm, which indicates the presence of anthocyanin compounds.

Table 2.6 Anthocyanidin Variations and Absorption Spectra

Anthocyanin	R3	R4	R5	Aglycon	R1	R2	λmax (nm)	Visible Colour
Cyanidin	OH	OH	H	Pelargonidin	H	H	494 nm	Orange
Delphinidin	OH	OH	OH	Cyanidin	OH	H	506 nm	Orange-Red
Malvidin	OCH3	OH	OCH3	Peonidin	OMe	H	508 nm	Orange-Red
Pelargonidin	H	OH	H	Delphinidin	OH	OH	508 nm	Red
Peonidin	OCH3	OH	H	Petunidin	OMe	OH	508 nm	Red
Petunidin	OCH3	OH	OH	Malvidin	OMe	OMe	510 nm	Bluish-Red

2.6.5.1 The pH effect on Anthocyanin

The stability of anthocyanin pigments, encompassing shades of red, blue, and purple, can be compromised by alterations in factors such as pH, oxygen levels, exposure to light, and temperature variations in the presence of sugar (Suh et al., 2003). Literature analysis indicates that anthocyanins exhibit a red hue under acidic conditions, particularly at a low pH. In an acidic milieu, typically around pH = 1, anthocyanins manifest as the flavylium cation form, resulting in their red coloration and high solubility in water. This configuration is responsible for the generation of both red and purple shades. As the pH escalates within the range of 2 to 4, the dominant color shifts to blue (Jenshi et al., 2011; Wahyuningsih and Ramelan, n.d.).

Anthocyanins are stable at low pH. It becomes less stable when exposed to heat, causing a loss of colour and browning. As a result, high temperatures, increased sugar levels, pH, and ascorbic

acid can affect the rate of destruction. Due to the ionic nature of the molecular structure, the colour of anthocyanins is influenced by pH: some anthocyanins are red in acid solutions, violet or purple in neutral solutions, and blue in alkaline media (Castañeda-Ovando et al., 2009; Kang et al., 2021; Khoo, 2017). Anthocyanins possess a structural element referred to as the flavylium cation (depicted as the red circle), which accounts for the phenomenon observed. Under conditions of low pH, the cyanidin molecule within anthocyanins undergoes protonation, resulting in the formation of a positively charged ion. With a rise in pH, the molecules undergo deprotonation, causing them to adopt a negatively charged ion configuration. This behavior is pivotal in explaining why colorants containing anthocyanins are generally effective only within pH levels lower than four.Additionally, anthocyanins can act as pH indicators (Castañeda-Ovando et al., 2009; Pina et al., 2012).

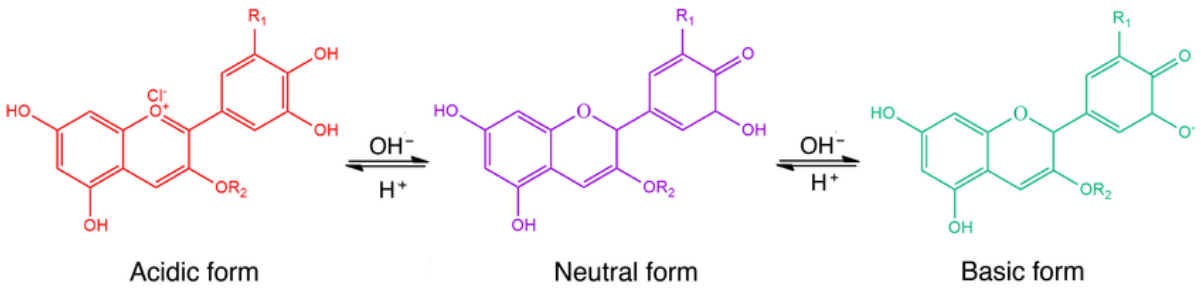

Acidic pH<4 Neutral pH=7-8 Basic pH>7

Figure 2.4 In the depicted chemical structure, the anthocyanin molecule contains hydroxyl (OH) and/or methyl ether (O-CH3) groups attached to its carbon rings. This configuration is responsible for the color change response observed under different pH conditions

Source (Kan et al., 2016).

2.6.5.2 The Effect of Enzyme on Anthocyanins

Anthocyanoses are the name generally given to enzymes that take part in anthocyanin degradation. There are two groups of enzymes (hydrolyze glycosidases and PPO) in plant tissue that are responsible for anthocyanin degradation based on enzymatic activities as reported by some literature (Sandoval-Castro et al., 2017).

Polyphenol oxidases (PPO) act on anthocyanins in the presence of o-diphenols via a coupled oxidation mechanism (Sandoval-torres and Barriada-bernal, 2017). In the presence of PPO, anthocyanins are degraded enzymatically and these enzymes may play a major role in the degradation of anthocyanins in some fruits like strawberries. One of the factors that might explain the retention of anthocyanins when lower temperatures are used is the denaturation of

PPO by the effect of the drying temperaturePPO (Polyphenol oxidase) displays notable heat stability; however, its activity diminishes when subjected to temperatures exceeding 50°C for an extended period.(Informa et al., 2006; Nunes et al., 2005; Sandoval-torres and Barriada-bernal, 2017). This process is frequently observed within plant tissues and facilitates the oxidative conversion of catechol and other ortho-dihydroxy phenyls into ortho-quinones. These ortho-quinones can subsequently engage in reactions with each other, amino acids, or other phenolic compounds, which may include anthocyanins. Consequently, this sequence of events yields compounds of higher molecular weight, often brown, or transformed products displaying greater molecular. The intricacy arises due to the comparatively diminished oxidation-reduction potential of these enzymes (Méndez-Lagunas et al., 2017). Peroxidase (POD), an enzyme present across a broad spectrum of organisms ranging from plants and humans to bacteria, serves the role of decomposing hydrogen peroxide (H2O2). This compound is produced as a byproduct during the utilization of oxygen for respiration (Méndez-Lagunas et al., 2017).

They are also known to oxidize the anthocyanin utilizing peroxides. In fruits and berries, PPO and POD are both often present, and they are responsible for the majority of anthocyanin degradation (Peñaloza et al., 2022).

2.6.5.3 The Effect of Oxygen on Anthocyanins

The deterioration of anthocyanins can occasionally stem from their exposure to oxygen, which can lead to degradation through either direct oxidation or indirect oxidation pathways. Notably, the interplay between ascorbic acid and oxygen can synergistically contribute to the degradation of anthocyanins. The most substantial reduction in pigment content is observed when anthocyanins are subjected to elevated levels of both oxygen and ascorbic acid (Heng et al., 2003).

Furthermore, the degradation of anthocyanins can also occur via indirect oxidation involving hydrogen peroxide (H2O2), which is generated during the aerobic oxidation of ascorbic acid. Research findings indicate that the introduction of H2O2 prompts swift discolouration of pelargonidin 3-glucoside solutions. The ensuing oxidation products have the potential to impact subsequent degradation or polymerization processes. Additionally, the direct oxidation of hemiacetal or chalcone species may contribute to the formation of precipitates or cloudiness in fruit juices (Heng et al., 2003).

Earlier research has highlighted the potential of high-oxygen treatments to enhance the antioxidant capacity of certain fruits, as exemplified by blueberries. Additionally, there seems to exist a potential connection between total phenolic, anthocyanin levels, and antioxidant capacity in blueberries. The work conducted by Yonghua Zheng and colleagues highlights the substantial impact of high-oxygen treatments on various fruits. Specifically, oxygen concentrations ranging from 60% to 100% tend to result in a notably reduced decay rate and elevated total anthocyanin content following a five-week storage period (Heng et al., 2003).

2.6.5.4 Co-pigmentation effect

Co-pigmentation is a solution phenomenon in which pigments and other non-coloured organic components form molecular associations or complexes. This effect would generally result in an enhancement in the optical absorbance and certain instances would cause a shift in the wavelength of the maximum absorbance of the pigment. The study conducted by Castañeda-Ovando and colleagues in 2009 introduces the concept of co-pigmentation. Co-pigmentation refers to a phenomenon wherein pigments interact with colourless organic compounds, metallic ions, or other molecules, resulting in the formation of molecular complexes. This interaction often leads to a change or enhancement in the intensity of colour. This phenomenon is of significant importance in various fields, including food science, where colour plays a crucial role in determining product acceptance and quality.

Extensive research across disciplines suggests that the co-pigmentation of anthocyanins with other compounds, referred to as co-pigments, serves as a fundamental mechanism for stabilizing and preserving colour within plants (Boulton, 2001; Castañeda-Ovando et al., 2009).

Co-pigments are typically devoid of color themselves, but upon being combined with an anthocyanin solution, an interplay transpires that yields a hyperchromic effect and a shift towards longer wavelengths in the optical absorption spectra (UV–Vis region). These co-pigments encompass a range of substances including flavonoids, alkaloids, amino acids, organic acids, nucleotides, polysaccharides, metals, or even additional anthocyanins (Castañeda-Ovando et al., 2009).

2.6.5.5 The Temperature Effect on Anthocyanin

The stability of anthocyanins and the speed at which they degrade are notably impacted by temperature. Similar to many chemical reactions, specific structural attributes that enhance pH stability, including methoxylation, glycosylation, and acylation, also contribute to heightened thermal stability. As temperature rises, there is an observable escalation in the degradation of

anthocyanins, leading to a more pronounced breakdown (Jenshi et al., 2011). Therefore, the use of thermal methods is not recommended for extraction of anthocyanins. High temperature may damage the componets and a low temperatures do not have enough energy to promote the migration of them (Yuniati et al., 2021). Ultrasonic extraction is recomende at frequency of 60 Hz (24) kHz.

Jenshi Roobha et al in their paper studied the effect of 8 different temperatures which were 0, 10, 20, 30, 40, 50, 60 and 70˚C on the level of anthocyanin extracted from Musa acuminata bract for 5 days. Their samples were measured at a wavelength of 520 nm. From their analysis, they reported the destruction of anthocyanins at the temperature of 50^0C and higher. They also stated that there was an increase in the optical absorbance of Musa acuminata bract anthocyanin which is stable at temperatures 0, 10, and 20˚C (Jenshi et al., 2011).

From their experiments, they suggested that the faster rate of destruction of anthocyanin at higher temperatures was due to hydrolyzation of the 3-Glycoside structure, which has a protective effect on unstable anthocyanin. They also made an alternative suggestion, which is the hydrolyzation of the pyridinium ring, which resulted in the production of chalcone, and that it was responsible for the brown colour-developed in the food containing anthocyanin (Jenshi et al., 2011).

Generally, from the observations of most reports, an increase in temperature would produce a decrease in the co-pigment bond intensity and its hyperchromic shift. Co-pigment complexes are exothermic and are particularly sensitive to temperature (Chen et al., 2022; Dangles and Brouillard, 1992; Jenshi et al., 2011).

Also, it has been reported that the degradation of anthocyanins in strawberries during drying was related to the temperature of the drying. It was also supported by theoretical molecular modelling that showed a bond deformation of the chemical structure leading to changes in their aromatic behaviour and a decrease in anthocyanins concentration (López-Ortiz et al., 2020).

2.6.5.6 The effect of Light on Anthocyanins

Light is the most important environmental factor influencing anthocyanin biosynthesis in plants (Jackma, 1987).

Anthocyanins extracted from organic sources are typically susceptible to instability when exposed to ultraviolet (UV) or visible light, as well as other forms of ionizing radiation. Light exposure accelerates the pace at which anthocyanins degrade thermally, primarily due to the creation of an excited state known as the flavylium cation (Jenshi et al., 2011).

The Exposure of growing plants and food storage to light of different wavelengths might trigger some distinct physiological processes in plants which can lead to changes in the plant pigments some of which are anthocyanins, phenolic compounds etc. and also alter their associated enzymes. The initiation of anthocyanin synthesis by white light is facilitated through an associated increase in PAL (Phenylalanine ammonia-lyase) activity. Conversely, under the influence of red light and UV-C irradiation, there is a noticeable tendency towards the inhibition or even degradation of anthocyanins. These observations align with the alterations in PAL activity that correspond to each light condition. Intriguingly, blue light yielded a comparable enhancement in anthocyanin content within the spear tips, mirroring the outcomes achieved in the control group. (Huyskens-keil et al., 2020; Renan, 2010). These results could be related to the changes in anthocyanins during drying.

Light from the Sun which comprises UV light, Visible light, and infrared-light, tends to affect the concentration of anthocyanin within the food during solar drying. From the reports of various works in the literature, the degradation of anthocyanins was due to UV light, incandescent light and IR-light49 and UV-C light50 (Ortiz et al., 2021). Therefore, different efforts are focused on improving anthocyanin retention during the solar drying process of foods using solar filters as covering materials and building materials in dryers (Nair et al., 2020; Ortiz et al., 2021; Pineda et al., n.d.).

Therefore in this research, we focused on the retention or increase in the bio-active content of the fig during drying through the use of solar filters in the building material.

2.7 The Drying Process

The process of dehydration consists of the removal of moisture from the produce by heat, usually in the presence of a controlled flow of air (Pardhi and Bhagoria, 2013). Drying might be defined as a process of the removal of moisture due to simultaneous heat and mass transfer.

2.7.1 The Solar drying Systems

In solar drying, two primary energy transport phenomena characterize the drying systems: passive and active systems. Active solar drying systems are also referred to as forced convection systems. These systems allow for optimal airflow to be maintained throughout the drying process within the dryer. This control over airflow helps regulate temperature and moisture levels over a wide range, irrespective of varying weather conditions. Notably, active systems involve energy transport within fluid loops, central systems that redirect fluid flows to different subsystems, and solar collectors that employ forced convection as the mode of heat

transfer. These systems utilize external energy sources to distribute solar energy through mechanisms such as fans, pumps, or other mechanical devices. At times, electricity is necessary to operate pumps, fans, and other mechanical components to ensure efficient energy distribution.

Conversely, passive solar energy systems function without the need for additional energy sources. They rely on natural buoyancy effects to facilitate heat circulation for the drying process (Tiwari, 2016).

2.7.2 Solar drying Classifications

Solar dryers are devices that use solar energy to dry materials, particularly food. There are four general types of solar dryers: Direct, hybrid, Mixed mode dryers and indirect. Direct solar dryers expose the substance to dehydration in direct sunlight (Ikrang, 2014).

2.7.2.1 Direct and indirect solar dryers

Direct solar dryers use the direct sunlight on drying chamber and then on food materils. An absorbing surface is necessary to collect the sunlight and converts it into heat. The covering material of the driers can be: glass, polyetylene, polycarbonate or another transparent or semitransparent material (Pardhi and Bhagoria, 2013).

In indirect solar dryers the heating source can be obtained from outside of the drying chamber. Furtermore, the sunlight are not in touch with the food matrix. The heated air is then passed over the substance to be dried and exits upwards often through a chimney, taking moisture released from the substance with it.

2.7.2.2 Mixed mode dryers

In these dryers, the solar radiation incide on both: food material and the solar collector to provide the heat required for the drying operation. This technology includes different covering materials and solar technologies to improve the efficience (Roman-roldal 2021).

2.7.2.3 Hybrid solar dryers

In these dryers, combine sunlight for heating source and other fosil fuel technologies. For example, electricity or gas (Ikrang, 2014; Pardhi and Bhagoria, 2013; Tiwari, 2016).

All dryers are designed considering the following features: heat loss reduction, better air distribution, and better temperature distribution, to increase the efficiency of the dryer (Ikrang, 2014; Roman Gutierrez, 2022). Some of these driers include solar filter materials to improve food quality (Nair et al., 2020).

Therefore in this work, we made use of the solar filter as a building material for the benchtop cabinet dryer to improve the retention of the bio-active compounds.

2.7.3 Drying Kinetics

The combined macroscopic and microscopic mechanisms of heat and mass transfer during drying are referred to as the drying kinetics, and they depend on the drying conditions, the type of dryer, and the properties of the materials to be dried (Samuel and Olalekan, 2016). Studying drying kinetics can help one select the best drying technique and regulate the drying processes. Additionally, engineering and process improvement depends on it. Considering that drying kinetics involves process factors and is used to illustrate the elimination of moisture from products, a better understanding of drying rate will facilitate the creation of a drying rate model.

2.7.4 Drying behaviour of fig

In this section, the drying behaviour of fig is discussed

2.8 Safe water content in dried fig

Water present in all food usually takes two forms: one is the free or available water while the other is the water that is bound to different molecules such as proteins and carbohydrates Available water can support the growth of bacteria, yeast and mould, which can affect the safety and quality of food.

In drying the water content of the food and the water activity of the food must be considered(A Jackson, 2010).

Over an extended period, both food scientists and producers have recognized texture as a crucial quality factor that significantly impacts consumer preferences towards food products. Texture can be elucidated as a set of physical attributes originating from the structural components of food, primarily perceived through the sense of touch. Texture encompasses a spectrum of characteristics, including smoothness or roughness, softness or hardness, and fineness or coarseness. It pertains to how a food item responds to forces like deformation, comminution, and flow, and this aspect is quantitatively expressed based on parameters such as mass, time, and distance (Ansari et al., 2014).

Numerous factors and attributes, including cellular components, biochemical constituents, water content, and the composition of cell walls, collectively exert influence on the texture of fruits and vegetables. Consequently, any external factors that impact these attributes have the potential to modify the texture, consequently affecting the overall quality of the final product (Guiné and Barroca, 2011).

2.9 Moisture ratio in food

In the context of solar drying, the moisture ratio (MR) refers to the ratio of the mass of water vapor present in a material being dried to the mass of the dry solid in that material: (Taiwo, A., Fashina, A.B., Ola, 2014)

Moiture ratio= $MR = \frac{mass\ of\ water\ vapour}{mass\ of\ dry\ solids}$

Where $MR\ is\ the$ moisture ratio

2.9.1 Thin layer Drying Models

In the concept of drying, a thin layer could be described as a layer of sufficient product thickness to allow uniform air characteristics to be considered throughout the layer and are without variance. The thin-layer drying process also refers to the drying of individual particles or grains of material that are entirely exposed to the drying air. The process is frequently divided into two drying periods which are the period of constant drying speed and the period of decreasing drying speed (Inyang et al., 2018).

The modelling of the thin layer drying of figs, dried under the sun in the open air was studied by Togrul while the behaviour of mechanically dried figs was extensively studied by Babalis. In the latter study, the influence of the drying conditions on the drying constants and the moisture diffusivity was also determined (Babalis et al., 2006; Babalis and Belessiotis, 2004; Ikrang, 2014; Inyang et al., 2018; Pehlivan, 2004). Different agricultural products' drying rates are described using a variety of thin-layer drying formulae. The three types of thin-layer drying models are theoretical, semi-theoretical, and empirical. The solution of Fick's second law provides the most well-studied theoretical model for thin layer drying of various foods (Inyang et al., 2018).

2.9.1.1 Theoretical Method

The categorization of models used in this context is primarily divided into three groups. Theoretical models are rooted in the second principle of the diffusion law, as put forth by Fick. Semi-theoretical models, on the other hand, typically incorporate concepts derived from both Newton's law of cooling and Fick's second law, along with its modifications. The third category focuses on assessing external resistance to moisture transfer between the air and the product. In contrast, theoretical models exclusively consider the internal resistance to moisture transfer within the product itself (Henderson, 1974; Inyang et al., 2018; Whitaker et al., 1969).

2.9.1.2 Empirical Method

An approach based on experimental data and dimensionless analysis is termed the empirical method. According to empirical drying models, there is a direct correlation between drying time and average moisture content. The basic principles of the drying process are not taken into consideration by empirical models, which can only describe the drying curve under ideal drying conditions and not the processes that take place during drying. Empirical models aid in comprehending the trend of both dependent and independent experimental/process variables. The main issues with empirical models are their heavy reliance on experimental data and their lack of detail about heat and mass transfer during drying (Coradi and Melo, 2014; Fernando and Amarasinghe, 2016; Inyang et al., 2018).

2.9.1.3 Semi-Empirical Method

Semi-theoretical models have been created to simplify the use and fit the drying data of the food material to be dried. To achieve a balance between theory and usability, much focus has been placed on creating semi-theoretical models. These models often use mass transfer to implement Newton's Law of Cooling. It is assumed that the environment is isothermal and that the product's surface is the sole place where resistance to moisture transfer exists when applying this law. The streamlined general series solutions of Fick's second law are semi-theoretical models. The Henderson and Pabis, Page and Modified Page, Henderson and Pabis, and Model of Two Terms are some semi-theoretical models (Inyang et al., 2018; Kemp and Smithkline, 2011; Panchariya et al., 2002; Parry, 1985).

Table 2.7 Table of Models derived from the solution of the equation of Newton of cooling and other derivatives of Fick's second law

	Model name	Equation	Reference
Models from Newton's law of cooling	Newton	$W = \exp(-kt)$	(A.S., 1998)
	Page	$W = \exp(-kt^n)$	(Page, 1949)
	Modified Page	$W = \exp(-(kt)^n)$	
Models from Fick's law of Diffusion	Henderson and Pabis	$W = a.\exp(-kt)$	
	Logarithmic	$W = a.\exp(-kt) + c$	
	Two-term	$W = a.\exp(-kt) + b.\exp(-k_1 t)$	
	Two terms exponential	$W = a.\exp(-kt) + (1-a)\exp(-k_1 t)$	
	Midilli and Kucuk	$W = a.\exp(-kt^n) + bt$	
Empirical Models	Wang and Singh	$W = 1 + at + bt^2$	

Therefore need to model the drying behaviour using these covering materials to investigate the moisture content loss as there are previously no models describing the drying of figs using the solar filter as a building material of solar dryers.

2.9.2 Drying Constant

The combination of drying transport parameters including moisture diffusivity, thermal conductivity, density, specific heat, interface heat, and mass coefficients make up the drying constant in the thin layer drying concept (Inyang et al., 2018; Karathanos, 1999). To use any transport equation, one must be familiar with both transport and material properties.

2.10 Review of some Related Literature on drying kinetics

Several researchers have investigated the influence of drying conditions on the drying kinetics of various agricultural products to evaluate the most suitable and efficient model for describing the drying features.

In the research conducted by F. Sabet Sarvestani et al., a comprehensive exploration of the thin-layer drying characteristics of Figs (Ficus carica) was carried out. Throughout the study, diverse drying conditions were examined, involving variations in temperature. Notably, the impact of temperature on the drying rate was found to hold greater significance compared to the other parameters. This highlights the pivotal role of temperature in influencing the drying kinetics of figs..(Sarvestani et al., 2014).

Utkucan Şahin et al compared the drying kinetics of non-pretreated (fresh) and pretreated Sarılop (Ficus carica L.) variety figs (Şahin and Öztürk, 2016).

Arun K. Raj and his team conducted a study aimed at assessing feasibility and establishing a universal drying characteristic curve within an indirect mode multi-tray solar cabinet dryer. Their research involved merging tray rearrangement patterns with the dryer performance index (DPI) approach, leading to a comprehensive analysis of how four key factors influence drying kinetics. This comprehensive analysis resulted in the creation of a generalized curve. One noteworthy finding from the conducted experiments is the notable influence of tray arrangement on the effectiveness of the dryer performance index method, particularly within the context of an indoor indirect-mode solar cabinet dryer. Interestingly, the assessment of the dryer performance index for Tray 3 alone proves sufficient in offering valuable insights into the overall dryer performance (Raj and Jayaraj, 2021).

Rifat Jabeen et al designed a laboratory-scale cabinet dryer equipped with a connected weighing balance to monitor product weight changes within the dryer. Their experiments focused on investigating the impact of process parameters, specifically temperature and thickness, on the drying kinetics of potatoes. The study outcomes indicated that utilizing their self-designed laboratory dryer facilitated the reduction of post-harvest losses through successful potato drying. The research encompassed the drying of potato slices of different thicknesses across temperatures ranging from 60 to 70°C (Jabeen et al., 2015).

Norhasmanina Norhad et al examined the drying kinetics of mango using a tray and oven dryer at varying temperatures (40, 50, and 60 °C) with a consistent airflow rate of 1.3 m/s. The study

aimed to analyze the effects of drying time, temperature, and air velocity on mango drying, compare the physical attributes of dried mango samples, and identify the most suitable drying kinetics model for each drying method. The research highlighted that an increased drying time led to reduced moisture content and an augmented drying rate. Temperature and air velocity also played a role, with higher values of these parameters correlating to increased drying rates. The researchers proposed that the Henderson and Pabis model was the best fit for the drying of mango in a tray dryer, specifically at 60°C, with R^2 and RMSE values of 0.9249 and 0.0910, respectively (Norhadi et al., 2020).

Taiwo et al conducted earlier experiments indicating that it took 16 hours to sun-dry 4.5 kg of peeled cassava chips to a safe moisture content of 13.9% w/w during the rainy season in August. Conversely, using a cabinet dryer during the same period of the year, the same mass of peeled fresh cassava chips reached an average safe moisture content of 12.2% w/w within only 3 hours (Taiwo, A., Fashina, A.B., Ola, 2014).

Luqman E. investigated the drying kinetics of pineapple slices using a Solar Conduction Dryer (SCD). The study entailed developing suitable thin-layer drying models for prediction and assessing the performance of the SCD. Throughout the experimentation, ambient temperatures ranged from 24 to 37°C, while the dryer's temperature varied between 25 and 46°C. Results indicated that the SCD consistently maintained higher temperatures than the ambient surroundings. These drying conditions in the SCD proved favorable for pineapple drying and aligned well with findings from other researchers(Daud and Simate, 2017).

CHAPTER 3

3 MATERIALS AND METHOD

3.1 Study Area

The study area is Temixco, Morelos which is the fourth largest city in the Mexican State of Morelos. It stands at 18°51'N 99°14'W and has a height of 1,290 meters (4,232 feet).in the west-northwestern part of the state. The city is mostly associated with high solar irradiance and temperature. The temperature commonly fluctuates between 52°F and 90°F, with infrequent occurrences below 47°F or exceeding 96°F during the day which makes it possible for solar drying experiments to be carried out.

3.2 General analysis of the Experiment.

In this study, sliced fig cut longitudinally were dried with two separate solar cabinet dryers and with direct solar drying as a reference. The first building material for the cabinet dryer was cellular polycarbonate material treated with copper chalcogenide (sulphide/selenide) which would be called "CELL" in this work. They act as solar radiation filters for blocking its UV and Violet-Blue spectral components. The building material for the second cabinet dryer was cellular polycarbonate material without treatment and termed ordinary - "ORD."

Fig *3.1*

Figure *3.1* and Figure 3.2 below describe the cellular polycarbonate cabinet dryer used for the experiment outlet and inlet view (CELL) respectively. Figure 3.2 below shows the ordinary polycarbonate cabinet dryer. Subsequently, we also analyzed the chemical composition of the dried samples. The bio-active substance analyzed was total anthocyanins. In addition, we studied some drying behaviour for the figs such as drying kinetics, and drying rate and we were able to predict the best model suitable to describe the drying kinetics of fig.

3.2.1 Raw materials

The samples of the fresh figs (*ficus carica*) were sourced from a local market in Temixco, Morelos. About 2 kg of the fresh fig was purchased and used for the experiment. The fresh figs were all harvested when they were ripe, which was the normal practice for commercial harvesting in Mexico. The fig samples were harvested at the beginning of February 2022, which is a season that is widely regarded as the peak of the production of figs in Mexico. The fresh fig samples harvested were then washed and placed in a plastic container and were next stored in a freezer at −10 °C before the drying experiment.

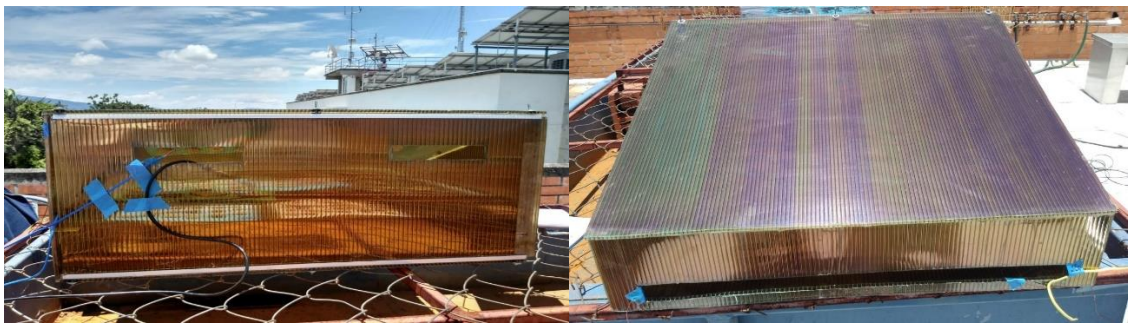

Fig 3.1

Figure 3.1 Left, the Cellular polycarbonate material treated with copper chalcogenide sulphide/selenide Cabinet dryer (CELL) Front view (outlet); right, cellular polycarbonate material treated with copper chalcogenide sulphide/selenide Cabinet dryer (CELL) Inlet view

Figure 3.2 The ordinary *polycarbonate bench-top cabinet dryer (ORD)*

3.2.2 Drying equipment and design

The drying was done with the help of a benchtop cabinet dryer built with cellular polycarbonate material treated with copper chalcogenide (sulphide/selenide) and an ordinary cellular polycarbonate dryer without such treatment. Both the dryers were designed by the Renewable Energy Institute –UNAM in Temixco, Morelos, Mexico. Each of the cabinet dryers contained two perforated trays. The dryer operates by the principle of natural convection whereby the solar radiation from the sun heats the roof of the dryer. This way, the inlet air also gets heated up thereby blowing through the tray before leaving the dryer through the outlet vent. The vents

were designed in such a way as to ensure an even distribution of hot air through the vents to the samples for drying (Roman Gutierrez, 2022).

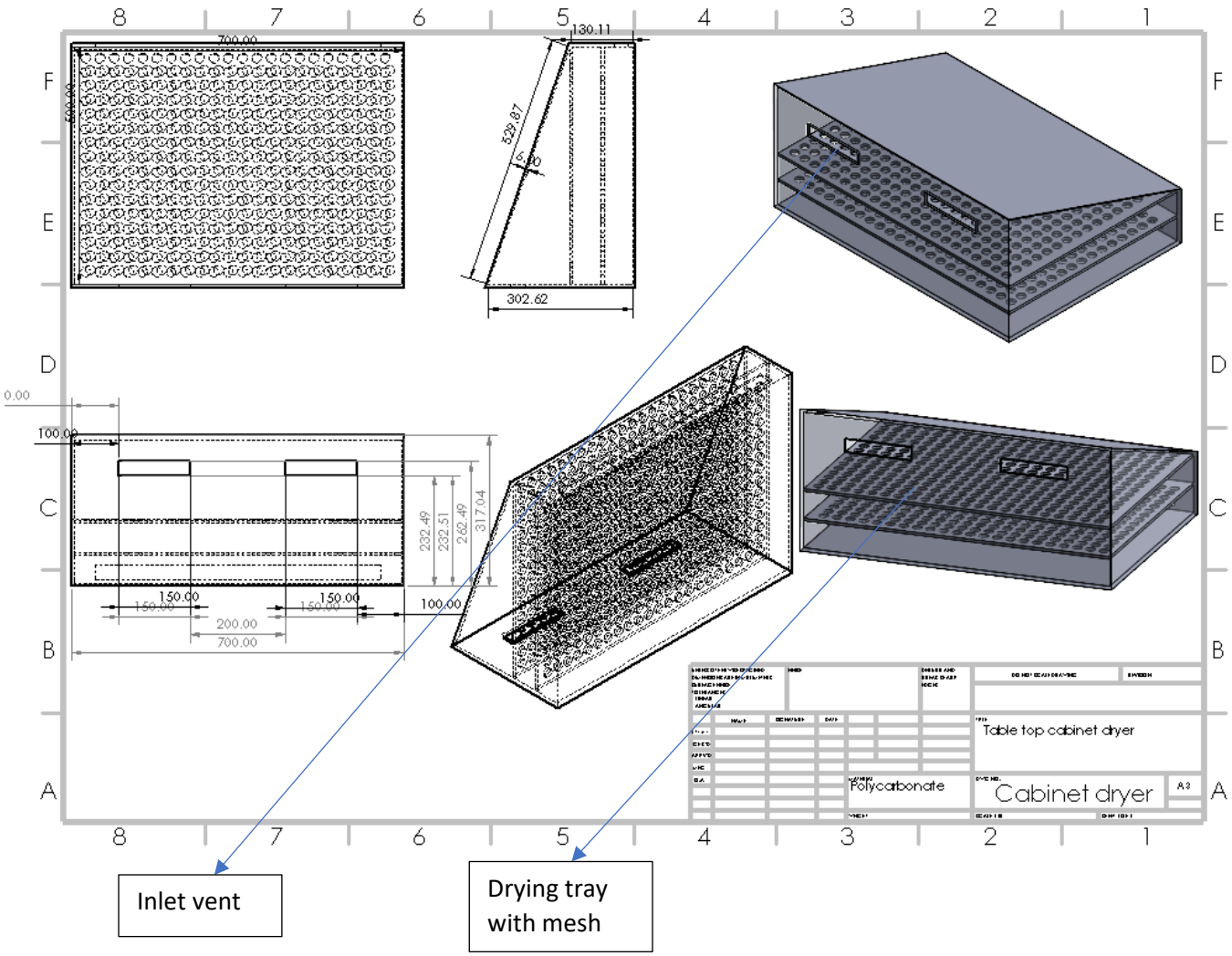

Figure 3.3 Schematic diagram of the bench top Cabinet dryer (Roman Gutierrez, 2022).

3.3 Optical properties of the Cabinet dryer

The chemical aspect of the cabinet dryer design, which is the property of the cabinet dryer that blocks the UV light from the sun which interacts with pigments such as Anthocyanin from the figs would be adopted using copper chalcogenide (sulphide/selenide) thin films applied by chemical deposition on cellular polycarbonate sheet, which has been proven to block UV light from the sun (Nair et al., 2020).

3.4 Drying

The washed fig samples were required to be dried further until their water activity (Aw) reached about 0.60–0.65 to create a shelf-stable product. In this study, two drying methods were employed. The first one involved using a benchtop cabinet dryer built with anti-reflective filters and dries at a relatively high temperature while the second drying method was the ordinary polycarbonate benchtop cabinet dryer. Figure *3.2* below. For these two different types of dryers, we established various drying curves.

3.4.1 Drying Method

Our drying tests were done in March 2022, between 9:30 am and 5:00 pm and the drying was performed continuously. The CELL and ORD benchtop cabinet prototypes were developed at the Renewable Energy Institute (IER- UNAM).

A *B*

Figure 3.4 Fig A shows the picture of the electric oven used for parts of the experiments while Fig B shows the process for the slicing of the figs before drying

The samples in the fridge were brought out to defrost before drying. The sorted and washed samples were then sliced transversely by a pen knife with a desired thickness of 1.5mm and diameter of 2.5 cm as shown above. The slicing helps the drying to take place with efficacy concerning the mass transfer. The relationship between the diameter and the thickness of the sliced fig is about 20 times which is generally referred to as thin layer drying. The sliced fig was then sent for drying with various drying methods described below. The results of both

cabinet dryers were compared with those obtained in the electric oven dryer. Independent samples were collected periodically from the dryer for physical and chemical measurements. The equation below describes the moisture content for each sample. Weight loss in the drying sample was determined periodically by using a balance (BPS40plus, Boeco, Germany). This weight loss would be used for the determination of the moisture content (X) in the sample.

$$X_t = \frac{Msh - Mss}{Mss} \qquad 3.1$$

Where, X_t, is the moisture ratio at any given time t, Msh and Mss are the mass of the wet sample and the mass of the dried solid sample respectively.

We also reported the drying kinetics as time-dependent normalized moisture content (MR). The MR was calculated as follows by equation 3.2. which is Fick's diffusion equation.

3.2

$$MR = \frac{X_{(t)} - X_e}{X_0 - X_e}$$

Where MR is the normalized moisture content or moisture ratio, $X_{(t)}$ is the moisture at any given time (t) X_e is the equilibrium moisture content while X_0 is the initial moisture content.

The value of MR is relatively smaller when compared with values of X_0 and X_e and can therefore be reduced to equation 3.3 below (Norhadi et al., 2020).

3.3

$$MR = \frac{X_{(t)}}{X_0}$$

Figure 3.5 Left, drying of sliced fig performed with the ordinary polycarbonate cabinet dryer (ORD); and right, drying in its final stage

Fig 3.6

Figure 3.6 Left, drying performed with the cellular polycarbonate cabinet dryer (CELL) before drying, right, drying performed with the cellular polycarbonate cabinet dryer (CELL) after drying.

Figure 3.7 Left, drying performed under direct solar drying (D.S) before drying; right, drying performed under direct solar drying (D.S) after drying

3.5 Some of the materials used for the experimental measurements

Some of the materials used for the drying experiment are mentioned below: We used 3 different types of sensors to measure temperature, relative humidity and air velocity inside the dryer.

Other parameters measured were solar irradiance, wind speed and relative humidity in the ambient.

3.5.1 Temperature

A K-type thermocouple as shown in Figure 3.8 was placed inside the drying tray compartment at various positions (top, roof, bottom, inlet, outlet and ambient temperature). These were utilized to determine the drying temperature for each drying experiment (ORD, CELL, and D.S.) as well as for the reference (control) experiment. The data were recorded using a 48-channel data acquisition system (MAC-14 Cole-Parmer®) connected to a laptop computer that takes reading automatically. Each solar dryer had six thermocouples attached to it, and the temperature was monitored every thirty seconds.

Figure 3.8 The K-type thermocouple for taking a reading with the laptop computer for the analysis.

3.5.2 Wind Speed

The anemometer as shown below was used to measure the average Wind speed at the inlet and outlet of the dryer periodically as the drying progressed.

3.9

Figure 3.9 Left, the Digital Balance; right, the anemometer.

3.5.3 UV irradiance and Relative humidity.

We employed the services of the meteorological station located in Temixco, Morelos, UNAM ESOLMET-IER-UNAM (http://esolmet.ier.unam.mx/Tipos_consulta.php) for the measurement of the UV irradiance and relative humidity outside of the dryers used. We analyzed the data acquired every 10 min using a data acquisition system (CR1000, Campbell Scientific, USA). For each experiment, the half-hourly averages were considered.

3.6 Extraction of Organic compounds

After the drying was completed, each of the 0.5 g slices of the fig was placed in a clean container for the extraction process. We performed the extraction by using two successive 5 mL of methanol-water mixture at an 8:2 ratio for total anthocyanins (TA) and Flavonoids measurements (TF) and two successive methanol-water mixture at an 8:2 ratio acidified (0.1%) for total phenolic compounds (TPC) measurements as described by (López-Ortiz et al., 2021; Rodríguez-Ramírez et al., 2021). We then performed ultrasonic bathing with the ultrasonic machine as shown in Figure *3.10* below for twenty minutes for enhanced extraction purposes. The supernatant was obtained after the extraction procedure. The final aqueous organic extract was filtered using a Pasteur pipette filled with cotton and celite. Then it was kept at 4 °C until TPC and TA analysis were made. A dry matter basis was used to determine all the parameters.

Figure 3.10 The ultrasonic bathing of the sample and the ultra-sonic machine

3.6.1 Anthocyanin Determination

Following the methods described by (Eisele et al., 2005; Jiang et al., 2018). The total content of monomeric anthocyanins content was determined using the pH-differential method.

Two distinct buffer systems were employed in our study: a sodium acetate buffer at a concentration of 0.04 M with a pH of 4.5, and a potassium chloride buffer at a concentration of 0.025 M with a pH of 1.0. Total anthocyanin content (TA) was quantified in terms of cyanidin-3-glucoside equivalent. To calculate this, we utilized a molar extinction coefficient (ε) of 26,900 L/mol·cm, a dilution factor (DF) of 1, and the molecular weight (MW) of cyanidin-3-glucoside, which is 449.2 g/mol. Thermo Scientific's Genesys 105 UV-VIS spectrophotometer as shown in Figure 3.12 was used to measure the samples' optical absorbance (A) at 510 and 700 nm for two pH levels. In terms of milligrams of cyanidin-3-glucoside equivalents per litre (mg/L), anthocyanin concentration (CTA) was measured.

The anthocyanin concentration and absorbance A were calculated by Equation 3.4 below.

3.4

$$TA = \frac{A\ x\ MWx\ dfx\ 10^3}{\varepsilon\ x\ p}$$

where

3.5

$$A = (A_{510nm} - A_{700nm})pH\ 1.0 - (A_{510nm} - A_{700nm})pH\ 4.5;$$

$$MW = (molecular\ weight$$

$$= 449.2\ \frac{g}{mol}\ for\ cyanidin - 3 - glucoside\ (cyd - 3 - glu)$$

$$DF = dilution\ factor$$

$$\varepsilon = molar\ extintion\ cooeficient\ 26900\ \frac{L}{mol * cm}\ \ and\ p = path\ length\ in\ cm$$

10^3=factor for conversion from gram to milligram, V_s is the volume of the solution used for extraction (mL) *and w is the weight of dried solids.*

$$TA = \frac{C_{TA}.V_s}{1000.w}$$

3.6

Figure 3.11 The fig extracts labelled and stored for analyses

3.6.2 Total phenolic content determination.

According to (Pantelidis et al., 2007; Singleton et al., 1999) total phenolic compounds in samples in aqueous extracts were assessed using a modified Folin-Ciocalteu colourimetric method. The calibration curve was created using gallic acid equivalent (0-36mg_{GAE}/100 mL). At 750 nm, the optical absorbance was measured. The total phenolic content (TPC,mgGAE/gdm) was calculated using the equation below.

3.7

$$TPC = \frac{C_{TPC}.V_S}{100.w}$$

In the given equation above C_{TPC} is the total phenolic content concentration (mg_{GAE}/100mL), Vs represents the volume of the solution used for extraction (mL) and w signifies the sample weight (gdm) expressed in grams per dried matter.

3.6.3 Flavonoid determination

The aluminium chloride colourimetric test was used to quantify the total flavonoid content as described by (Zhishen et al., 1999). Following 30 min of processing at 25 °C, the optical absorbance was measured at 510 nm with the use of a spectrophotometer. The fig's total flavonoids (TF) were expressed as mg of equivalent quercetin per gram of dry matter (mg_{QE}/gds.). A reference curve was created using dilutions of quercetin (20–100 mg/L). The averages and standard deviations of three separate determinations were used to calculate all results (each performed in triplicate).

Figure 3.12 The spectrophotometer

3.6.4 Antioxidant Capacity Determination

We applied the procedure described by (Brand-Williams et al., 1995; Rufino et al., 2007) to assess antioxidant activity using the stable free radical 1,1-diphenyl-2-picrylhydrazyl (DPPH). A spectrophotometer was used to measure the optical absorbance at 517 nm following a reaction for 30 minutes at 25 °C (S10, Thermo Scientific, USA). The fig's antioxidant activity was measured in terms of milligrams of ascorbic acid equivalent (AAE) per gram of dry matter (ds) in both its raw and dried forms. Ascorbic acid was used to produce a calibration curve (0–25 mg/100 mL).

The antioxidant capacity can be calculated by the formula below:

3.8

$$AA_{mgAAE/gdm} = \frac{C_{AA} x V_s}{100 x d.m}$$

3.7 Colour

Using a colourimeter, we assess the colour using CIELAB indices (International Commission on Illumination, Vienna) (Kingwell, JZ-300, China) as shown in Figure 3.13 below.

Figure 3.13 The Colorimeter

3.8 The Color characteristics of figs

The analysis for the values of colour for the fresh and dried figs was done using the colourimeter of model: (Kingwell, JZ-300, China) that was recommended by the International Commission on Illumination (CIE) colour coordinates L*, a* and b. ("International Commission on Illumination - Wikipedia," n.d.).

Identifying Color Differences Using CIE L*a*b* Coordinates.

ΔL (L sample minus L* standard):** This indicates the difference in lightness and darkness, where a positive value denotes a lighter shade and a negative value signifies a darker shade.

Δa (a sample minus a* standard):** This quantifies the distinction in the red and green components, with a positive value implying a redder hue and a negative value suggesting a greener hue.

Δb (b sample minus b* standard):** This measures the variation in the yellow and blue components, with a positive value indicating a yellower shade and a negative value indicating a bluer shade.

During the experiment, three samples were chosen from each tray and individually labelled for colour measurement. The colour values of these samples were documented as the drying

process progressed. These colour assessments were conducted for all employed drying methods. Similar tests were conducted on figs stored in a refrigerator for two weeks.

Additionally, the hue angle, as one of the measured parameters, characterizes the relative proportions of redness and yellowness:

0°/360° for red/magenta, 90° for yellow, 180° for greenand 270° for blue or purple. Values between these basic colours describe intermediate shades (Kortei et al., 2015; Kortei and Akonor, 2015; Seerangurayar et al., 2018). Colour variations were assessed using the following parameters:

We calculate the luminosity L* which represents the lightness or the darkness of the sample and it ranges from 0-100. Also, the chromaticity parameters a* which denotes the Redness +a to greenness -a range from +60 (red) to -60 (green) lastly, the b* parameter that denotes the yellowness +b to blueness -b { ranging from +60 (yellow) to –60 (blue)}. Before the measurement, the calorimeter was first calibrated with a white standard tile provided by the manufacturer (Barroca, 2012).

For the colour measurements, three fig slices were chosen at random. Throughout the drying process, the colour was checked every 30 minutes. The colour angle hue was assessed by Eq 3.9 below.

3.9

$$Hue\ angle\ (H) = tan^{-1}\left(\frac{b^*}{a^*}\right)$$

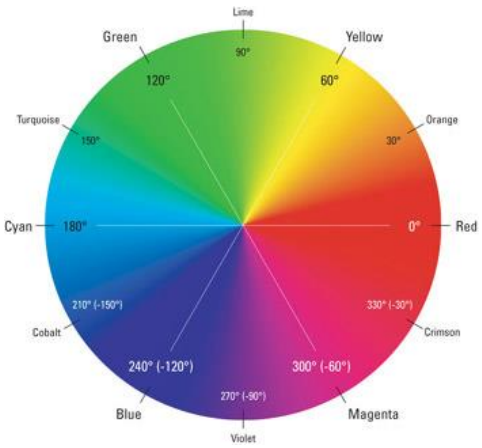

Figure 3.14 The colour wheel for Hue angle.

We also calculated the total colour change given by Equation 3.10 below

3.10

$$Total\ color\ change\ \Delta E = \sqrt{(L_0^* - L^*)^2 + (a_0^* - a^*)^2 + (b_0^* - b^*)^2}$$

Where, L_0^*, a_0^* and b_0^*, are the L*, a*, and b* values of the fresh figs to be dried while L*, a*, and b* are corresponding values of the figs during drying at each respective time (Barroca, 2012). When the value of ΔE is greater than 1.5 and less than 3 one can consider a significant colour change. When the value of ΔE is less than 3 we consider a strong differences between the samples (Guiné and Barroca, 2012).

3.9 Empirical and Semi-empirical modelling

Table 3.1 Table of Empirical and semi-empirical modelling in drying

Nonlinear regression was performed on the Gauss-Newton algorithm to estimate the model parameters as shown in the table Table 3.1 below Mathematical models were fitted to the drying data.

Model Name	Equation	Reference
Newton	$MR = exp(-kt)$	(Norhadi et al., 2020)
Henderson and Pabis	$MR = a.exp(-kt)$	(Daud and Simate, 2017)
Wang and Singh	$MR = 1 + at + bt^2$	(Gr et al., 2021)
Logarithmic	$MR = a.exp(-kt) + c$	(Jabeen et al., 2015)
Two-term exponential	$MR = a.exp(-kt) + (1 - a)exp(-kat)$	(Leeratanarak et al., 2006)

3.9.1 Statistical analysis

The data for the drying analysis was analyzed using the Number Cruncher Statistical Systems (2020) NCSS software and Microsoft Excel (365). The model's fitting quality to the experimental data was assessed using the coefficient of determination R^2 as shown in equation 3.13 below, it is a statistical measure that represents the proportion of the variance for a dependent variable that's explained by an independent variable or variables in a regression model. The statistical errors were calculated numerically by Excel and the root mean square error (RMSE) and chi-square error X^2 were generated by NCSS as shown by the equations 3.11 and 3.12 respectively. The ideal value for the Root means the square error is "Zero" therefore a smaller value would indicate that the data points fall closer to the curve-fitted line (Borah et

al., 2015). For the evaluation of the best fit of the experimental data to the model a low value of Root mean square error and a high value of R^2 value should be obtained (Borah et al., 2015)

3.11

$$RMSE = \sqrt{\frac{1}{N}\sum_{i=1}^{N}\left(MR_{pre,i} - MR_{exp,i}\right)^2}$$

3.12

$$X^2 = \frac{\sum_{i=1}^{N}\left(MR_{exp,i} - MR_{pre,i}\right)^2}{N - n}$$

3.13

$$R^2 = \frac{\sum_{i=1}^{N}\left(MR_{pre,i} - MR_{exp,avg}\right)^2}{\sum_{i=1}^{N}\left(MR_{exp,i} - MR_{exp,avg}\right)^2}$$

CHAPTER 4

4 RESULTS AND DISCUSSIONS

The experiments conducted and described in this research aimed to enhance our comprehension of the factors influencing the drying rate and quality of Mexican figs, along with the preservation of their bioactive compounds. The study delves into various drying methods, exploring their impact on freshly harvested figs and those stored for two weeks at a refrigerated temperature of 10°C. To evaluate the quality of dried Mexican figs based on composition, the anthocyanin content was assessed using spectroscopic methods, comparing the levels before and after drying. The research also examines colour parameters, such as total colour change, lightness, redness ratio, and hue angle, concerning the drying process and fresh figs.

4.1 Drying Kinetics

Figure 4.1 below shows the drying kinetics for the freshly harvested Mexican fig for various methods or drying procedures using direct solar (D.S), ordinary polycarbonate (ORD) and cellular polycarbonate (CELL). The temperature for the drying was plotted against the time for three drying conditions as well as solar radiation.

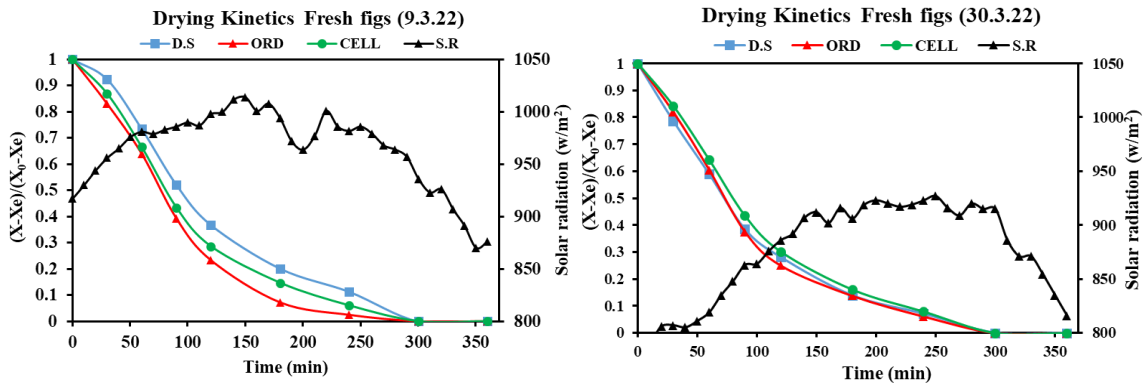

A *B*

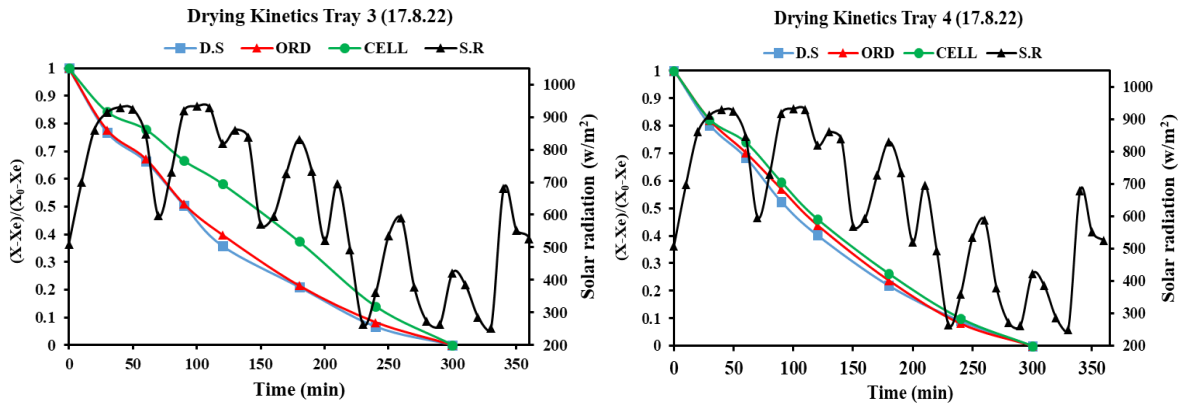

C

D

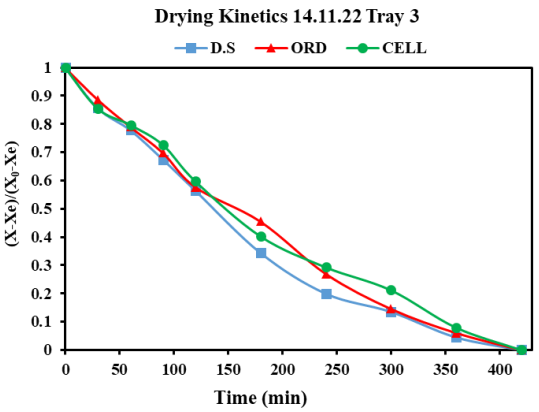

E

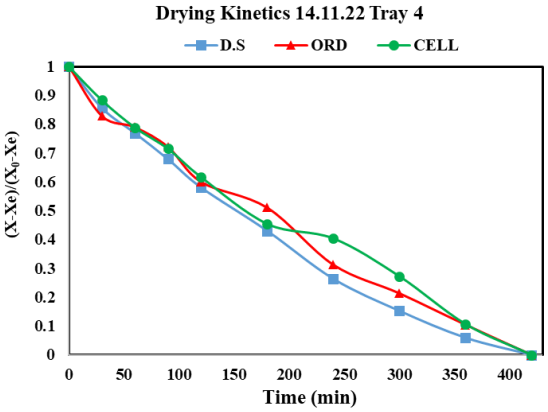

F

Figure 4.1 Fig A shows the drying kinetics for fresh figs dried in early March with solar Irradiance. Fig B shows the drying kinetics of figs after 2 weeks of storage in the refrigerator with solar irradiance. Fig C and D show the drying kinetics for figs dried in August Tray 3 (bottom of the dryer) and Tray 4 (top of the dryer). Fig E and F show the drying kinetics of figs dried in November with solar irradiance. All were dried with different drying methods (Direct solar, Ordinary polycarbonate, Cellular polycarbonate).

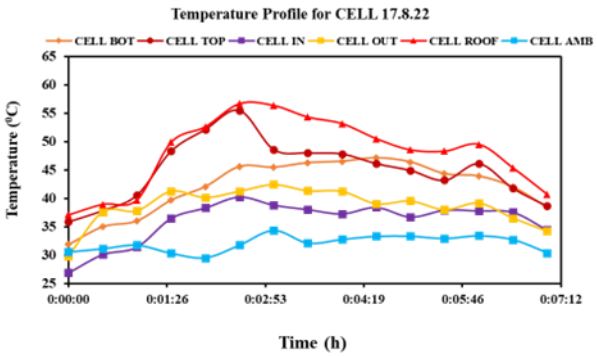

A

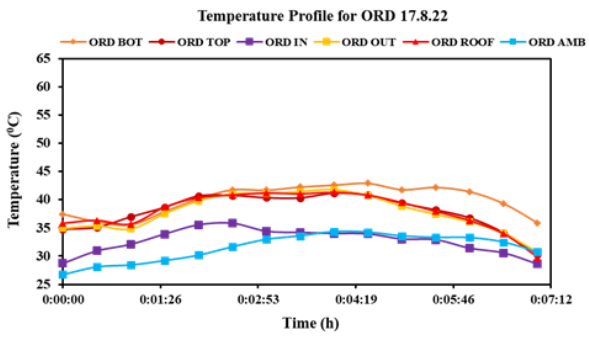

B

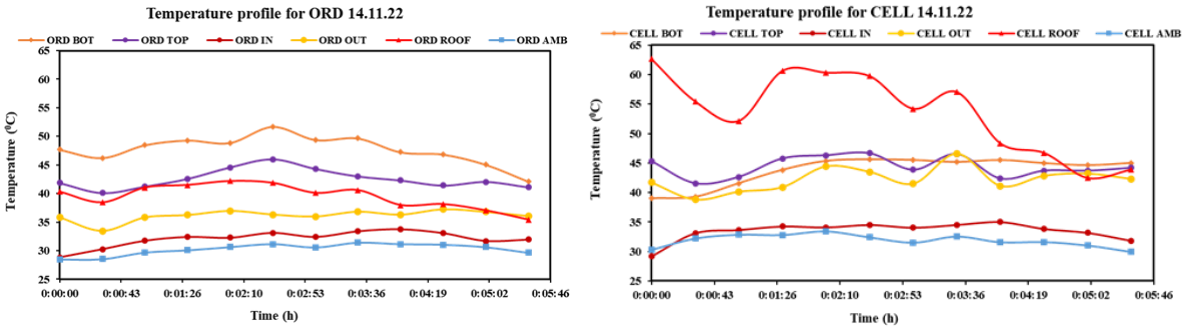

C *D*

Figure 4.2 fig A shows the graph of the temperature variation for fresh fig dried in August with the cellular polycarbonate with sensors positioned (bottom, top, inlet, outlet, roof, ambient) while fig B shows the graph of temperature variation for fresh fig dried with the ordinary polycarbonate for same sensor positions. fig C shows the graph of the temperature variation for fresh figs dried in November with the cellular polycarbonate with sensors positioned (bottom, top, inlet, outlet, roof, ambient) while fig D shows the graph of temperature variation for fresh figs dried with the ordinary polycarbonate for same sensor positions.

4.2 Effect of drying time

As the drying of the fresh figs took place, we observed that the weight of the fresh fig samples continued to decrease rapidly during the first three to four hours of drying. The moisture content for the fig reduced rapidly from 0.6 to 0.3 within the first two-three hours of drying, this reduced moisture content occurred because the temperature continued to increase at the early hours of drying in the dryers used as shown in the figure below. Thus the rising temperature led to a decrease in moisture content. Also, as the drying time increased, we experienced increasing solar radiation of about 1000w/m^2 which was also responsible for the rapid reduction in moisture content as shown in Figure 4.1. Further into the drying, the weight continued to decrease gradually, as we took readings, we observed that there was a mass transfer process which consists of the removal of water from the fig due to the evaporation or loss of moisture from the surface of the fig samples. From the graph Figure 4.1 above, we could deduce that the drying was more rapid with the ordinary polycarbonate material than with figs dried under direct sunlight. Therefore, with this material, we obtained faster drying. The lower relative humidity between 15-30%, as can be seen from Figure 4.3 below, contributed to lowering the moisture content in the sample.

We observed the drying was faster with the ordinary polycarbonate than the cellular polycarbonate (UV-Blue light solar filter) material because of the difference in optical properties of the materials, the transmittance of the ordinary polycarbonate material was higher (T: 83%) (Nair et al., 2020) than the cellular polycarbonate (T: 42%), and the absorbance on

the cellular polycarbonate higher than the ordinary polycarbonate. As a result, the temperature on the surface of the cellular polycarbonate (57 °C and 62°C) resulted in a major heat lost. Also, the temperature of the ordinary polycarbonate (42°C) causes a lesser heat lost.

For the drying kinetics for the figs stored in the refrigerator for two weeks (drying performed in late March 2022) we observed a trend slightly similar to the drying of fresh figs, as illustrated in Figure 4.1 above, the drying done with ordinary polycarbonate was also faster than other drying methods this might also be explained by similar observations as regard solar radiation for the particular day of drying, the peak solar radiation recorded for 30th of March, 2022 was about (920w/m^2) as can be seen from Figure 4.1 below obtained from **(The IER-UNAM Solar metric and Meteorological station (ESOLMET-IER).** We also recorded a high wind speed for the drying performed for late March between 1-5m/s as shown in Figure 4.3, this was responsible for the losses in some of the energy absorbed by the cellular polycarbonate material.

From the drying of figs performed in August 2022, we observed that the drying was performed at different layers of the dryer the top and the bottom of the dryer as shown in Figure *3.2* above we recorded a higher temperature at the top the dryer as recorded by the thermocouple about 55^{0}C and about 42^{0}C at the bottom of the cellular polycarbonate dryer as shown in Figure 4.2 above. The faster drying recorded at the top of the dryer for August was attributed to the higher temperature at the top of the dryer when compared to the slower drying observed at the bottom of the dryer. We also recorded a lower solar irradiance which was a cloudy day of about 900w/m^2.

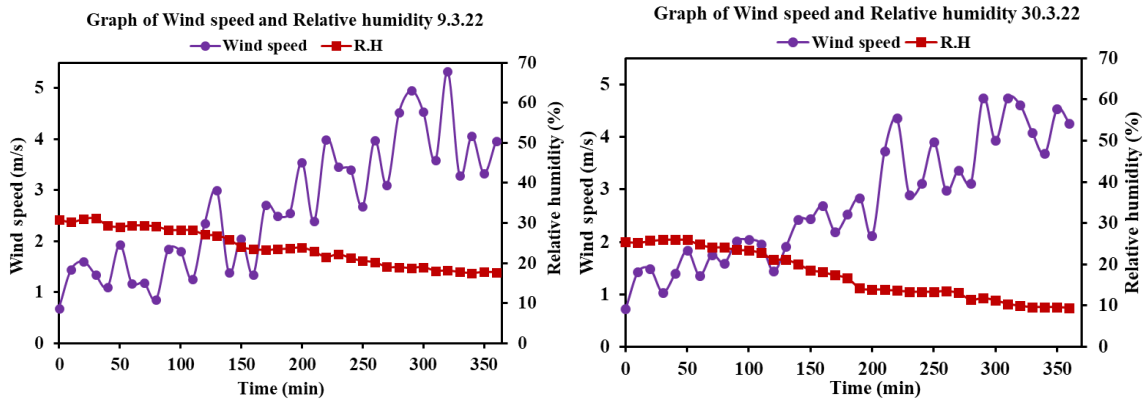

A *B*

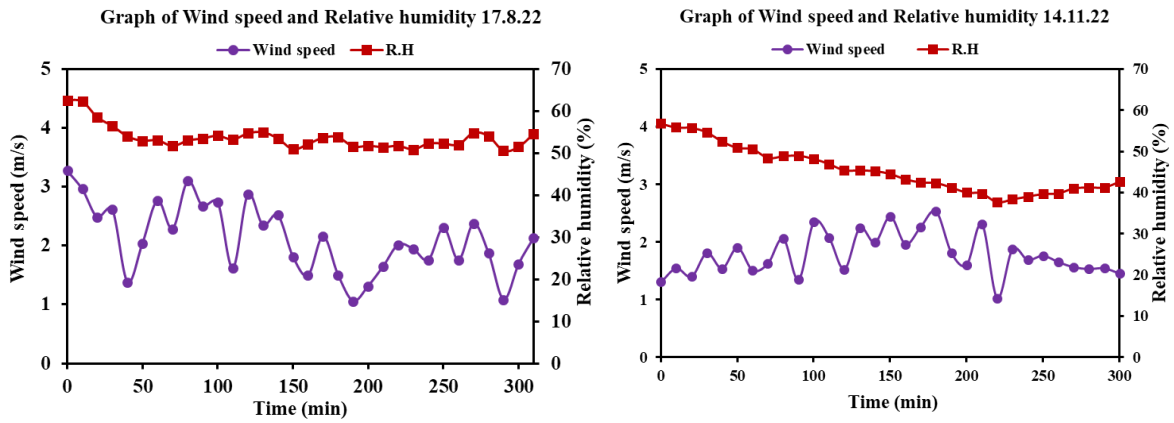

C *D*

Figure 4.3 Graph showing the Wind speed and relative humidity for each particular day Fig A shows experiments conducted in early March, fig B shows the ones done in Late March while Fig C shows the ones conducted in August and lastly, fig D shows the experiments done in November).

Our observation from the drying kinetics agrees with some data reported which shows the drying time depends on drying temperature, solar irradiance on the sample, wind speed around the dryer and the ambient relative humidity. Samples which were dried at a higher solar irradiance had a shorter drying time because of a higher driving force for heat transfer and vice versa as reported by Leeratanarak et al (Leeratanarak et al., 2006).

Norhasmanina Norhadi et al. made a report which is consistent with our observations that as the drying time increases, the moisture content of the sample would decrease and vice versa. He maintained that the moisture content in the sample for analysis is either diffused or evaporated to the drying medium existing in the dryers over time, and thus the samples would continue drying (Norhadi et al., 2020).

From the report of Juliana M Silver et al., as they analyzed figs treated osmotically and non-treated their results correspond with the observations we made for the non-treated figs, they dried figs at 55, 65 and 75°C with air-velocity of 1.4 m/s. The initial moisture contents of osmotically treated and non-treated figs were 66 and 84 wt.% (wet basis), respectively which is similar to our observation of 82% (wet basis) (Silva et al., 2013).

4.3 Effect of drying temperature on drying rate

The data we obtained for the ambient temperature during the experiment ranged from 28 ^{0}C which is the lowest temperature to about 35 ^{0}C while drying with the direct solar. The graph plotted above Figure 4.2 shows the relation between the temperature and the drying time for

the various drying modes we analyzed which were realized after about 8 hours of drying. There is also a relation between the temperature of drying and the weight of the samples being analyzed, the graph shows that the rising temperature led to an increase in the drying rate and the rate of weight loss, Figure 4.4 as drying involves the mass transfer process consisting of the removal of water or other solvents by convection and diffusion. The reason for the increased drying rate could be a higher temperature that would have been able to provide or supply more heat energy in the heat transfer process. Thus, we can observe that more moisture content was reduced within the first 1 hour of drying at a higher temperature.

Changes in the drying temperature affect changes in the drying rate in non-isothermal or periodic drying (López-Ortiz et al., 2023; Martynenko, 2018). In this instance, the fig also showed a similar trend in the drying rate. This phenomenon occurs as a result of the temperature rise brought about by the high solar radiation. The drying temperature in the cabinet dryer (CELL) ranged from 40-60^{0}C during the mid-day. This increasing temperature led to an increase in drying rate during the first 2 hours of drying. After the critical moisture content was attained, the drying rate dropped. This happens because the moisture on the fig was not enough to maintain an increased drying rate as shown by the drying rate curves shown below in Figure 4.4. Also, there is no free water available at the surface of the material and the amount of water migrating from the interior to the surface is not enough to maintain a constant drying rate.

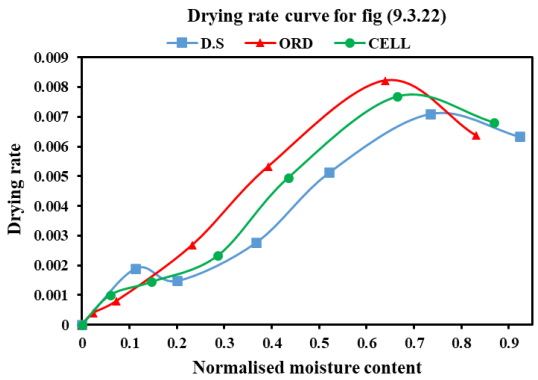

A

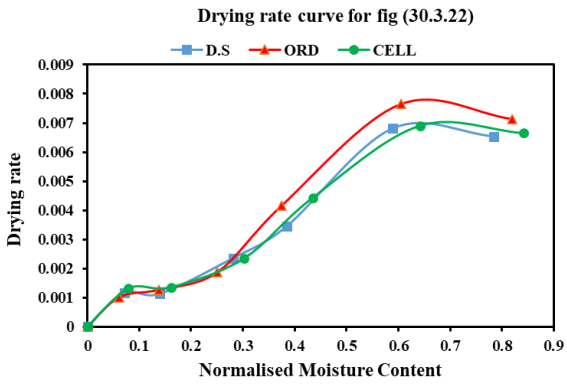

B

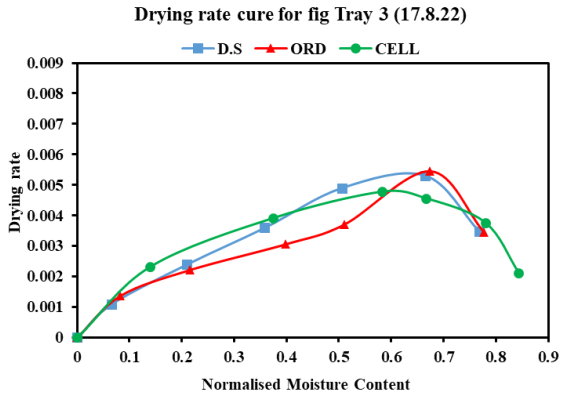

C

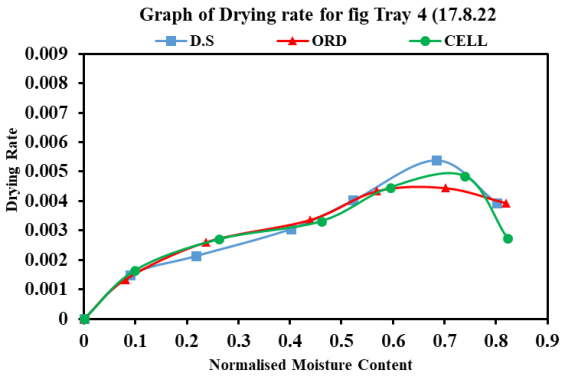

D

Figure 4.4 Fig A shows the drying rate curve for fresh fig. Fig B shows the drying rate of figs after 2 weeks in the refrigerator. Fig C shows the drying rate of drying for figs dried in August at the bottom of the dryer while Fig D shows the figs dried at the top of the dryer.

This observation we reported is in agreement with previous work that mentioned that at higher temperatures the drying rate would increase (Şahin and Öztürk, 2018). Besides the higher temperature (around 65^0C) on the roof, we obtained the highest heat loss due to the wind speed around the solar dryer. When the drying was done with the cellular polycarbonate dryer made from (copper chalcogenide sulphide/selenide: Abs=0.41, Trans=0.40, Ref=0.19) thin films as can be seen from the graph, the energy from the solar radiation was mostly absorbed on the roof. Therefore, a lower amount of energy was able to penetrate the cellular dryer. While higher energy efficiently passed through the ORD dryer when compared to the absorbance in the ordinary polycarbonate (Abs= 0.1, Trans=0.83, Ref=0.07) (Nair et al., 2020). Therefore, the drying rate was a bit faster when using the ordinary polycarbonate dryer for drying, because major energy resides directly on the food surface. The efficiency of the convective heat transfer rate was also a possible reason for the temperature discrepancies between the top and bottom of the trays. Also, the optical properties as reported by Nair et al. were responsible for the rising temperature in the drying medium in the different trays (Nair et al., 2020).

Our observations also correspond to the report by Sabet et al. his experiments on the drying kinetics of fig show the variation of dimensionless moisture content with drying time at 40, 50, 60, and 70°C, he stated that the exponential behaviour of drying curves is evident, also reiterating that the drying time decreases by a rising air temperature (Sarvestani et al., 2014).

The effect of wind speed was well noticed when drying under direct sunlight. From the readings we obtained during the drying with the help of the anemometer and also data obtained from the Esolmet, the value we got ranged from 1.0-5.0m/s for the drying performed. These results also facilitated the faster drying of the figs and led to increased weight loss and in turn improved the removal of moisture content from the figs in the tray in the open sun drying. The above information is correct for drying performed in August 2022.

For the second drying, performed on the 30th of March 2022, we obtained also a relatively lower R.H. and a lower wind speed similar to the first drying performed. (5-25%) and (1.0-4.5m/s) this perhaps made the drying under direct solar slower than the ordinary polycarbonate dryer.

4.4 Empirical and semi-empirical modelling

Table 4.1 below shows the mathematical models used by different authors to characterize the kinetic drying process in food. We analyzed 3 different mathematical models (Newton/Lewis, Wang and Singh, and Henderson and Pabis) gave a good fit and thus obtained a model that we can say best suits the drying kinetics of figs.

Table 4.1 Parameters for the fresh fig drying model.

Model	Drying Method	k	a	b
Newton/Lewis	Direct solar	0.00782	-	-
	Ordinary polycarbonate	0.01048	-	-
	Cellular polycarbonate	0.00929	-	-
	Electric oven	0.00763	-	-
Wang and Singh	Direct solar	-	-0.00587	0.00001
	Ordinary polycarbonate	-	-0.00747	0.00001
	Cellular polycarbonate	-	-0.00681	0.00001
	Electric oven	-	-0.0057	0.00001
Henderson and Pabis	Direct solar	0.0086	1.09287	-
	Ordinary polycarbonate	0.01121	1.07007	-
	Cellular polycarbonate	0.01001	1.07337	-
	Electric oven	0.00832	1.08374	-

Table 4.2 Parameters for the 2 weeks fig drying model.

Model	Drying Method	k	a	b
Newton/Lewis	Direct solar	0.01024	-	-
	Ordinary polycarbonate	0.0103	-	-
	Cellular polycarbonate	0.00927	-	-
	Electric oven	0.00929	-	-
Wang and Singh	Direct solar	-	-0.0072	0.00001
	Ordinary polycarbonate	-	-0.00727	0.00001
	Cellular polycarbonate	-	-0.00676	0.00001
	Electric oven	-	-0.00667	0.00001
Henderson and Pabis	Direct solar	0.01061	1.03331	-
	Ordinary polycarbonate	0.01085	1.05054	-
	Cellular polycarbonate	0.00983	1.05592	-
	Electric oven	0.00929	0.99969	-

Table 4.3 The results for the thin layer drying modelling for fresh fig to obtain the line of best fit

Model	Drying Method	R^2	X^2	RMSE
Newton/Lewis	Direct solar	0.96069	0.0058766	0.0722746
	Ordinary polycarbonate	0.96954	0.0044963	0.0632199
	Cellular polycarbonate	0.97253	0.0039902	0.0595554
	Electric oven	0.9642	0.0052389	0.0682411
Wang and Singh	Direct solar	0.9867	0.010981	0.092416
	Ordinary polycarbonate	0.98731	0.048976	0.195172
	Cellular polycarbonate	0.98867	0.009922	0.087846
	Electric oven	0.99229	0.0174999	0.116666
Henderson and Pabis	Direct solar	0.97211	0.004765	0.060876
	Ordinary polycarbonate	0.97534	0.004161	0.056889
	Cellular polycarbonate	0.97928	0.003439	0.05172
	Electric oven	0.97384	0.004375	0.058333

Table 4.4 The results for the thin layer drying modelling for 2 weeks fig to obtain a line of best fit.

Model	Drying Method	R^2	X^2	RMSE
Newton/Lewis	Direct solar	0.99194	0.0010485	0.0305284
	Ordinary polycarbonate	0.9843	0.002139	0.0436046
	Cellular polycarbonate	0.98257	0.00240048	0.04619261
	Electric oven	0.98473	0.00187054	0.04077629
Wang and Singh	Direct solar	0.98526	0.031411	0.156304
	Ordinary polycarbonate	0.98319	0.03628	0.167981
	Cellular polycarbonate	0.99111	0.008255	0.080131
	Electric oven	0.99229	0.00678	0.072616
Henderson and Pabis	Direct solar	0.99341	0.0009805	0.0276155
	Ordinary polycarbonate	0.98754	0.0019412	0.0388559
	Cellular polycarbonate	0.98669	0.0020947	0.0403632
	Electric oven	0.98473	0.0021377	0.040776

Table 4.3 and Table 4.4 shows the model for the kinetics of solar drying for the fresh and 2 weeks dried fig. The above data were fitted to the thin layer models as listed using Number Cruncher Statistical Systems (NCSS) 2020 and the results presented above and in the Appendices. The adequacy of the model's prediction quality was assessed using several key metrics: reduced chi-square ($\chi 2$), root mean square error (RMSE), and coefficient of correlation (R^2). For the present research work, we analyzed 12 models as listed in the literature and the models were fitted to the experimental data. We then observed that only three models which are the Newton/Lewis, Wang and Singh, Henderson and Pabis models were with a varied degree of quality fit, able to fit the experimental data analyzed. We further observed that from the three models that showed some degree of quality fit, Wang and Singh's model best represents the kinetics of the fig drying process because it had a better fit when compared to

other mathematical models. Our conclusions were deduced based on a relatively higher value of R^2 and a low χ^2.

For the Wang and Singh model in the analysis for the fresh dried figs, the R^2 value ranged from 0.987-0.99229 and RSME ranged from 0.088-0.200. The χ^2 value ranged from 0.001-0.049. Furthermore, with the Newton/Lewis model, drying with the cellular polycarbonate had a better fit when compared to the experimental data with an R^2 value of 0.973, RMSE value of 0.060 and χ^2 value of 0.004. Generally, with the Newton/Lewis model for the fresh fig the statistical value for R^2 ranged from 0.961-0.972, χ^2 value ranged from 0.00399-0.00588 and RMSE value ranged from 0.059555-0.07227. For the two weeks of dried figs, the Newton/Lewis model has a value for R^2 range from 0.98257-0.99194, χ^2 value range from 0.00104-0.002401 and RMSE ranged from 0.03052-0.046192. Similarly, for the Henderson and Pabis model, we have the χ^2 value range from 0.00343-0.004765 for the fresh fig and a χ^2 value that ranged from 0.00098-0.002138 for two weeks fig, for the R^2 the values ranged from 0.97211-0.97928 for fresh fig and 0.98473-0.99341 for two weeks dried figs and for the RMSE value, we got values that ranged from 0.027615-0.06088 for both fresh and two weeks dried figs.

The Wang and Singh Model, established in 1978, was designed to facilitate the drying of rough rice grains under specific conditions: temperatures ranging from 30 to 350 degrees Celsius and relative humidity spanning 25% to 95%. This model is particularly tailored for thin layers of grain (Ozdemir and Devres, 2000). The Wang and Singh model is of the form $MR = M_0 + at + bt^2$ or $MR = 1 + at + bt^2$

(Babalis et al., 2006) observed that the two-term exponential model demonstrated the best performance in fitting the experimental data, when they fitted several mathematical thin-layer drying models, to experimental data obtained when figs were mechanically dried in the range of mean air temperatures of 55–85 ^{0}C and air velocity values from 0.5 m/s to 3 m/s in an experimental mechanical dryer.

(Xanthopoulos et al., 2010) reported that the Logarithmic model was the best-fitted model for the unpeeled figs, while for the peeled figs the best-fitted model was the Modified Henderson & Pabis model, they further reported that the discrepancy with the Logarithmic model was less than 3% of RMSE.

4.5 Discussions on Anthocyanin

The analysis of the anthocyanin composition of the dried Mexican fig was characterized by the UV-Vis spectroscopy approach, the TA content was measured as per the association of official analytical chemists (AOAC) method using the pH differential method at two different visible range wavelengths (510nm and 700nm). This method has been used by previous researchers for the determination of total monomeric anthocyanin content, based on the structural change of the anthocyanin chromophore between pH 1.0 and 4.5 (Eisele et al., 2005). In the experiment, two buffer solutions were utilized: potassium chloride at a concentration of 0.025 M with a pH of 1.0, and sodium acetate at a concentration of 0.04 M with a pH of 4.5.

The Anthocyanin content was determined using the method described by Wrolstad, where the variations in absorbances were employed to calculate the content (Eisele et al., 2005).

4.6 Kinetics of Anthocyanin

The kinetics of Anthocyanin for Mexican figs for freshly purchased figs and figs stored in the refrigerator for 2 weeks at 10°C then both sliced longitudinally and dried using the direct solar, cellular polycarbonate, ordinary polycarbonate and electric oven are shown in Figure 4.5 below. Each drying test for this experiment was carried out for about 360 min.

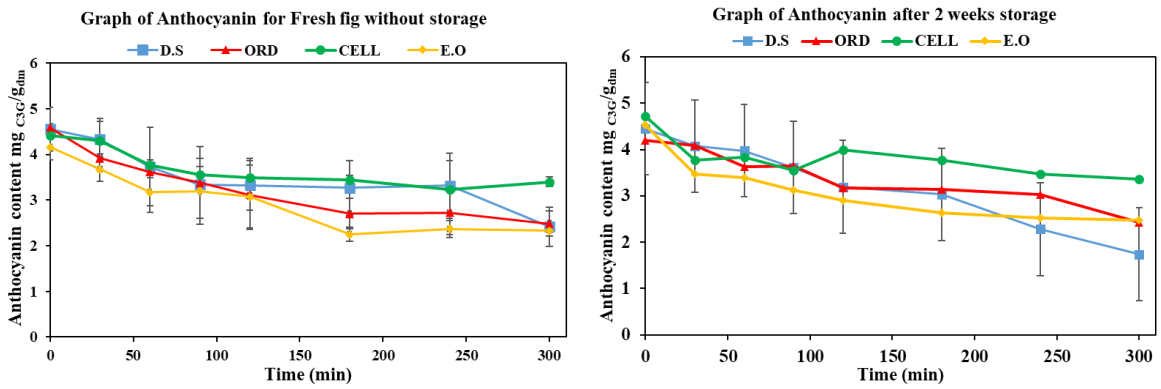

A *B*

Figure 4.5 Kinetics of Total anthocyanin content dried with (Direct solar, Ordinary polycarbonate, Cellular polycarbonate, and Electric oven)Fig A shows the Total anthocyanin content for fresh figs without storage while Fig B shows the Kinetics of Total anthocyanin content for figs stored in the refrigerator for 2 weeks

Anthocyanin generally contributes to the colour appearance of most fruits and vegetables, and they have a wide range of health-related benefits. They also tend to be unstable and quickly degrade under high thermal treatments (Y. Zhang et al., 2020). It was thus considered

imperative to study and observe the retention ability under some selected drying temperature conditions.

From the results obtained, we found significant differences ($\alpha = 0.5$) in total anthocyanin content due to treatments and the drying time for both experiments conducted. The average anthocyanin content for the figs studied ranged from 4.2 ± 0.05 mg_{C3G}/g_{dm} for fresh figs to about 4.7 ± 0.05 mg_{C3G}/g_{dm} for figs stored in the refrigerator.

There was a slight increase in the anthocyanin content for the figs stored in the refrigerator as shown in Figure 4.5. The increase in the concentration of anthocyanins in the figs stored in the refrigerator for two weeks could be attributed to the increased ripeness of the fruits, which in turn might be due to the anthocyanin biosynthesis that is characterized by the upregulation of phenylpropanoid pathway and chalcone synthase enzyme (CHS). This enzyme is one of the key enzymes regulating the pathway (Belwal et al., 2019; Karaaslan et al., 2015). The ripening process of the figs which is also accompanied by a noticeable colour change increases significantly as the biosynthesis of the anthocyanins increases (Pfannhauser, 2005).

Anah et al. conducted a study that yielded analogous findings. They conducted a comparison of anthocyanin levels and their distribution within ripe and unripe fig fruits. Notably, they observed an overall increase in the total anthocyanin content among all ripe fruits when compared to their unripe counterparts. Among the various fig varieties they examined, the Mission variety exhibited the highest anthocyanin content. Their reported anthocyanin content for this variety was 11.0 mg C3G/gdm, which surpassed our observations. This variation in results could potentially be attributed to differences in the specific fig variety analyzed between their study and ours (Olomon et al., 2006).

From Figure 4.5 it can be observed that during the drying process, there was a slight continuous reduction in the total anthocyanin content for the first 240-300 minutes of drying using the cellular polycarbonate, though the net reduction was minimal as compared to the other drying processes (3.3 mg $_{C3G}/g_{dm}$) this was followed by a significant increase in the TA, we observed from the experiment that the copper chalcogenide (sulfide/selenide) thin films applied by chemical deposition on filtered polycarbonate sheet as proposed by (Nair et al., 2020) was the drying process that retained the highest value of TA. A similar observation was noticed while drying with the ordinary polycarbonate dryer, where continuous reduction in TA was also noticed as the drying progressed, for the drying performed with the help of the electric oven and the drying done with direct solar, we observed the least retained value of TA.

Figure 4.5 shows the kinetics of TA after two weeks of storage in the refrigerator at 10°C. We report a slightly different observation though similar to the fresh fig, in the dryers with the cellular polycarbonate material there was an initial decrease in the TA within the first 1 hour of drying, this was followed by a significant increase for the next 2 hours, a slow and steady decrease in the TA was then observed till the drying was completed. (3.4 mg $_{C3G}/g_{dm}$). When the drying was conducted with the help of the ordinary polycarbonate, we observed a reduction in the TA for the first 2 hours (4.2-3.6 mg $_{C3G}/g_{dm}$) followed by a slight increase (3.62-3.65 mg $_{C3G}/g_{dm}$), for the next 2 hours, for the final drying duration the TA steadily decreased till it attained a value of (2.43 mg $_{C3G}/g_{dm}$) the drying performed with the aid of the cellular or filtered polycarbonate was able to retain more TA for the two experiments performed. We observed that the drying done in the electric oven and under the direct solar has the lowest anthocyanin after the drying was completed. Naturally, as food dries, less water is present, which can cause an increase in the concentration of anthocyanins and other colours. However, several variables, including the amount and length of sunshine exposure, the ambient temperature and humidity, and the initial concentration of the pigment in the food, might affect how anthocyanins alter during open sun drying. The stability of anthocyanins during drying is a crucial factor to maintain the quality of the dried food product even though they can have positive health effects and contribute to the sensory qualities of food (Belwal et al., 2019; Dueñas et al., 2008; Nassour et al., 2020; Nemzer et al., 2018).

Based on the outcomes of the various drying methods employed in our experiments, a consistent trend was observed. Initially, there was a notable decrease in the total anthocyanin content (TA) during the early stages of the drying process. However, as the drying progressed towards its conclusion, a similar reduction in TA was observed. These observations align with the reports obtained from the study of (Méndez-Lagunas et al., 2017; Rodríguez-Ramírez et al., 2021). where they analyzed the convective drying kinetics of strawberries and agree with our findings for this observation.

4.7 Collaborative reports on Anthocyanin

The reduction in the TA could be attributed to an increase in the drying temperature, from our experiments there was a steady increase in the temperature at the beginning of drying, as can be seen from Figure 4.2 the increase in the drying temperature was consistent with 3 different drying methods, perhaps the increased solar radiation was responsible for this. From Figure 4.1 also, the kinetics of drying as shown below collaborates with the fact that there is a direct

relationship between solar radiation intensity, drying temperature, moisture loss and anthocyanins content, as we can also observe a rapid decrease in moisture content and sample weight. Some other factors like UV light, incandescent light and IR light can also contribute to the degradation of anthocyanins (Ortiz et al., 2021).

A study performed on the thermal and light degradation kinetics of anthocyanin extract from mangos teen peel shows that there was a reduction in the TA at a very fast rate. This reduction in the TA was caused by the luminosity emitted by infrared light, this enabled the TA degradation rate to be high during the storage time, then followed by ultraviolet light, incandescent, and fluorescent light (Renan, 2010).

The kinetics of anthocyanins as observed from Figure 4.5, showed that the fresh figs dried with the cellular polycarbonate had the TA increase at some point within the drying and at the final stages of drying, this behaviour was also noticed when drying with the solid polycarbonate material, we could attribute this behaviour to some possible reasons; this might be due to the temperature of processing of the anthocyanin (Zhang et al., 2019). The increase could also signify that there is a partial incidence of UV radiation in the food during drying, this could increase the retention of anthocyanins during the drying (Kataoka et al., 2003; López-Ortiz et al., 2021, 2020).

Various researchers have studied the effect of UV light on the concentration of anthocyanin in some fruits using drying covers that possess some anti-UV properties, the report of Kataoka collaborates with our observation, he reported that cover material for drying had a significant influence on the concentration of anthocyanin. According to the findings outlined in his reports, a noteworthy observation was the considerable decline in the anthocyanin concentration when using covering materials that hindered the penetration of UV light. Conversely, when a cover material permitting UV light penetration in the UV-A region (320–400 nm) was utilized, a substantial elevation in anthocyanin concentration was favourably observed (Kataoka et al., 2003). Generally, there had been many reports by researchers that validated the claim about the effect of ultraviolet light in increasing the anthocyanin concentration (Kataoka et al., 2003; Rodríguez-Ramírez et al., 2021).

4.8 Measurement of Colour Kinetics

Figure *4.6* and Figure *4.7* below illustrate the colour changes for the selected fig samples for drying. The graph shows the CILAB colour parameters for the fig, in its fresh form and after

drying with different conditions and methods. The colour analysis was also performed for figs stored in the refrigerator for 2 weeks. From our experiments, we could conclude that the drying methods used (D.S, ORD, CELL, E.O), and the interaction between them had significant effects ($p \leq 0.05$) on the colour characteristics analyzed for figs. The initial values for the L*, a* and b* coordinates of the fresh fig were 62.3, 19.05 and 22.23 respectively. Subsequently, as the drying progressed there was a gradual reduction in the value of the L* lightness ratio for all the drying methods, this reduction was more pronounced with drying performed in the direct solar. This reduction observed with the direct solar drying could be a result of the direct exposure of the fig to sunlight and thus the reason for the darker appearance, as also reported by (T. et al., 2019). There is also a relationship between the moisture loss and the lightness ratio: Food loses moisture as it dries, which can lead to a buildup of pigments and other substances that reduces the lightness and change the colour of the fig while drying. The reduction of the L* value was least in the drying done with the ORD and the CELL

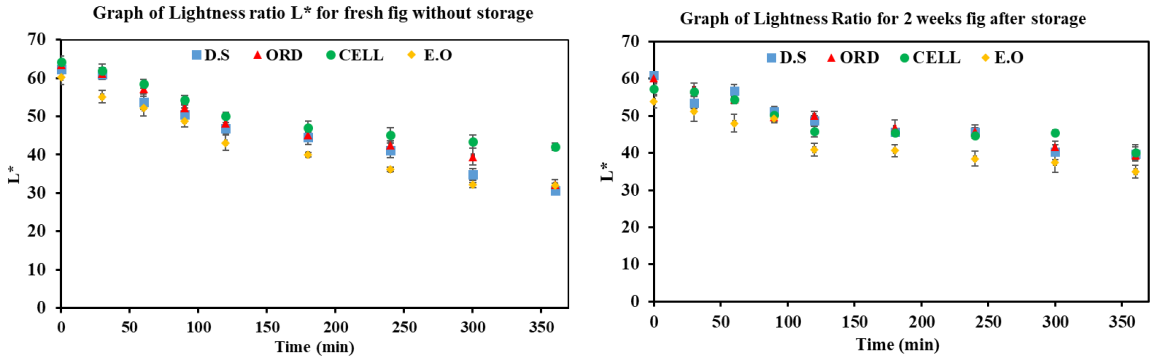

A *B*

Figure 4.6 Kinetics of Lightness ratio for figs dried with (Direct solar, Ordinary polycarbonate, Cellular polycarbonate, Electric oven) Fig A shows the Kinetics of Lightness ratio of fresh figs while Fig B shows the Kinetics of Lightness ratio of figs stored in the refrigerator for 2 weeks.

The report presented by (Maskan, 2001) was consistent with our findings when they studied the colour kinetics of kiwifruits their findings revealed that the colour of kiwifruits was affected regardless of the drying method they used. They reported that the L* value decreased with drying time for all drying methods, the falling value of L* they observed indicated that their samples were turning darker as it is a measure of the light-dark axis. The loss of the L* value from our study was characterized by the darker colour of the fig as the drying progressed, this phenomenon was reported by the research of various authors (Maskan, 2006, 2001; Soysal et al., 2009; Suh et al., 2003). The reason for this loss of L* value could be due to the

decomposition of colour pigments and the enzymatic browning effect (Ávila and Silva, 1999; Falguera et al., 2011; Guiné and Barroca, 2012; Soysal et al., 2009; T. et al., 2019). The L* value for the drying done in the electric oven for both the fresh and 2 weeks figs also showed a gradual and steady reduction in the L* value perhaps because it was not exposed to direct sunlight, and it had a steady operating temperature of about 50^0C. We report a similar observation for all colour parameters for the figs stored in the refrigerator for two weeks the initial L*, a* and b* values were (60.4, 18.04, and 21.43), these slight differences might be due to the length of time it was kept in the refrigerator.

From Figure *4.7* we observed a ΔE value that increased for all drying methods and the increase was more noticeable when drying was done with direct sunlight. This same phenomenon was reported by (T. et al., 2019). when they performed the colour kinetics of dates. From Figure *4.7* below we notice that the ΔE at the beginning and end of the drying was (5.7 and 33.3) D.S and (3.8 and 20.7) for CELL. The colour change for the drying performed in the E.O. and the polycarbonate were not so pronounced as the ones recorded in the direct solar drying invariably had a lower colour variation, this could be explained by the absence of direct solar radiation.

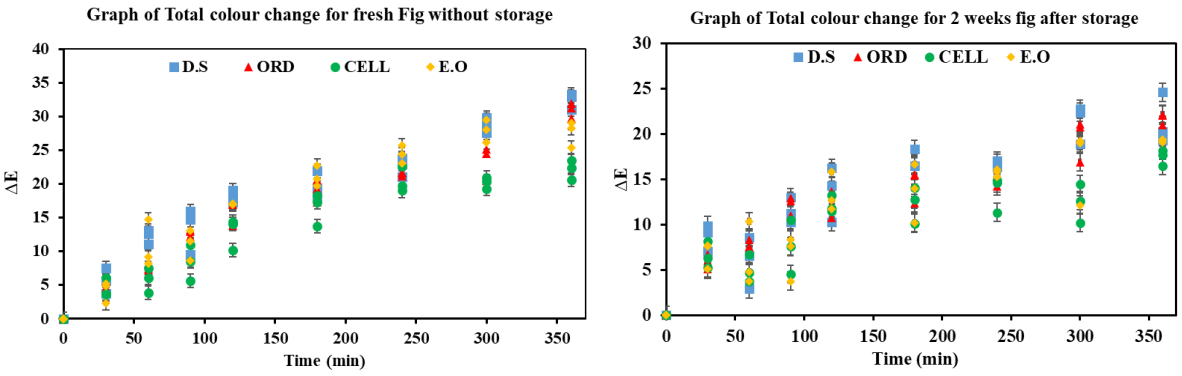

A *B*

Figure 4.7 Kinetics of Total colour change of figs dried with (Direct solar, Ordinary polycarbonate, Cellular polycarbonate, Electric oven) Fig A shows the Kinetics of Total colour change for fresh figs while Fig B shows the Kinetics of Total colour change for figs stored in the refrigerator for 2 weeks.

The total colour difference or change ΔE, is a combination of the L*, a* and b* values, as stated in equation 3.10, it is a colourimetric parameter which is extensively used in the characterization of the colour variation in agricultural foods during processing (Guiné and Barroca, 2012).

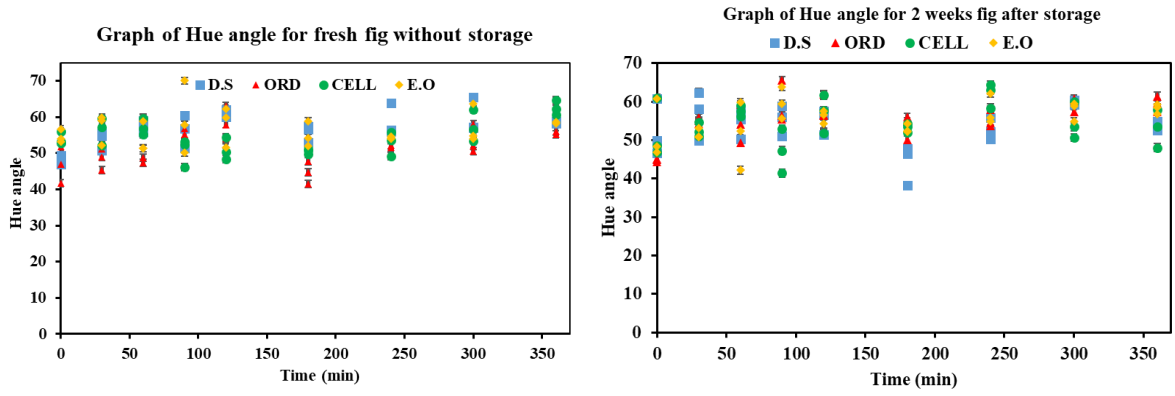

A *B*

Figure 4.8 Kinetics of Hue angle for figs dried with (Direct solar, Ordinary polycarbonate, Cellular polycarbonate, Electric oven) Fig A shows the Kinetics of Hue angle for fresh figs while Fig B shows the Kinetics of Hue angle for figs stored for 2 weeks in the refrigerator

The hue angle (Ho) describes the relative amounts of redness and yellowness of a sample. As is observed from Figure *4.8*, the hue angle values increased slowly with an initial value at the beginning of the drying from 49.4 degrees to about 58.1 degrees at the end of the drying when the drying was performed under direct sunlight. Chemical modifications are a possible reason for the changes in the hue angle. The pigments that give food its colour can undergo chemical modifications because of exposure to heat and sunshine during the fig drying, which may result in a change in hue angle. For instance, when drying of the figs was done, anthocyanins, which give figs their red colour, might disintegrate into other compounds, changing the hue angle. The hue angle chart shown in Figure 3.14 above, shows after drying the colour of the fig where in between red and yellow. The dried samples from other drying methods used each had a relative increase in the hue angle.

Our results were consistent with the report of (Sharifian et al., 2013) where they analyzed the colour Change of fig fruit using microwave drying. They reported that the hue angle values increased slowly with microwave power intensity. The values they obtained ranged from 1.21 radians at 0.5 W/g MW power intensity to 1.32 radians at 2.5 W/g MW power intensity. Our observation also collaborates with the results from other researchers (Kortei and Sciences, 2015; Yemis, 2012).

For the a* colour parameter indicates the redness or greenness of a sample while the b* colour parameter measures the yellowness or blueness of a product. Generally, the b* values tend to increase with an increase in solar intensity likewise a* value. The differences in our drying conditions contributed to differences in a* values we obtained. The colour of the fig we dried

was affected by a variety of drying conditions, which includes the amount of sunlight, the temperature of drying, and the humidity. Generally, food may turn discoloured or lose its vibrancy if the temperature is too high or the humidity level is too low. We report a relatively slow reduction in the a* value for the drying methods used in this experiment. Our result agrees with those of (Ozkan, 2007). when they dried spinach in the microwave. However, we noticed a slight reduction in the b* values then followed by a relative increase towards the end of drying this might be due to the increase in drying time and an increase in the surface temperature which promotes browning reactions (Sharifian et al., 2013).

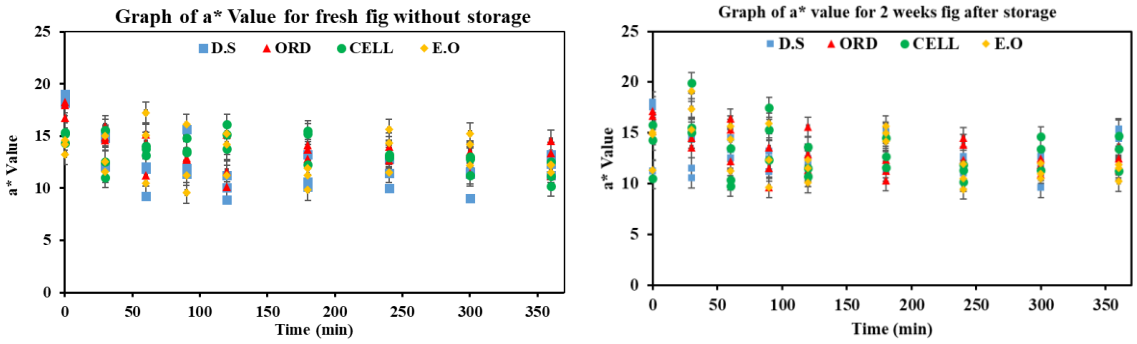

A *B*

Figure 4.9 Kinetics of redness ratio (a*) of figs dried with (Direct solar, Ordinary polycarbonate, Cellular polycarbonate, Electric oven) Fig A shows the Kinetics of redness ratio (a*) of fresh figs dried while Fig B shows the Kinetics of redness ratio (a*) of figs stored in the refrigerator for 2 weeks.

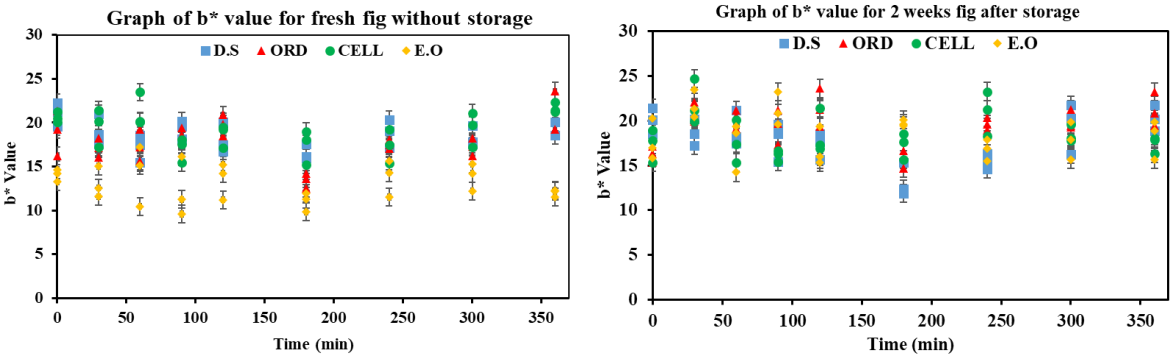

A *B*

Figure 4.10 Kinetics of (b*) value for figs dried with (Direct solar, Ordinary polycarbonate, Cellular polycarbonate, and Electric oven. Fig A shows the Kinetics of the (b*) value for fresh figs dried while Fig B shows the Kinetics of the (b*) value of figs stored in the refrigerator for 2 weeks.

CHAPTER 5

5 CONCLUSIONS AND RECOMMENDATIONS

5.1 Conclusion

Four different drying conditions were analyzed for this present study (Direct solar drying, Ordinary polycarbonate, cellular polycarbonate, and the electric oven). We compared also the different drying conditions for figs stored in the refrigerator for two weeks to minimize the drying time and maximize product quality in terms of colour and anthocyanin content.

Our results show that the anthocyanin content is better retained from the experiments which use the cellular polycarbonate type cabinet dryers than in the ordinary polycarbonate type cabinet dryer, direct solar and electric oven dryers respectively due to the copper chalcogenide (sulphide/selenide) thin films on cellular polycarbonate sheet used in designing the cabinet dryer due to their ability to block some amount of UV radiation. We also observed a slightly higher anthocyanin content when we compared our results from the figs stored in the refrigerator for two weeks.

From the result of this work, the Wang and Singh model can predict the drying moisture ratio of Mexican figs with a high degree of accuracy.

The total colour change ΔE, Lightness ratio L*, Hue angle Redness ratio a* and b* value of solar dried figs at fresh and two weeks were investigated. The cellular polycarbonate type dryer has the highest colour stability from the ΔE point of view. The lightness ratio was also better retained than other drying methods. Similar observations were reported for figs stored in the refrigerator for two weeks. Given the above reasons, we can comfortably conclude that the cellular polycarbonate dryer would be recommended for better drying when considering colour parameters.

The result on drying kinetics showed that high temperature and low relative humidity were the main parameters that reduced the drying time of the figs. The design nature and material for the polycarbonate (ORD) type dryer permitted a smooth heat and air exchange between the surrounding and the cabinet dryer enabling faster drying than direct solar drying and electric oven drying. The design material (CELL) also retains the surrounding heat thereby significantly increasing the temperature on the roof and the heat loss. There were no significant differences between fresh and two weeks figs concerning the drying kinetics.

5.2 Recommendation

Before the decision on a solar *dryer* is *to be* taken, the nature of the food, the climate of the area, and the technical and economic environment in which the dryer will be operated have to be analyzed.

In the present work, the drying was conducted using direct solar drying, an electric oven, and the cabinet-type solar dryer where the relative humidity and air velocity, were relatively low. However, there was no steady temperature while the drying progressed with the cabinet-type dryer, the temperature kept on fluctuating as solar irradiation and relative humidity for that day were not constant. We also need to prevent heat loss from the CELL cabinet dryer by adding a transparent insulating system (transparent materials-air-CELL material).

It is therefore recommended that further research should be conducted in such a way as to introduce a ground-breaking design of the cabinet-type dryer that will ensure a more uniform temperature distribution inside the dryer by performing further simulations on the model for the cabinet-type dryer that can predict the best positions for the air duct for a smoother and more efficient air, heat and mass transfer from the surrounding to the dryer. With the proposed advances in the design, better relative humidity with air velocity, and regulated temperature values could be achieved inside the dryer.

The model derived from this design will not only help to better predict the drying performance but also reduce the drying time and ensure a better quality of the dried figs by way of preserving the colour and retaining some valuable nutritional content in the fig.

It is of significant importance to investigate the shelf life of the dried figs, particularly concerning factors such as pigment degradation and the colour preferences of consumers.

Another point worth mentioning is the effect of varying thicknesses in the slicing of the figs perhaps due to the imperfect nature of man there could be some discrepancies in the sliced figs. We, therefore, recommend that a slicing machine be developed and fabricated for future use in the slicing of figs.

REFERENCES

A.S., M., 1998. Handbook of Industrial Drying. CRC Press, Boca Ratón.

A, J.A., 2010. Water Content and Water Activity_ Two Factors That Affect Food Safety _ Manitoba Agriculture, Food and Rural Development _ Province of Manitoba. Manitoba.

Abdel-Aty, A.M., Hamed, M.B., Salama, W.H., Ali, M.M., Fahmy, A.S., Mohamed, S.A., n.d. Ficus carica, Ficus sycomorus and Euphorbia tirucalli latex extracts: Phytochemical screening, antioxidant and cytotoxic properties. Biocatal. Agric. Biotechnol.

Alexandra Pazmiño-Durán, E., Mónica Giusti, M., Wrolstad, R.E., Glória, M.B.A., 2001. Anthocyanins from Oxalis triangularis as potential food colorants. Food Chem. 75, 211–216.

Ansari, S., Maftoon-Azad, N., Farahnaky, A., Hosseini, E., Badii, F., 2014. Effect of moisture content on textural attributes of dried figs. Int. Agrophysics 28, 403–412. https://doi.org/10.2478/intag-2014-0031

Ávila, I.M.L.B., Silva, C.L.M., 1999. Modelling kinetics of thermal degradation of colour in peach puree. J. Food Eng. 39, 161–166. https://doi.org/10.1016/S0260-8774(98)00157-5

Babalis, S.J., Belessiotis, V.G., 2004. Influence of the drying conditions on the drying constants and moisture diffusivity during the thin-layer drying of figs 65, 449–458. https://doi.org/10.1016/j.jfoodeng.2004.02.005

Babalis, S.J., Papanicolaou, E., Kyriakis, N., Belessiotis, V.G., 2006. Evaluation of thin-layer drying models for describing drying kinetics of figs (Ficus carica) 75, 205–214. https://doi.org/10.1016/j.jfoodeng.2005.04.008

Badgujar, S.B., Patel, V. V., Bandivdekar, A.H., Mahajan, R.T., 2014a. Traditional uses, phytochemistry and pharmacology of Ficus carica: A review. Pharm. Biol. 52, 1487–1503. https://doi.org/10.3109/13880209.2014.892515

Badgujar, S.B., Patel, V. V., Bandivdekar, A.H., Mahajan, R.T., 2014b. Traditional uses, phytochemistry and pharmacology of Ficus carica: A review. Pharm. Biol. 52, 1487–1503. https://doi.org/10.3109/13880209.2014.892515

Barolo, M.I., Ruiz Mostacero, N., López, S.N., 2014. Ficus carica L. (Moraceae): An ancient source of food and health. Food Chem. 164, 119–127.

https://doi.org/10.1016/J.FOODCHEM.2014.04.112

Barrett, D.M., Beaulieu, J.C., Shewfelt, R., 2010. Color, flavor, texture, and nutritional quality of fresh-cut fruits and vegetables: Desirable levels, instrumental and sensory measurement, and the effects of processing. Crit. Rev. Food Sci. Nutr. 50, 369–389. https://doi.org/10.1080/10408391003626322

Barroca, G. and, 2012. Effect of drying treatments on texture and color of vegetables (pumpkin and green pepper) 3–10. https://doi.org/10.1016/j.fbp.2011.01.003

Belwal, T., Pandey, A., Bhatt, I.D., Rawal, R.S., Luo, Z., 2019. Trends of polyphenolics and anthocyanins accumulation along ripening stages of wild edible fruits of Indian Himalayan region. Sci. Rep. 1–11. https://doi.org/10.1038/s41598-019-42270-2

Bonghi, C., Serrano, M., Lomolino, G., Inglese, P., Allegra, A., Gallotta, A., Carimi, F., Mercati, F., Martinelli, F., 2018. Metabolic Profiling and Post-harvest Behavior of "Dottato" Fig (Ficus carica L.) Fruit Covered With an Edible Coating From O. ficus-indica. https://doi.org/10.3389/fpls.2018.01321

Borah, A., Hazarika, K., Khayer, S.M., 2015. Drying kinetics of whole and sliced turmeric rhizomes (Curcuma longa L.) in a solar conduction dryer. Inf. Process. Agric. 2, 85–92. https://doi.org/https://doi.org/10.1016/j.inpa.2015.06.002

Boulton, R., 2001. The Copigmentation of Anthocyanins and Its Role in the Color of Red Wine : A Critical Review 2, 67–87.

Bouzo, C.A., Travadelo, M., Gariglio, N.F., 2012. Effect of different packaging materials on postharvest quality of fresh fig fruit. Int. J. Agric. Biol. 14, 821–825.

Brand-Williams, W., Cuvelier, M.E., Berset, C., 1995. Use of a free radical method to evaluate antioxidant activity. LWT - Food Sci. Technol. 28, 25–30. https://doi.org/https://doi.org/10.1016/S0023-6438(95)80008-5

Britannica, T.E. of E., 2023. Fig [WWW Document]. URL https://www.britannica.com/plant/fig (accessed 8.6.23).

Castañeda-Ovando, A., Pacheco-Hernández, M. de L., Páez-Hernández, M.E., Rodríguez, J.A., Galán-Vidal, C.A., 2009. Chemical studies of anthocyanins: A review. Food Chem. 113, 859–871. https://doi.org/10.1016/j.foodchem.2008.09.001

Chen, X., Gao, Q., Liao, S., Zou, Y., Yan, J., Li, Q., 2022. Co-Pigmentation Mechanism and Thermal Reaction Kinetics of Mulberry Anthocyanins with Different Phenolic Acids.

Condit, I.J., 1955. Fig varieties: a monograph. Hilgardia 23, 323–538. https://doi.org/10.3733/HILG.V23N11P323

Congress, A.E., Engineering, C., 2007. Session T5-K : Theme-5 Keynote Lectures 16–20.

Coradi, P.C., Melo, E.D.C., 2014. Mathematical modeling of the drying kinetics of the leaves of lemon grass (Cymbopogon citratus Stapf) and its effects on quality 43–56.

Da-Costa-Rocha, I., Bonnlaender, B., Sievers, H., Pischel, I., Heinrich, M., 2014. Hibiscus sabdariffa L. - a phytochemical and pharmacological review. Food Chem. 165, 424–443. https://doi.org/10.1016/j.foodchem.2014.05.002

Dangles, O., Brouillard, R., 1992. Spectroscopic Method Based on the Anthocyanin Copigmentation Interaction and Applied to the Quantitative Study of Molecular Complexes.

Daud, L.E.I., Simate, I.N., 2017. Drying Kinetics of Sliced Pineapples in a Solar Conduction Dryer 7, 14–26. https://doi.org/10.5539/eer.v7n2p14

David G. Frodin, 1394. History and concepts of the big plant genera. Taxon 53, 753–776.

DINCER, I., 1998. Moisture Loss from Wood Products During Drying—Part I: Moisture Diffusivities and Moisture Transfer Coefficients. Energy Sources 20, 67–75. https://doi.org/10.1080/00908319808970044

Dueñas, M., Pérez-Alonso, J.J., Santos-Buelga, C., Escribano-Bailón, T., 2008. Anthocyanin composition in fig (Ficus carica L.). J. Food Compos. Anal. 21, 107–115. https://doi.org/10.1016/j.jfca.2007.09.002

Eisele, T., Giusti, M.M., Hofsommer, H., Koswig, S., Krueger, D.A., Kupina, S., Martin, S.K., Martinsen, B.K., Miller, T.C., Paquette, F., Ryabkova, A., Skrede, G., Trenn, U., Wightman, J.D., 2005. Determination of Total Monomeric Anthocyanin Pigment Content of Fruit Juices, Beverages, Natural Colorants, and Wines by the pH Differential Method: Collaborative Study 1269–1278.

El-Sebaii, A.A., Shalaby, S., 2012. Solar drying of agricultural products: A review. Renew. Sustain. Energy Rev. - RENEW Sustain ENERGY REV 16.

https://doi.org/10.1016/j.rser.2011.07.134

Ertan, B., Şenkayas, H., Tuncay, Ö., 2019. Postharvest logistics performance of fresh fig varieties in Turkey. Sci. Hortic. (Amsterdam). 257, 108769. https://doi.org/10.1016/J.SCIENTA.2019.108769

Falguera, V., Quintero, J.P., Jiménez, A., Muñoz, J.A., Ibarz, A., 2011. Edible films and coatings: Structures, active functions and trends in their use. Trends Food Sci. Technol. 22, 292–303. https://doi.org/10.1016/J.TIFS.2011.02.004

Femenia, A., 2016. Improvement of the Quality and the Shelf Life of Figs (Ficus carica) Using an Alginate – Chitosan Edible Film. Food Bioprocess Technol. https://doi.org/10.1007/s11947-016-1796-9

Fernando, J.A.K.M., Amarasinghe, A.D.U.S., 2016. Drying kinetics and mathematical modeling of hot air drying of coconut coir pith. Springerplus 5, 807. https://doi.org/10.1186/s40064-016-2387-y

Fig Produce, S.P., 2022. Adriatic fig Information [WWW Document]. URL https://specialtyproduce.com/produce/Adriatic_Figs_5272.php (accessed 12.19.22).

Filippone, P.T., 2019. The History of Figs [WWW Document].

Giusti, M.M., Wrolstad, R.E., 2003. Acylated anthocyanins from edible sources and their applications in food systems 14, 217–225. https://doi.org/10.1016/S1369-703X(02)00221-8

Gr, D.E., Mori-mestanza, D., Muñ, L.D., Cayo-colca, I.S., 2021. Kinetics Drying of Blackberry Bagasse and Degradation of Anthocyanins and Bioactive Properties 1–12.

Guiné, R., Barroca, M., 2012. Effect of drying treatments on texture and color of vegetables (pumpkin and green pepper). Food Bioprod. Process. - FOOD BIOPROD Process 90. https://doi.org/10.1016/j.fbp.2011.01.003

Guiné, R., Barroca, M., 2011. Influence of freeze-drying treatment on the texture of mushrooms and onions. J. Food Sci. Technol 3, 26–31.

Hemmer, W., Focke, M., Marzban, G., Swoboda, I., Jarisch, R., Laimer, M., 2010. Identification of Bet v 1-related allergens in fig and other Moraceae fruits. Clin. Exp. Allergy 40, 679–687. https://doi.org/10.1111/J.1365-2222.2010.03486.X

Henderson, S.M., 1974. Progress in Developing the Thin Layer Drying Equation 1–3.

Heng, Y.O.Z., Ang, C.H.Y.W., Ang, S.H.Y.W., Heng, W.E.I.Z., 2003. Effect of High-Oxygen Atmospheres on Blueberry Phenolics , Anthocyanins , and Antioxidant Capacity 7162–7169.

Hssaini, L., Charafi, J., Razouk, R., Hernández, F., Fauconnier, M., Ennahli, S., Hanine, H., 2020a. Assessment of Morphological Traits and Fruit Metabolites in Eleven Fig Varieties (Ficus Carica L.). Int. J. Fruit Sci. 20, 8–28. https://doi.org/10.1080/15538362.2019.1701615

Hssaini, L., Charafi, J., Razouk, R., Hernández, F., Fauconnier, M., Ennahli, S., Hanine, H., 2020b. Assessment of Morphological Traits and Fruit Metabolites in Eleven Fig Varieties (Ficus Carica L.). Int. J. Fruit Sci. 20, 8–28. https://doi.org/10.1080/15538362.2019.1701615

Huarte, E., Juániz, I., Cid, C., de Peña, M.-P., 2021. Impact of blanching and frying heating rate/time on the antioxidant capacity and (poly)phenols of cardoon stalks (Cynara cardunculus L. var. altilis DC). Int. J. Gastron. Food Sci. 26, 100415. https://doi.org/https://doi.org/10.1016/j.ijgfs.2021.100415

Huyskens-keil, S., Eichholz-dündar, I., Hassenberg, K., Herppich, W.B., 2020. Postharvest Biology and Technology Impact of light quality (white , red , blue light and UV-C irradiation) on changes in anthocyanin content and dynamics of PAL and POD activities in apical and basal spear sections of white asparagus after harvest. Postharvest Biol. Technol. 161, 111069. https://doi.org/10.1016/j.postharvbio.2019.111069

Ikrang, E.G., 2014. Development of a Model for Thin Layer Solar Drying of Salted Fish Fillets. PhD Thesis, in: Department of Agricultural and Bioresources Engineering, University of Nigeria, Nsukka.

Informa, F., Number, W.R., House, M., Street, M., 2006. Preparative Biochemistry and Biotechnology Some Biochemical Properties of Polyphenol Oxidase from Celery 37–41. https://doi.org/10.1081/PB-200031054

International Commission on Illumination - Wikipedia [WWW Document], n.d. URL https://en.wikipedia.org/wiki/International_Commission_on_Illumination (accessed 6.26.22).

Inyang, U.E., Oboh, I.O., Etuk, B.R., 2018. Kinetic Models for Drying Techniques—Food Materials. Adv. Chem. Eng. Sci. 08, 27–48. https://doi.org/10.4236/aces.2018.82003

Jabeen, R., Aijaz, T., Gul, K., 2015. Drying kinetics of potato using a self-designed cabinet dryer. Cogent Food Agric. 1, 1036485. https://doi.org/10.1080/23311932.2015.1036485

Jackma, R.L., 1987. Anthocyanins as food colorants 201–247.

Jenshi, J., Saravanakumar, M., Aravindhan, K.M., Suganya, P., 2011. The effect of light , temperature , pH on stability of anthocyanin pigments in Musa acuminata bract. Res. plant Biol. 1, 5–12.

Jiang, T., Mao, Y., Sui, L., Yang, N., Li, S., Zhu, Z., Wang, C., Yin, S., He, J., He, Y., 2018. Beijing Engineering and Technology Research Center of Food Additives , Beijing Beijing Laboratory for Food Quality and Safety , Beijing Technology and Business. https://doi.org/10.1016/j.foodchem.2018.07.141

Jing, L., Zhang, Y.M., Luo, J.G., Kong, L.Y., 2015. Tirucallane-Type triterpenoids from the fruit of Ficus carica and their cytotoxic activity. Chem. Pharm. Bull. 63, 237–243. https://doi.org/10.1248/cpb.c14-00779

Kan, V., Vargo, E., Machover, N., Ishii, H., Pan, S., Chen, W., Kakehi, Y., 2016. Organic Primitives: Synthesis and Design of pH-Reactive Materials using Molecular I/O for Sensing, Actuation, and Interaction.

Kang, H.J., Ko, M.J., Chung, M.S., 2021. Anthocyanin structure and ph dependent extraction characteristics from blueberries (Vaccinium corymbosum) and chokeberries (aronia melanocarpa) in subcritical water state. Foods 10. https://doi.org/10.3390/foods10030527

Karaaslan, M., Mehmet, F., Asliye, Y., Hasan, K., 2015. Synthesis and accumulation of anthocyanins in sour cherries during ripening in accordance with antioxidant capacity development and chalcone synthase expression. Eur. Food Res. Technol. https://doi.org/10.1007/s00217-015-2530-y

Karathanos, V.T., 1999. Determination of water content of dried fruits by drying kinetics. J. Food Eng. 39, 337–344. https://doi.org/https://doi.org/10.1016/S0260-8774(98)00132-0

Kataoka, I., Sugiyama, A., Beppu, K., 2003. Role of Ultraviolet Radiation in Accumulation of Anthocyanin in Berries of “Gros Colman” Grapes (Vitis vinifera L.). J. Japanese Soc.

Hortic. Sci. 72, 1–6. https://doi.org/10.2503/jjshs.72.1

Kemp, I.C., Smithkline, G., 2011. Drying Models , Myths , and Misconceptions 1057–1066. https://doi.org/10.1002/ceat.201100061

Khoo, H.E., 2017. Anthocyanidins and anthocyanins : colored pigments as food , pharmaceutical ingredients , and the potential health benefits. Food Nutr. Res. 61. https://doi.org/10.1080/16546628.2017.1361779

Kim, S., Back, H., Oh, M., Rk, S.P., Meihua, J., Jeon, J., Kim, M., Kim, J., Shin, S., Chae, M., Chae, H., Chae, S., 2010. Effect of Ficus carica on Functional Constipation. FASEB J. 24. https://doi.org/10.1096/FASEBJ.24.1_SUPPLEMENT.LB348

Kortei, N., Odamtten, G., Mary, O., Appiah, V., Akonor, P., 2015. CROATIAN JOURNAL OF FOOD TECHNOLOGY, BIOTECHNOLOGY AND NUTRITION Determination of color parameters of gamma irradiated fresh and dried mushrooms during storage. Croat. J. Food Technol. Biotechnol. Nutr. 10, 66–71.

Kortei, N.K., Akonor, P.T., 2015. CORRELATION BETWEEN HUE-ANGLE AND COLOUR LIGHTNESS OF GAMMA CORRELATION BETWEEN HUE-ANGLE AND COLOUR LIGHTNESS OF GAMMA textural and sensory properties . Fresh al ., (2008) to store between 1-3 days at ambient. Ann. Food Sci. Technol. 16, 98–103.

Kortei, N.K., Sciences, A., 2015. CORRELATION BETWEEN HUE-ANGLE AND COLOUR LIGHTNESS OF GAMMA CORRELATION BETWEEN HUE-ANGLE AND COLOUR LIGHTNESS OF GAMMA textural and sensory properties . Fresh al ., (2008) to store between 1-3 days at ambient.

Leeratanarak, N., Devahastin, S., Chiewchan, N., 2006. Drying kinetics and quality of potato chips undergoing different drying techniques. J. Food Eng. 77, 635–643. https://doi.org/10.1016/j.jfoodeng.2005.07.022

López-Ortiz, A., Ituna-Yudonago, F., Gallardo-Brígido, J.C., Román-Roldán, N.I., Rodríguez-Ramírez, J., Martynenko, A., 2023. Energy analysis of drying basil (Ocimum basilicum) leaves in an active greenhouse solar dryer. J. Food Process Eng. 1–14. https://doi.org/10.1111/jfpe.14257

López-Ortiz, A., Méndez-Lagunas, L.L., Delesma, C., Longoria, A., Escobar, J., Muñiz, J., 2020. Understanding the drying kinetics of phenolic compounds in strawberries: An

experimental and density functional theory study. Innov. Food Sci. Emerg. Technol. 60, 102283. https://doi.org/10.1016/j.ifset.2019.102283

López-Ortiz, A., Silva Norman, A., García Valladares, O., 2021. Bioactive compounds conservation and energy-mass analysis in the solar greenhouse drying of blackberry pulps. Heat Mass Transf. und Stoffuebertragung 57, 1347–1361. https://doi.org/10.1007/s00231-021-03039-4

Lourdes, M. De, Abraham, J., Cortez, T., Duch, E.S., Lizama, A.P., Hernán, C., Méndez, H., 2013. Extraction and Stability of Anthocyanins Present in the Skin of the Dragon Fruit (Hylocereus undatus) 2013, 1221–1228.

Martynenko, A., 2018. Highlights. Food Bioprod. Process. https://doi.org/10.1016/j.fbp.2018.06.005

Maskan, M., 2006. Production of pomegranate (Punica granatum L.) juice concentrate by various heating methods: Colour degradation and kinetics. J. Food Eng. - J FOOD ENG 72, 218–224. https://doi.org/10.1016/j.jfoodeng.2004.11.012

Maskan, M., 2001. Kinetics of colour change of kiwifruits during hot air and microwave drying. J. Food Eng. 48, 169–175. https://doi.org/https://doi.org/10.1016/S0260-8774(00)00154-0

Mattioli, R., Francioso, A., Mosca, L., Silva, P., 2020. Anthocyanins: A Comprehensive Review of Their Chemical Properties and Health Effects on Cardiovascular and Neurodegenerative Diseases. Molecules 25. https://doi.org/10.3390/molecules25173809

Mawa, S., Husain, K., Jantan, I., 2013. Ficus carica L. (Moraceae): Phytochemistry, traditional uses and biological activities. Evidence-based Complement. Altern. Med. 2013. https://doi.org/10.1155/2013/974256

Méndez-Lagunas, L., Rodríguez-Ramírez, J., Cruz-Gracida, M., Sandoval-Torres, S., Barriada-Bernal, G., 2017. Convective drying kinetics of strawberry (Fragaria ananassa): Effects on antioxidant activity, anthocyanins and total phenolic content. Food Chem. 230, 174–181. https://doi.org/10.1016/J.FOODCHEM.2017.03.010

Miho Hatanaka, J.C., 2019. Figs: Benefits, side effects, and nutrition [WWW Document]. Med. News Today. URL https://www.medicalnewstoday.com/articles/327207 (accessed 2.1.22).

Nair, P.K., Espinosa-santana, A.L., Guerrero-martínez, L., López-ortiz, A., Nair, M.T.S., 2020. Prospects toward UV-blue filtered solar drying of agricultural farm produce using chemically deposited copper chalcogenide thin films on cellular polycarbonate. Sol. Energy 203, 123–135. https://doi.org/10.1016/j.solener.2020.04.012

Nassour, R., Ayash, A., Al-tameemi, K., 2020. Anthocyanin pigments : Structure and biological importance Anthocyanin pigments : Structure and biological importance.

Nawaz, H., Waheed, R., Nawaz, M., 2019. Phytochemical Composition, Antioxidant Potential, and Medicinal Significance of Ficus, in: Kahramanoglu, I., Kafkas, N.E., Küden, A., Çömlekçioğlu, S. (Eds.), Modern Fruit Industry. IntechOpen, Rijeka. https://doi.org/10.5772/intechopen.86562

Nemzer, B., Vargas, L., Xia, X., Sintara, M., Feng, H., 2018. Phytochemical and physical properties of blueberries, tart cherries, strawberries, and cranberries as affected by different drying methods. Food Chem. 262, 242–250. https://doi.org/10.1016/J.FOODCHEM.2018.04.047

Norhadi, N., Akhir, A.M., Rosli, N.R., Mulana, F., Kuala, U.S., Aceh, B., 2020. Drying kinetics of mango fruit using tray and oven dryer 3, 51–59.

Nunes, M.C.N., Brecht, J.K., Morais, A.M.M.B., Sargent, S.A., 2005. Possible influences of water loss and polyphenol oxidase activity on anthocyanin content and discoloration in fresh ripe strawberry (cv. Oso Grande) during storage of 1 degree C. J. Food Sci.

Olomon, A.N.A.T.S., Olubowicz, S.A.R.A.G., Ablowicz, Z.E.E.V.Y., Rossman, S.H.G., Ergman, M.A.B., Ottlieb, H.U.G.O.E.G., Ltman, A.R.I.E.A., Erem, Z.O.K., Laishman, M.O.A.F., 2006. Antioxidant Activities and Anthocyanin Content of Fresh Fruits of Common Fig (Ficus carica L .).

Ortiz, A.L., Pineda, I.Y.P., Lagunas, L.L.M., Ortega, A.B., 2021. Optical and thermal properties of edible coatings for application in solar drying. Sci. Rep. 1–16. https://doi.org/10.1038/s41598-021-88901-5

Ozdemir, M., Devres, Y.O., 2000. The thin layer drying characteristics of hazelnuts during roasting 42, 225–233.

Ozkan, I.A., 2007. Microwave drying characteristics of spinach 78, 577–583. https://doi.org/10.1016/j.jfoodeng.2005.10.026

Panchariya, P.C., Popovic, D., Sharma, A.L., 2002. Thin-layer modelling of black tea drying process. J. Food Eng. 52, 349–357. https://doi.org/https://doi.org/10.1016/S0260-8774(01)00126-1

Pantelidis, G.E., Vasilakakis, M., Manganaris, G.A., Diamantidis, G., 2007. Antioxidant capacity, phenol, anthocyanin and ascorbic acid contents in raspberries, blackberries, red currants, gooseberries and Cornelian cherries. Food Chem. 102, 777–783. https://doi.org/https://doi.org/10.1016/j.foodchem.2006.06.021

Panwar, N.L., Kaushik, S.C., Kothari, S., 2011. Role of renewable energy sources in environmental protection: A review. Renew. Sustain. Energy Rev. 15, 1513–1524. https://doi.org/10.1016/j.rser.2010.11.037

Pardhi, C.B., Bhagoria, J.L., 2013. Development and performance evaluation of mixed-mode solar dryer with forced convection 1–8.

Parry, J.L., 1985. Mathematical modelling and computer simulation of heat and mass transfer in agricultural grain drying: A review. J. Agric. Eng. Res. 32, 1–29. https://doi.org/https://doi.org/10.1016/0021-8634(85)90116-7

Pehlivan, D., 2004. Modelling of thin layer drying kinetics of some fruits under open-air sun drying process 65, 413–425. https://doi.org/10.1016/j.jfoodeng.2004.02.001

Peñaloza, S., Delesma, C., Muñiz, J., López-Ortiz, A., 2022. The anthocyanin's role on the food metabolic pathways, color and drying processes: An experimental and theoretical approach. Food Biosci. 47, 101700. https://doi.org/https://doi.org/10.1016/j.fbio.2022.101700

Peterson, J.M., Montgomery, S., Haddad, E., Kearney, L., Tonstad, S., 2011a. Effect of consumption of dried california mission figs on lipid concentrations. Ann. Nutr. Metab. 58, 232–238. https://doi.org/10.1159/000330112

Peterson, J.M., Montgomery, S., Haddad, E., Kearney, L., Tonstad, S., 2011b. Effect of consumption of dried california mission figs on lipid concentrations. Ann. Nutr. Metab. 58, 232–238. https://doi.org/10.1159/000330112

Pfannhauser, W., 2005. Determination of anthocyanins in four Croatian cultivars of sour cherries (Prunus cerasus) 575–578. https://doi.org/10.1007/s00217-004-1103-2

Pina, F., Melo, M.J., Laia, C.A.T., Parola, A.J., Lima, J.C., 2012. Chemistry and applications

of flavylium compounds: A handful of colours. Chem. Soc. Rev. 41, 869–908. https://doi.org/10.1039/c1cs15126f

Pineda, P., Ortega, B., Mart, G., Nair, P.K., n.d. Optical and thermal properties of edible coatings for application in solar drying.

Pirasteh, G., Saidur, R., Rahman, S.M.A., Rahim, N.A., 2014. A review on development of solar drying applications. Renew. Sustain. Energy Rev. 31, 133–148. https://doi.org/10.1016/j.rser.2013.11.052

Raj, A.K., Jayaraj, S., 2021. Development and assessment of generalized drying kinetics in multi-tray solar cabinet dryer. Sol. Energy 226, 112–121. https://doi.org/10.1016/j.solener.2021.08.034

Renan, A.S., 2010. Original article Thermal and light degradation kinetics of anthocyanin extracts from mangosteen peel (Garcinia mangostana L .) 1902–1908. https://doi.org/10.1111/j.1365-2621.2010.02351.x

Rodriguez-Amaya, D.B., 2019. Update on natural food pigments - A mini-review on carotenoids, anthocyanins, and betalains. Food Res. Int. 124, 200–205. https://doi.org/10.1016/j.foodres.2018.05.028

Rodríguez-Ramírez, J., Méndez-Lagunas, L.L., López-Ortiz, A., Muñiz-Becerá, S., Nair, K., 2021. Solar drying of strawberry using polycarbonate with UV protection and polyethylene covers: Influence on anthocyanin and total phenolic content. Sol. Energy 221, 120–130. https://doi.org/10.1016/j.solener.2021.04.025

Roman Gutierrez, D.M., 2022. Diseño, construcción y evaluación de un prototipo de secador solar tipo gabinete utilizando dos materiales de cubierta empleando CFD. Degree Thesis, in: FACULTAD DE CIENCIAS QUÍMICAS E INGENIERÍA, UNIVERSIDAD AUTÓNOMA DEL ESTADO DE MORELOS.

Rønsted, N., Salvo, G., Savolainen, V., 2007. Biogeographical and phylogenetic origins of African fig species (Ficus section Galoglychia). Mol. Phylogenet. Evol. 43, 190–201. https://doi.org/10.1016/j.ympev.2006.12.010

Ross, J.A., Kasum, C.M., 2002. Dietary flavonoids: bioavailability, metabolic effects, and safety. Annu. Rev. Nutr. 22, 19–34. https://doi.org/10.1146/annurev.nutr.22.111401.144957

Rufino, M., Alves, R., Brito, E., Morais, S., Sampaio, C., Pérez-Jimenez, J., 2007. Metodologia Científica: Determinaão da atividade antioxidante total em frutas pela captura do radical ABTS+. Embrapa Agroindústria Trop. Comun. Técnico 127.

Şahin, U., Öztürk, H.K., 2018. Comparison between Artificial Neural Network model and mathematical models for drying kinetics of osmotically dehydrated and fresh figs under open sun drying. J. Food Process Eng. 41. https://doi.org/10.1111/jfpe.12804

Şahin, U., Öztürk, H.K., 2016. Effects of pulsed vacuum osmotic dehydration (PVOD) on drying kinetics of figs (Ficus carica L). Innov. Food Sci. Emerg. Technol. 36, 104–111. https://doi.org/10.1016/j.ifset.2016.06.003

Samuel, A., Olalekan, A., 2016. Banana Drying Kinetics.

Sandoval-Castro, C.J., Valdez-Morales, M., Oomah, B.D., Gutiérrez-Dorado, R., Medina-Godoy, S., Espinosa-Alonso, L.G., 2017. Bioactive compounds and antioxidant activity in scalded Jalapeño pepper industrial byproduct (Capsicum annuum). J. Food Sci. Technol. 54, 1999–2010. https://doi.org/10.1007/s13197-017-2636-2

Sandoval-torres, S., Barriada-bernal, G., 2017. Convective drying kinetics of strawberry (Fragaria ananassa): effects on antioxidant activity, anthocyanins and total phenolic content. Food Chem. https://doi.org/10.1016/j.foodchem.2017.03.010

Sarvestani, F.S., Rahimi, A., Hatamipour, M.S., 2014. An experimental study on drying characteristics and kinetics of figs (Ficuscarica). Polish J. Chem. Technol. 16, 60–65. https://doi.org/10.2478/pjct-2014-0071

SaVanna Shoemaker, MS, RDN, L., 2020. All You Need to Know About Figs [WWW Document]. healthline. URL https://www.healthline.com/nutrition/figs-benefits (accessed 1.29.22).

Seerangurayar, T., Manickavasagan, A., Al-Ismaili, A.M., Al-Mulla, Y.A., 2018. Effect of carrier agents on physicochemical properties of foam-mat freeze-dried date powder. Dry. Technol. 36, 1292–1303. https://doi.org/10.1080/07373937.2017.1400557

Services, B. book, 2022. Figs – Produce Blue Book [WWW Document]. Inf. Serv. Technol. URL https://www.producebluebook.com/know-your-commodity/figs/ (accessed 3.4.22).

Sharifian, F., Modarres-motlagh, A., Komarizade, M.H., 2013. Colour Change Analysis of Fig Fruit during Microwave Drying 9, 107–114. https://doi.org/10.1515/ijfe-2012-0211

Sharma, B., Kumar, V., Kumar, S., Panesar, P., 2020. Microwave assisted extraction of phytochemicals from Ficus racemosa. Curr. Res. Green Sustain. Chem. 3. https://doi.org/10.1016/j.crgsc.2020.100020

Silva, J.M., Cantu, M.G., Rodrigues, V., Mazutti, M.A., 2013. Influence of Osmotic Pre-treatment on Convective Drying Kinetics of Figs 9, 187–196. https://doi.org/10.1515/ijfe-2012-0020

Singleton, V.L., Orthofer, R., Lamuela-Raventós, R.M., 1999. Analysis of total phenols and other oxidation substrates and antioxidants by means of Folin-Ciocalteu reagent. Methods Enzymol. 299, 152–178.

Sirijan, M., Pipattanawong, N., Saeng-on, B., Chaiprasart, P., 2020. Anthocyanin content, bioactive compounds and physico-chemical characteristics of potential new strawberry cultivars rich in-anthocyanins. J. Berry Res. 10, 397–410. https://doi.org/10.3233/jbr190487

Soysal, Y., Ayhan, Z., Es, O., 2009. Intermittent microwave – convective drying of red pepper : Drying kinetics , physical (colour and texture) and sensory quality 103, 455–463. https://doi.org/10.1016/j.biosystemseng.2009.05.010

Suh, H.J., Noh, D.O., Kang, C.S., Kim, J.M., Lee, S.W., 2003. Thermal kinetics of color degradation of mulberry fruit extract. Nahrung - Food 47, 132–135. https://doi.org/10.1002/food.200390024

T., S., Al-Ismaili, A.M., Janitha Jeewantha, L.H., Al-Habsi, N.A., 2019. Effect of solar drying methods on color kinetics and texture of dates. Food Bioprod. Process. 116, 227–239. https://doi.org/10.1016/j.fbp.2019.03.012

Taiwo, A., Fashina, A.B., Ola, F.A., 2014. Evaluation of a cabinet dryer developed for cassava chips. Int. J. Appl. Agric. Apic. Res. 10, 10-20–20.

Timberlake, C.F., Henry, B.S., 1988. Anthocyanins as natural food colorants. Prog. Clin. Biol. Res. 280, 107–121.

Tiwari, A., 2016. A Review on Solar Drying of Agricultural Produce 7. https://doi.org/10.4172/2157-7110.1000623

USDA nutritionix, 2016. Calories in Figs, raw [WWW Document]. nutritionix. URL https://www.nutritionix.com/i/usda/figs-raw-1-small-1-0.5-

dia/513fceb475b8dbbc21001015 (accessed 2.1.22).

Veberic, R., Jakopič, J., Stampar, F., 2008. Internal fruit quality of figs (Ficus carica L.) in the Northern Mediterranean Region. Ital. J. Food Sci. 20, 255–262.

Wahyuningsih, S., Ramelan, A.H., n.d. The Effect of pH and Color Stability of Anthocyanin on Food. https://doi.org/10.1088/1757-899X/193/1/012047

Walia, A., Kumar, N., Singh, R., Kumar, H., Kumar, V., Kaushik, R., Kumar, A.P., 2022. Bioactive Compounds in Ficus Fruits, Their Bioactivities, and Associated Health Benefits: A Review. J. Food Qual. 2022. https://doi.org/10.1155/2022/6597092

Wamucii, S., 2021. Figs Production in Mexico - Markets, Suppliers and Exporters [WWW Document]. Figs Prod. Mex. URL https://www.selinawamucii.com/insights/market/mexico/figs/ (accessed 12.12.22).

Wang, H., Cao, G., Prior, R.L., 1997. Oxygen Radical Absorbing Capacity of Anthocyanins. J. Agric. Food Chem. 45, 304–309. https://doi.org/10.1021/jf960421t

Wang, Z., Song, M., Li, Y., Chen, S., Ma, H., 2019. Differential color development and response to light deprivation of fig (Ficus carica L .) syconia peel and female flower tissues : transcriptome elucidation 1–15.

Watson, M., 2021. Guide to Common Varieties and Types of Figs [WWW Document]. URL https://www.thespruceeats.com/fig-varieties-4057270 (accessed 2.13.23).

Whitaker, T., J. Barre, H., M. Y. Hamdy, and, 1969. Theoretical and Experimental Studies of Diffusion in Spherical Bodies with a Variable Diffusion Coefficient. Trans. ASAE 12, 668–672. https://doi.org/https://doi.org/10.13031/2013.38924

Wojdyło, A., Nowicka, P., Carbonell-Barrachina, Á.A., Hernández, F., 2016. Phenolic compounds, antioxidant and antidiabetic activity of different cultivars of Ficus carica L. fruits. J. Funct. Foods 25, 421–432. https://doi.org/10.1016/J.JFF.2016.06.015

Xanthopoulos, G., Yanniotis, S., Lambrinos, G., 2010. Study of the drying behaviour in peeled and unpeeled whole figs. J. Food Eng. 97, 419–424. https://doi.org/10.1016/j.jfoodeng.2009.10.037

Yemis, O., 2012. Original article Changes in pigment profile and surface colour of fig (Ficus carica L .) during drying 1–10. https://doi.org/10.1111/j.1365-2621.2012.03025.x

Yuniati, Y., Elim, P.E., Alfanaar, R., Kusuma, H.S., Mahfud, 2021. Extraction of anthocyanin pigment from hibiscus sabdariffa l. By ultrasonic-assisted extraction. IOP Conf. Ser. Mater. Sci. Eng. 1010. https://doi.org/10.1088/1757-899X/1010/1/012032

Zhang, L., Wu, G., Wang, W., Yue, J., Yue, P., 2019. Anthocyanin profile , color and antioxidant activity of blueberry (Vaccinium ashei) juice as affected by thermal pretreatment. Int. J. Food Prop. 22, 1036–1046. https://doi.org/10.1080/10942912.2019.1625366

Zhang, X., Kong, W., Wang, Xingteng, Zhang, J., Liu, L., Wang, W., Liu, Y., Wang, Xun, Zhang, H., Deng, Q., 2020. Genetic diversity analysis of 34 fig varieties (Ficus carica L.) based on ISSR molecular marker. Genet. Resour. Crop Evol. 67, 913–921. https://doi.org/10.1007/s10722-020-00889-5

Zhang, Y., Sun, Y., Zhang, H., Mai, Q., Zhang, B., Li, H., Deng, Z., 2020. Food Bioscience The degradation rules of anthocyanins from eggplant peel and antioxidant capacity in fortified model food system during the thermal treatments. Food Biosci. 38, 100701. https://doi.org/10.1016/j.fbio.2020.100701

Zhishen, J., Mengcheng, T., Jianming, W., 1999. The determination of flavonoid contents in mulberry and their scavenging effects on superoxide radicals. Food Chem. 64, 555–559. https://doi.org/https://doi.org/10.1016/S0308-8146(98)00102-2

Appendices

Appendix A

Models for the Total Kinetics of drying

Models for Drying Kinetics (9.3.22)

Newtons Model Direct solar

Parameter Estimates for All Groups

Groups	Count	Iter's	R2	A
All	9	7	0.96069	0.00782

Function Plot

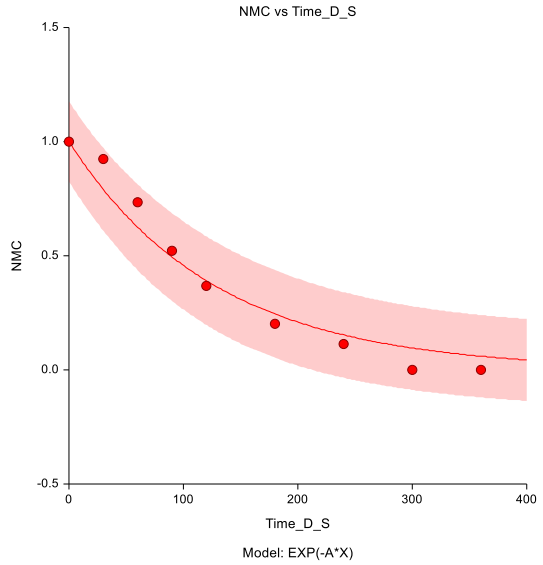

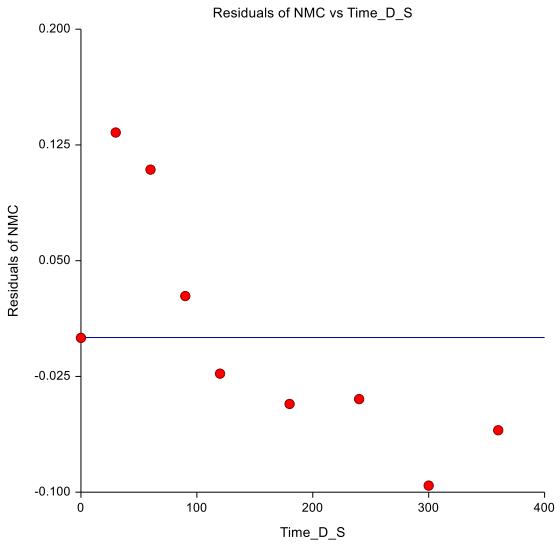

Analysis of Variance Table

Source	DF	Sum of Squares	Mean Square
Mean	1	1.65839	1.65839
Model	1	2.80729	2.80729
Error	8	0.04701	0.00588
Total (Adjusted)	8	1.19592	
Total	9	2.85431	

Models for Drying Kinetics (9.3.22)

Newtons Model ORD

Parameter Estimates for All Groups

Groups	Count	Iter's	R2	A
All	9	7	0.96954	0.01048

Function Plot

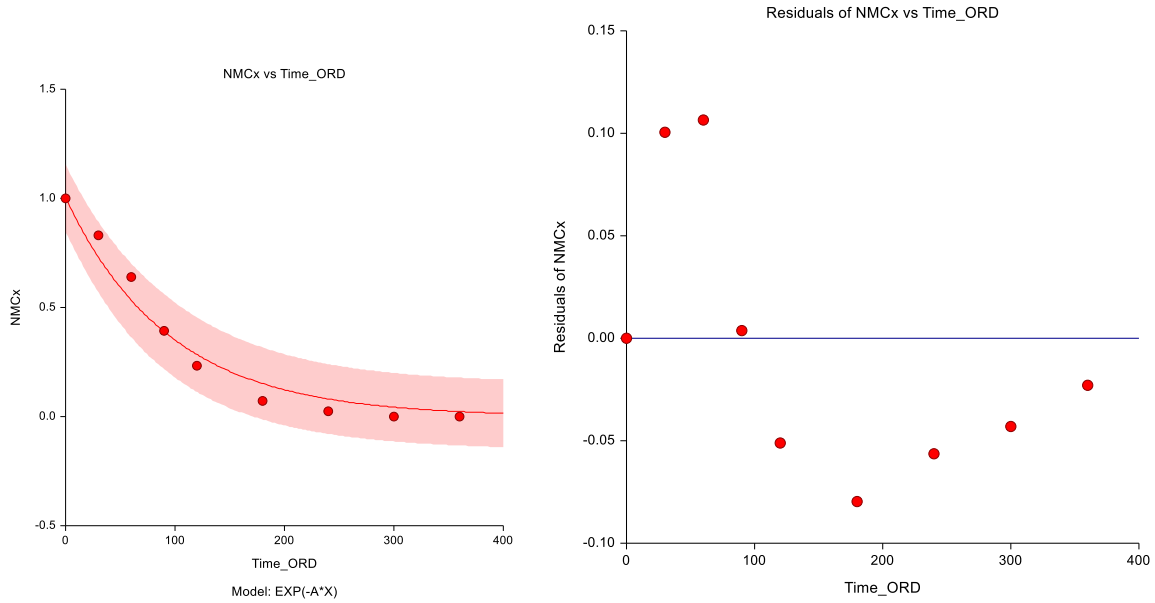

Analysis of Variance Table

Source	DF	Sum of Squares	Mean Square
Mean	1	1.13239	1.13239
Model	1	2.27749	2.27749
Error	8	0.03597	0.00450
Total (Adjusted)	8	1.18108	
Total	9	2.31346	

Models for Drying Kinetics (9.3.22)

Newtons Model CELL

Parameter Estimates for All Groups

Groups	Count	Iter's	R2	A
All	9	6	0.97253	0.00929

Function Plot

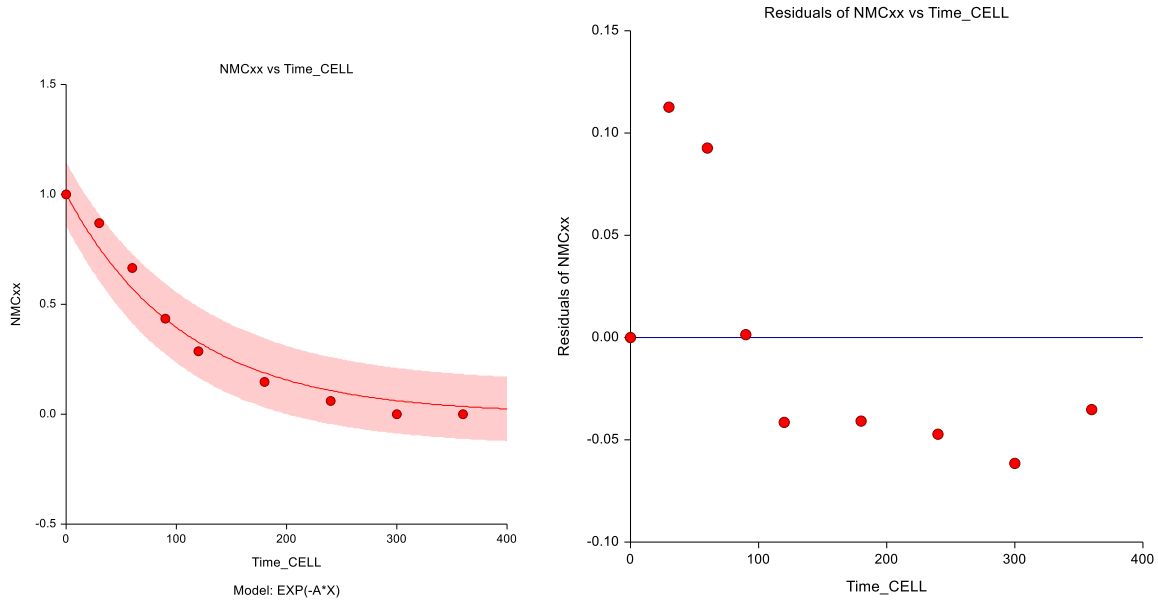

Analysis of Variance Table

Source	DF	Sum of Squares	Mean Square
Mean	1	1.33214	1.33214
Model	1	2.46237	2.46237
Error	8	0.03192	0.00399
Total (Adjusted)	8	1.16215	
Total	9	2.49429	

Models for Drying Kinetics (9.3.22)

Wang and Singh Model Direct solar

Parameter Estimates for All Groups

Groups	Count	Iter's	R2	A	B
All	9	5	0.98670	-0.00587	0.00001

Function Plot

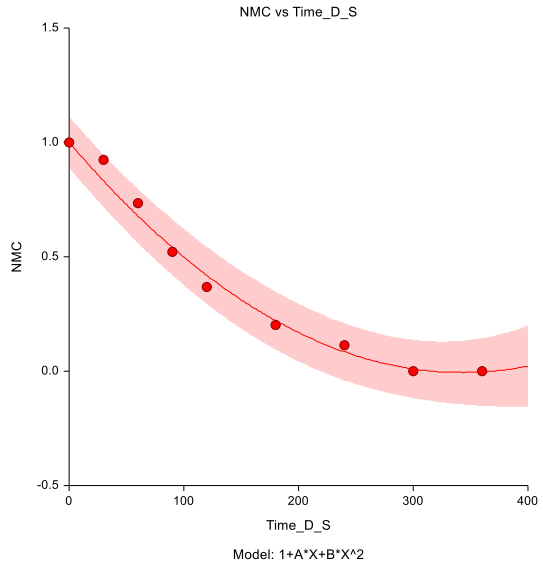

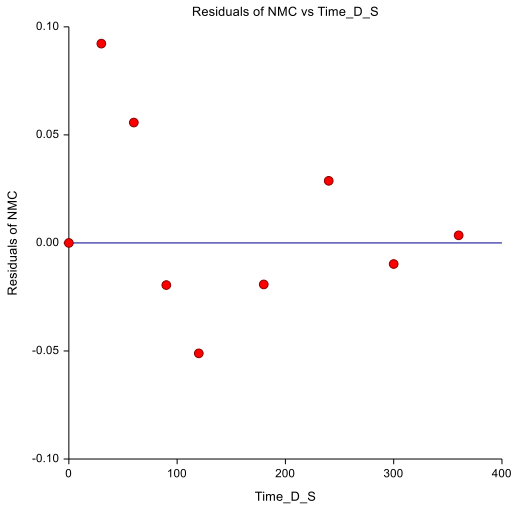

Analysis of Variance Table

Source	DF	Sum of Squares	Mean Square
Mean	1	1.65839	1.65839
Model	2	2.83840	1.41920
Model (Adjusted)	1	1.18001	1.18001
Error	7	0.01590	0.00227
Total (Adjusted)	8	1.19592	
Total	9	2.85431	

Models for Drying Kinetics (9.3.22)

Wang and Singh Model ORD

Parameter Estimates for All Groups

Groups	Count	Iter's	R2	A	B
All	9	5	0.98731	-0.00747	0.00001

Function Plot

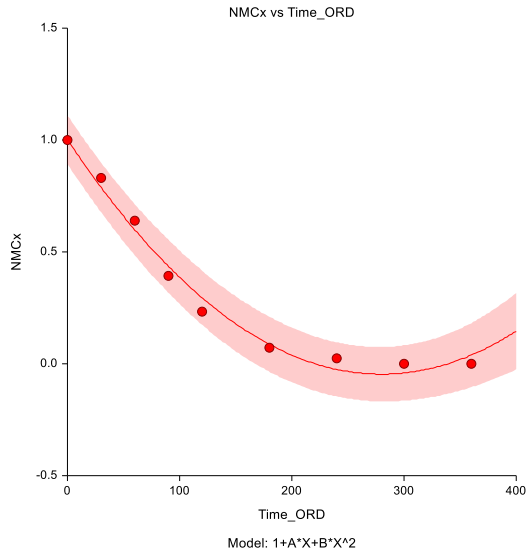

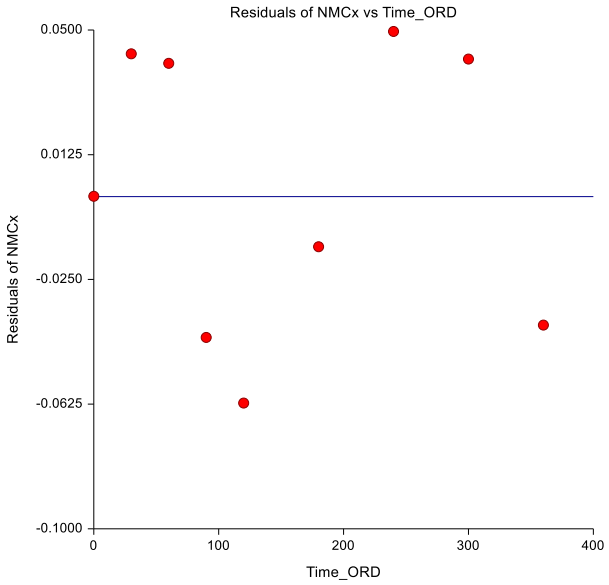

Analysis of Variance Table

Source	DF	Sum of Squares	Mean Square
Mean	1	1.13239	1.13239
Model	2	2.29847	1.14924
Model (Adjusted)	1	1.16608	1.16608
Error	7	0.01499	0.00214
Total (Adjusted)	8	1.18108	
Total	9	2.31346	

Models for Drying Kinetics (9.3.22)

Wang and Singh Model CELL

Parameter Estimates for All Groups

Groups	Count	Iter's	R2	A	B
All	9	5	0.98867	-0.00681	0.00001

Function Plot

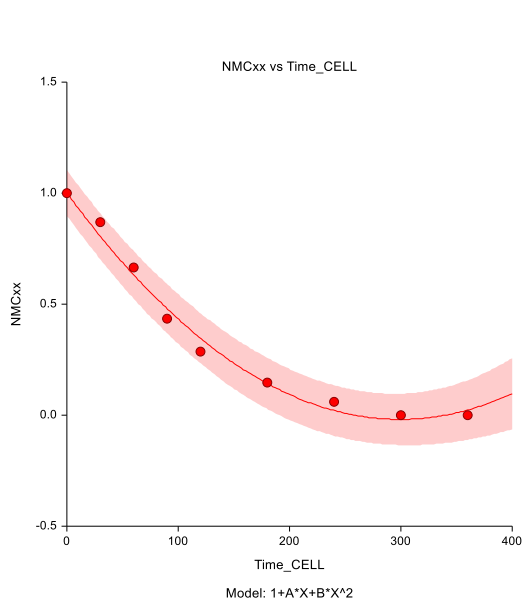

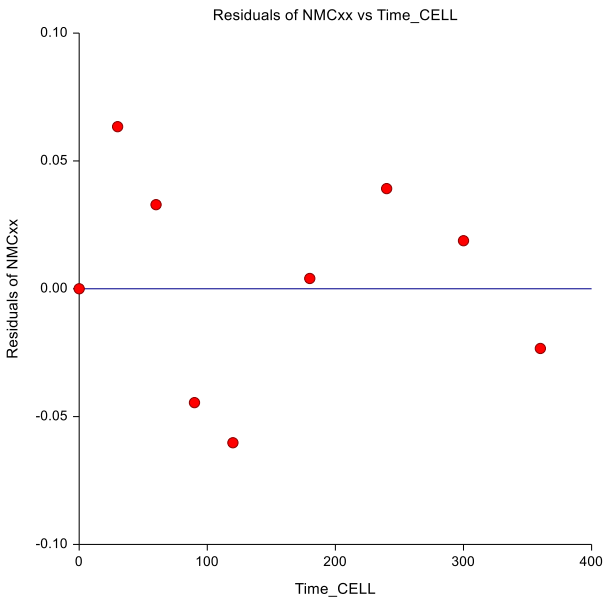

Analysis of Variance Table

Source	DF	Sum of Squares	Mean Square
Mean	1	1.33214	1.33214
Model	2	2.48113	1.24056
Model (Adjusted)	1	1.14899	1.14899
Error	7	0.01316	0.00188
Total (Adjusted)	8	1.16215	
Total	9	2.49429	

Models for Drying Kinetics (9.3.22)

Henderson and Pabis Model D.S

Parameter Estimates for All Groups

Groups	Count	Iter's	R2	A	B
All	9	8	0.97211	1.09287	0.00860

Function Plot

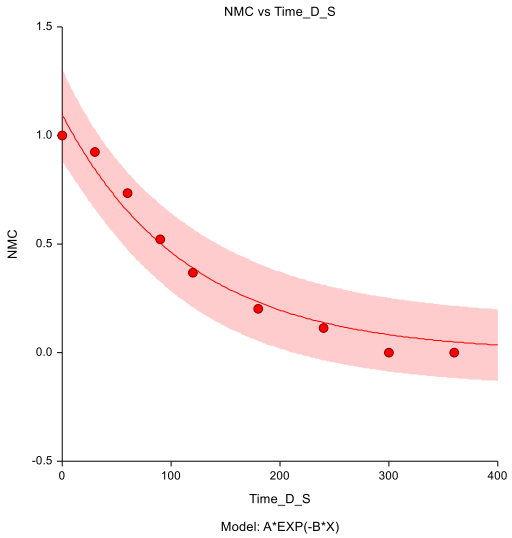

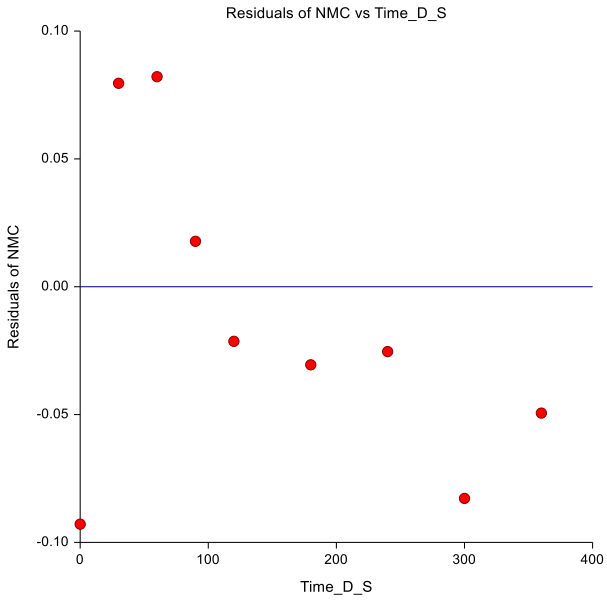

Analysis of Variance Table

Source	DF	Sum of Squares	Mean Square
Mean	1	1.65839	1.65839
Model	2	2.82095	1.41048
Model (Adjusted)	1	1.16257	1.16257
Error	7	0.03335	0.00476
Total (Adjusted)	8	1.19592	
Total	9	2.85431	

Models for Drying Kinetics (9.3.22)

Henderson and Pabis Model ORD

Parameter Estimates for All Groups

Groups	Count	Iter's	R2	A	B
All	9	7	0.97534	1.07007	0.01121

Function Plot

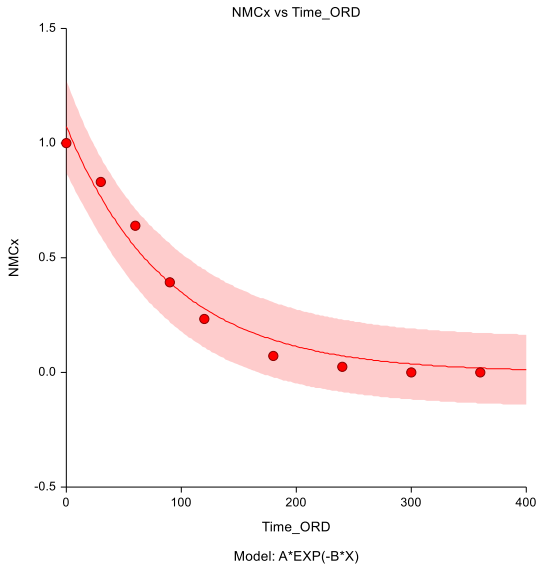

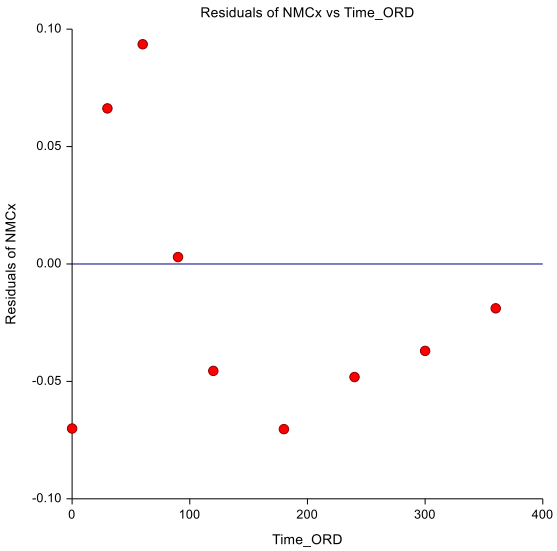

Analysis of Variance Table

Source	DF	Sum of Squares	Mean Square
Mean	1	1.13239	1.13239
Model	2	2.28434	1.14217
Model (Adjusted)	1	1.15195	1.15195
Error	7	0.02913	0.00416
Total (Adjusted)	8	1.18108	
Total	9	2.31346	

Models for Drying Kinetics (9.3.22)

Henderson and Pabis Model CELL

Parameter Estimates for All Groups

Groups	Count	Iter's	R2	A	B
All	9	8	0.97928	1.07337	0.01001

Function Plot

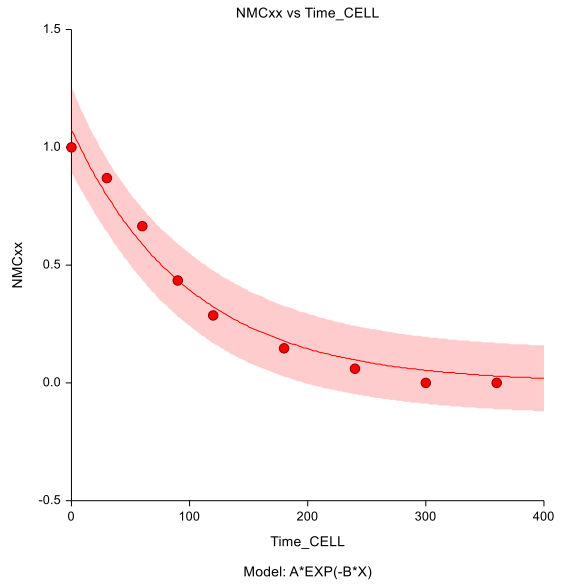

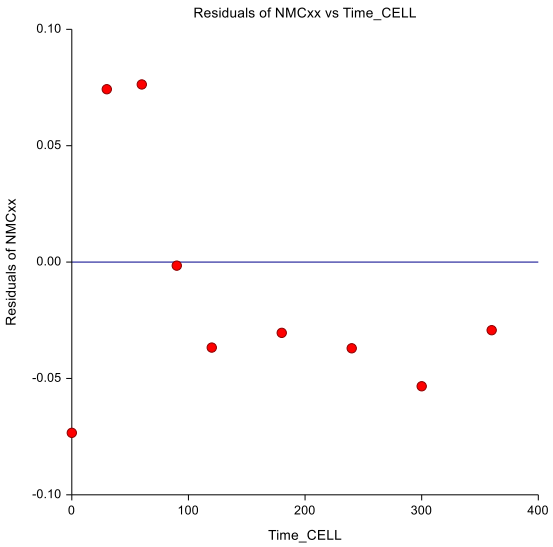

Analysis of Variance Table

Source	DF	Sum of Squares	Mean Square
Mean	1	1.33214	1.33214
Model	2	2.47022	1.23511
Model (Adjusted)	1	1.13808	1.13808
Error	7	0.02407	0.00344
Total (Adjusted)	8	1.16215	
Total	9	2.49429	

Models for Drying Kinetics (9.3.22)

Logarithmic Model D.S

Parameter Estimates for All Groups

Groups	Count	Iter's	R2	A	B	C
All	9	14	0.98556	1.22643	0.00630	-0.16292

Function Plot

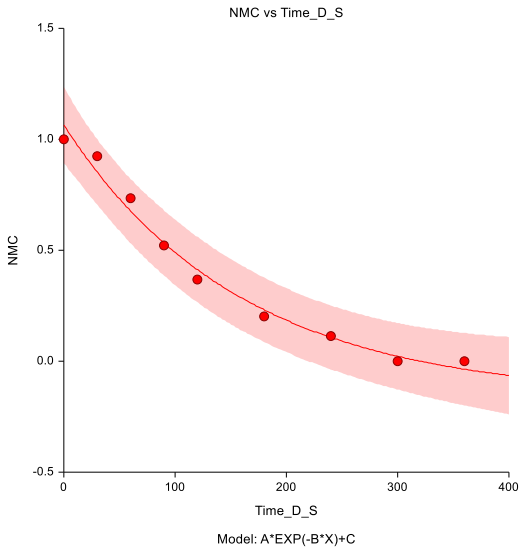

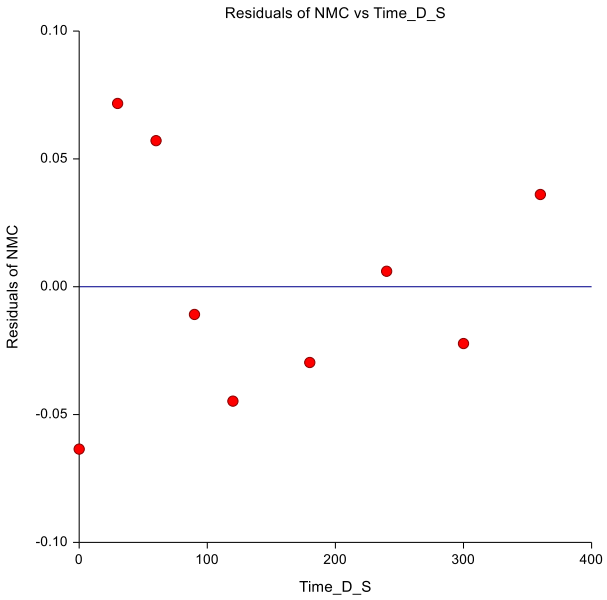

Analysis of Variance Table

Source	DF	Sum of Squares	Mean Square
Mean	1	1.65839	1.65839
Model	3	2.83704	0.94568
Model (Adjusted)	2	1.17865	0.58933
Error	6	0.01727	0.00288
Total (Adjusted)	8	1.19592	
Total	9	2.85431	

Models for Drying Kinetics (9.3.22)

Logarithmic Model ORD

Parameter Estimates for All Groups

Groups	Count	Iter's	R2	A	B	C
All	9	10	0.98313	1.13369	0.00947	-0.07903

Function Plot

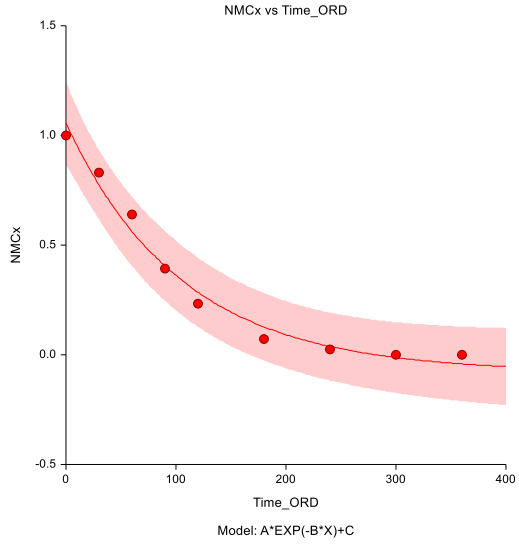

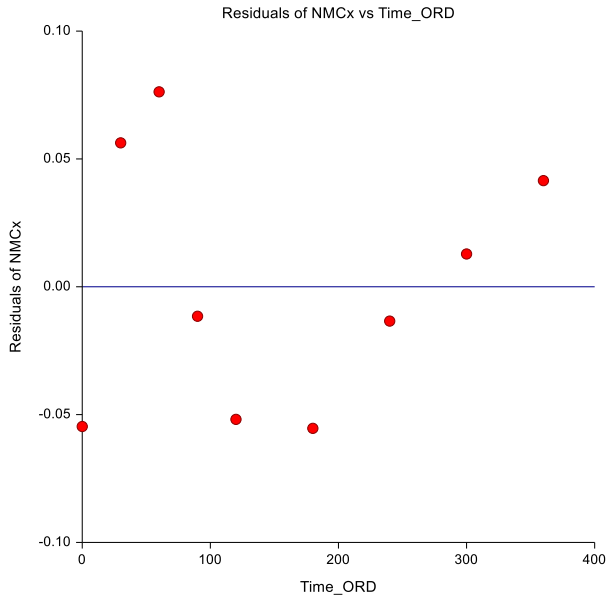

Analysis of Variance Table

Source	DF	Sum of Squares	Mean Square
Mean	1	1.13239	1.13239
Model	3	2.29354	0.76451
Model (Adjusted)	2	1.16115	0.58057
Error	6	0.01993	0.00332
Total (Adjusted)	8	1.18108	
Total	9	2.31346	

Models for Drying Kinetics (9.3.22)

Logarithmic Model CELL

Parameter Estimates for All Groups

Groups	Count	Iter's	R2	A	B	C
All	9	19	0.98712	1.14651	0.00823	-0.09218

Function Plot

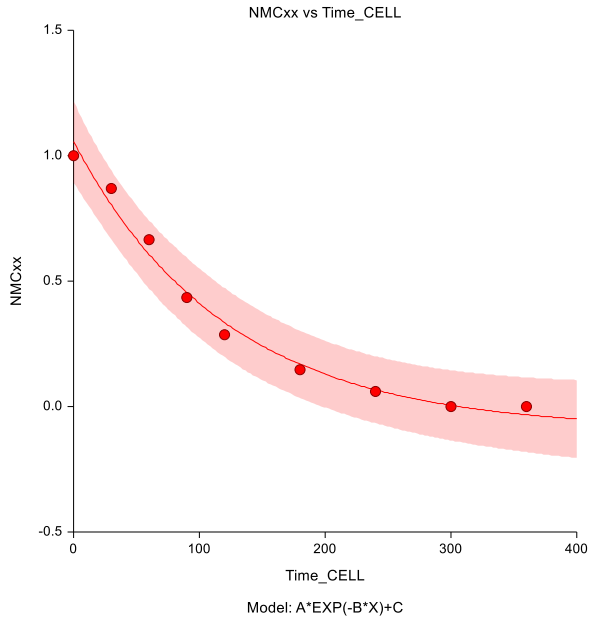

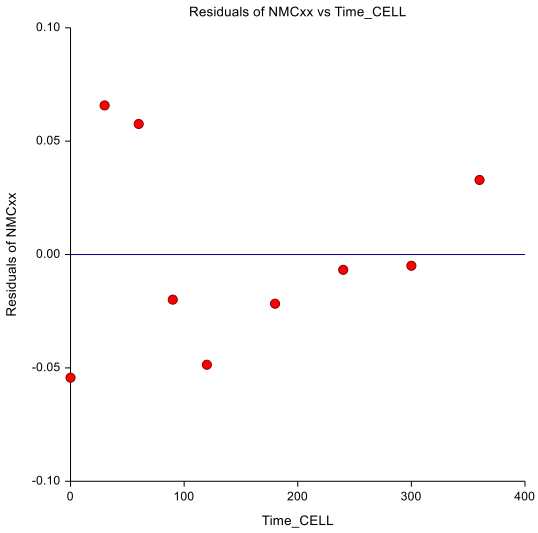

Analysis of Variance Table

Source	DF	Sum of Squares	Mean Square
Mean	1	1.33214	1.33214
Model	3	2.47932	0.82644
Model (Adjusted)	2	1.14718	0.57359
Error	6	0.01497	0.00250
Total (Adjusted)	8	1.16215	
Total	9	2.49429	

Models for Drying Kinetics (17.8.22)

Newtons Model Direct solar

Parameter Estimates for All Groups

Groups	Count	Iter's	R2	A
All	9	7	0.98272	0.00862

Function Plot

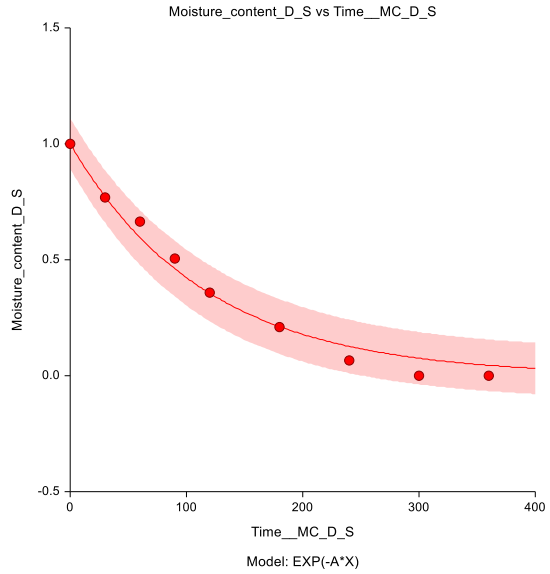

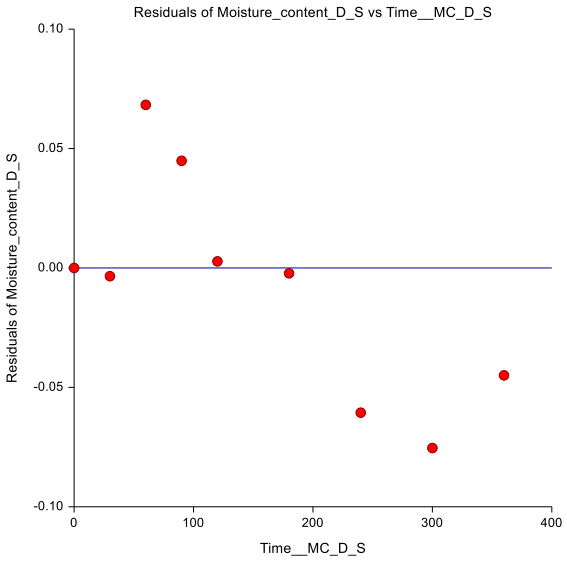

Analysis of Variance Table

Source	DF	Sum of Squares	Mean Square
Mean	1	1.41828	1.41828
Model	1	2.44679	2.44679
Error	8	0.01808	0.00226
Total (Adjusted)	8	1.04660	
Total	9	2.46487	

Models for Drying Kinetics (17.8.22)

Newtons Model ORD

Parameter Estimates for All Groups

Groups	Count	Iter's	R2	A
All	9	7	0.98178	0.00829

Function Plot

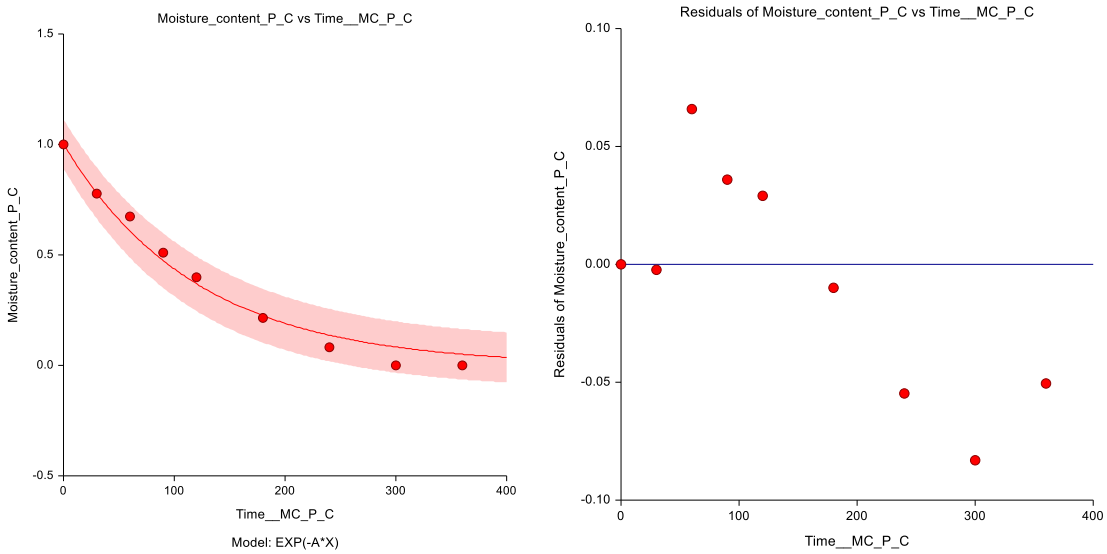

Analysis of Variance Table

Source	DF	Sum of Squares	Mean Square
Mean	1	1.48586	1.48586
Model	1	2.51151	2.51151
Error	8	0.01903	0.00238
Total (Adjusted)	8	1.04468	
Total	9	2.53054	

Models for Drying Kinetics (17.8.22)

Newtons Model CELL

Parameter Estimates for All Groups

Groups	Count	Iter's	R2	A
All	9	5	0.93420	0.00612

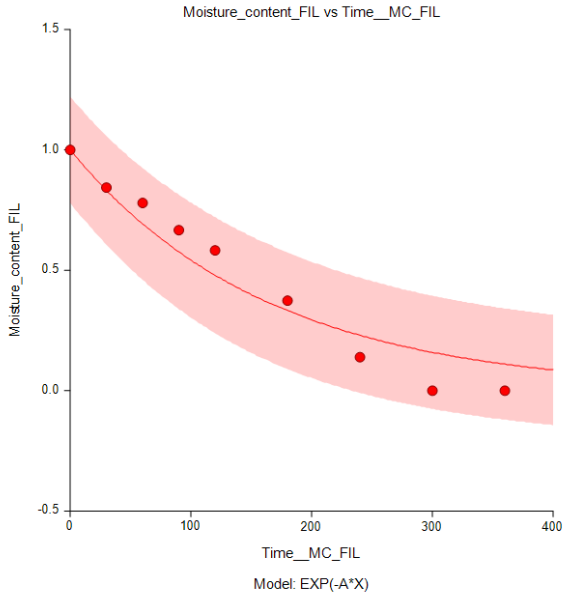

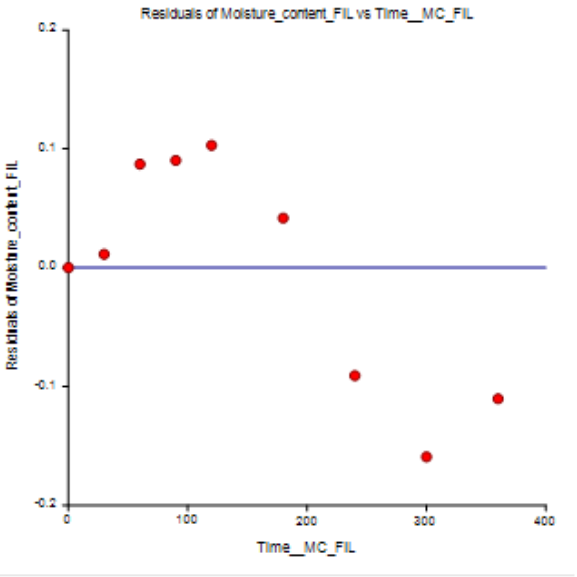

Analysis of Variance Table

Source	DF	Sum of Squares	Mean Square
Mean	1	2.13696	2.13696
Model	1	3.18840	3.18840
Error	8	0.07405	0.00926
Total (Adjusted)	8	1.12549	
Total	9	3.26245	

Models for Drying Kinetics (17.8.22)

Wang and Singh Model Direct solar

Parameter Estimates for All Groups

Groups	Count	Iter's	R2	A	B
All	9	4	0.99593	-0.00632	0.00001

Function Plot

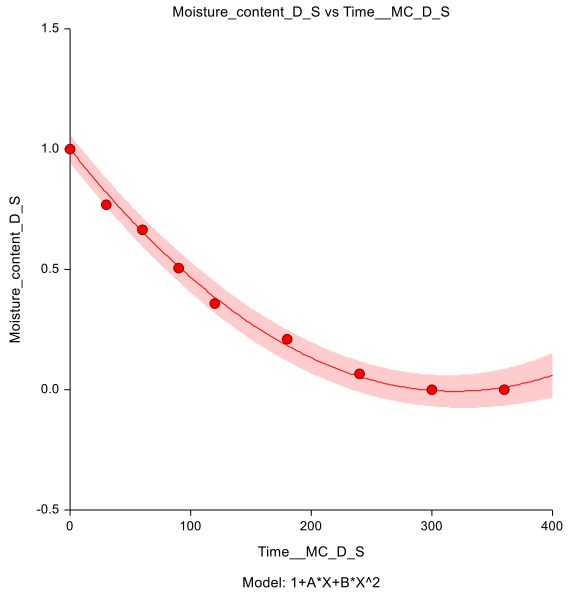

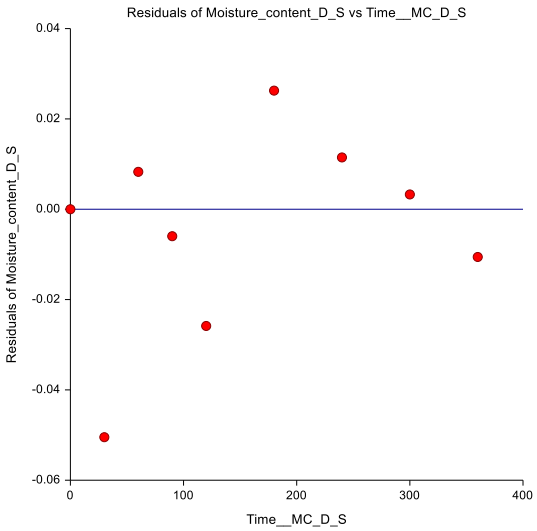

Analysis of Variance Table

Source	DF	Sum of Squares	Mean Square
Mean	1	1.41828	1.41828
Model	2	2.46061	1.23030
Model (Adjusted)	1	1.04233	1.04233
Error	7	0.00426	0.00061
Total (Adjusted)	8	1.04660	
Total	9	2.46487	

Models for Drying Kinetics (17.8.22)

Wang and Singh Model ORD

Parameter Estimates for All Groups

Groups	Count	Iter's	R2	A	B
All	9	5	0.99718	-0.00611	0.00001

Function Plot

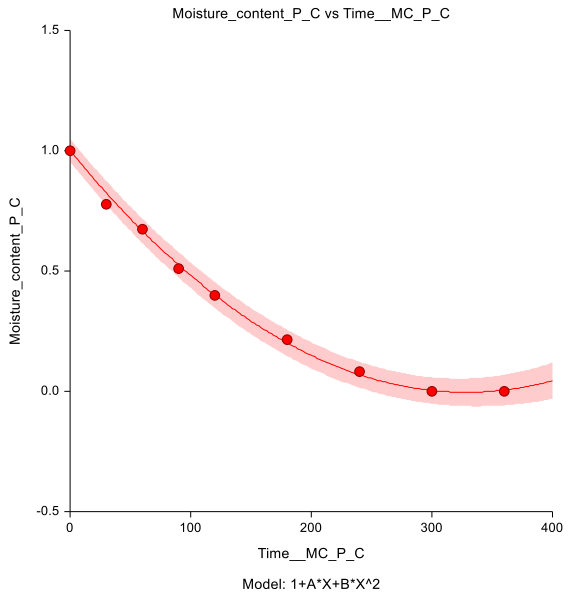

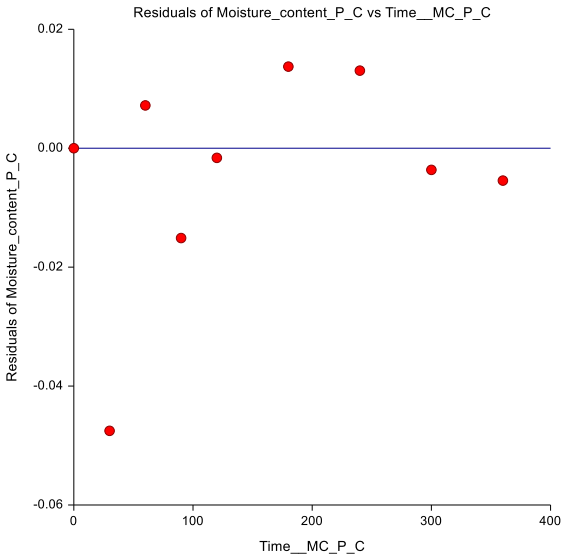

Analysis of Variance Table

Source	DF	Sum of Squares	Mean Square
Mean	1	1.48586	1.48586
Model	2	2.52760	1.26380
Model (Adjusted)	1	1.04174	1.04174
Error	7	0.00294	0.00042
Total (Adjusted)	8	1.04468	
Total	9	2.53054	

Models for Drying Kinetics (17.8.22)

Wang and Singh Model CELL

Parameter Estimates for All Groups

Groups	Count	Iter's	R2	A	B
All	9	6	0.98882	-0.00428	0.00000

Function Plot

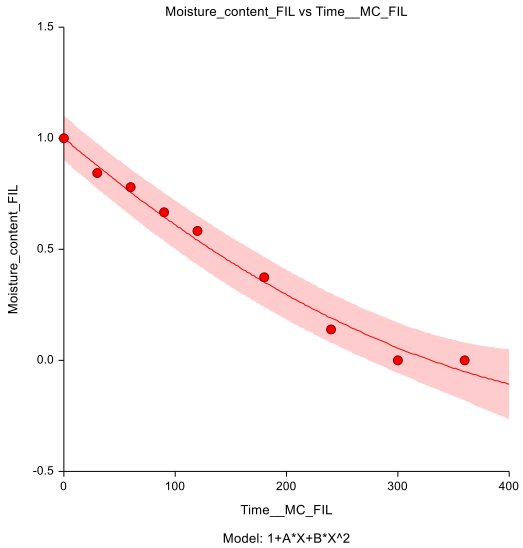

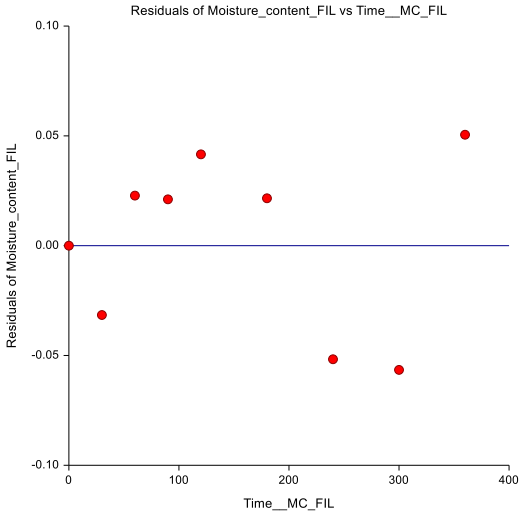

Analysis of Variance Table

Source	DF	Sum of Squares	Mean Square
Mean	1	2.13696	2.13696
Model	2	3.24987	1.62493
Model (Adjusted)	1	1.11290	1.11290
Error	7	0.01258	0.00180
Total (Adjusted)	8	1.12549	
Total	9	3.26245	

Models for Drying Kinetics (17.8.22)

Henderson and Pabis Model Direct Solar

Parameter Estimates for All Groups

Groups	Count	Iter's	R2	A	B
All	9	8	0.98393	1.02884	0.00889

Function Plot

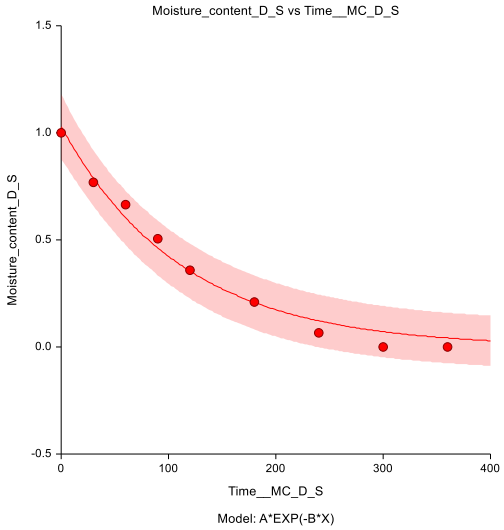

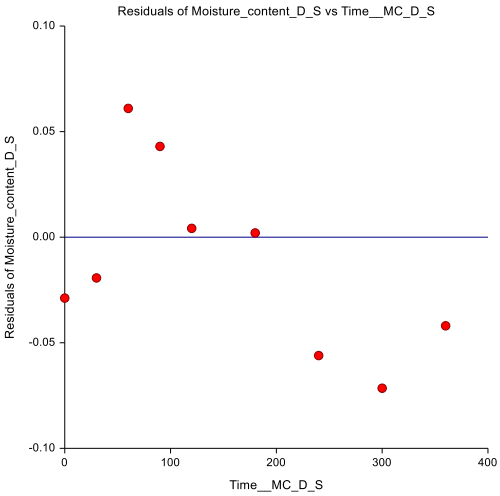

Analysis of Variance Table

Source	DF	Sum of Squares	Mean Square
Mean	1	1.41828	1.41828
Model	2	2.44806	1.22403
Model (Adjusted)	1	1.02978	1.02978
Error	7	0.01681	0.00240
Total (Adjusted)	8	1.04660	
Total	9	2.46487	

Models for Drying Kinetics (17.8.22)

Henderson and Pabis Model ORD

Parameter Estimates for All Groups

Groups	Count	Iter's	R2	A	B
All	9	8	0.98314	1.03018	0.00857

Function Plot

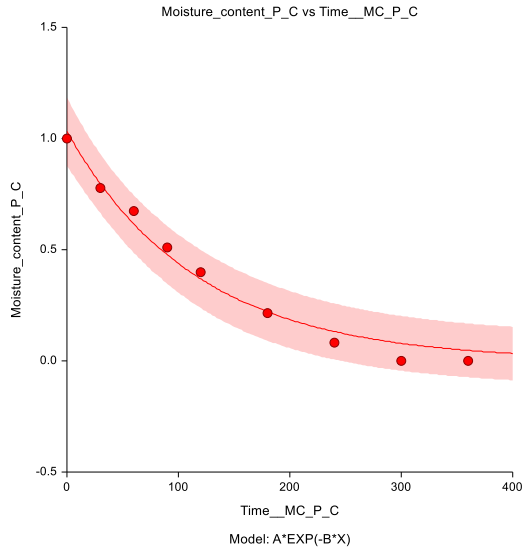

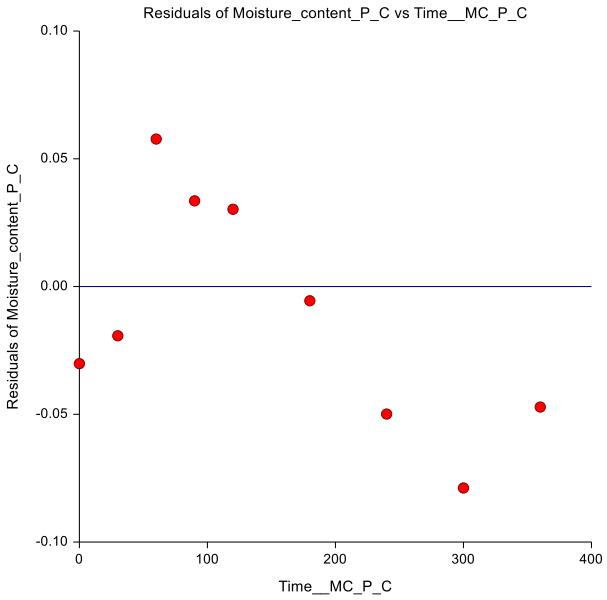

Analysis of Variance Table

Source	DF	Sum of Squares	Mean Square
Mean	1	1.48586	1.48586
Model	2	2.51293	1.25646
Model (Adjusted)	1	1.02706	1.02706
Error	7	0.01762	0.00252
Total (Adjusted)	8	1.04468	
Total	9	2.53054	

Models for Drying Kinetics (17.8.22)

Henderson and Pabis Model CELL

Parameter Estimates for All Groups

Groups	Count	Iter's	R2	A	B
All	9	8	0.94186	1.06852	0.00659

Function Plot

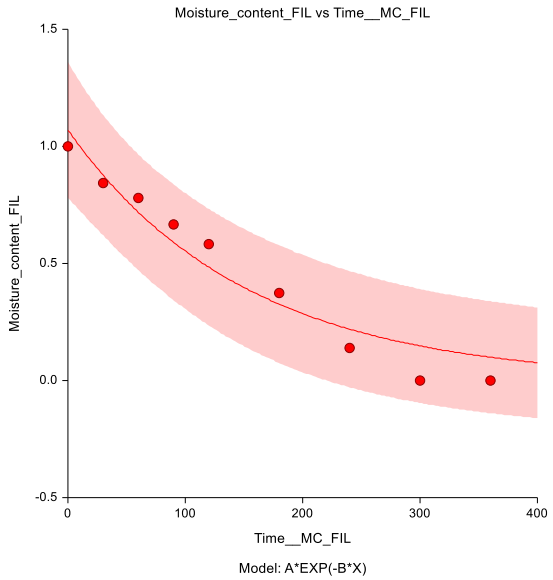

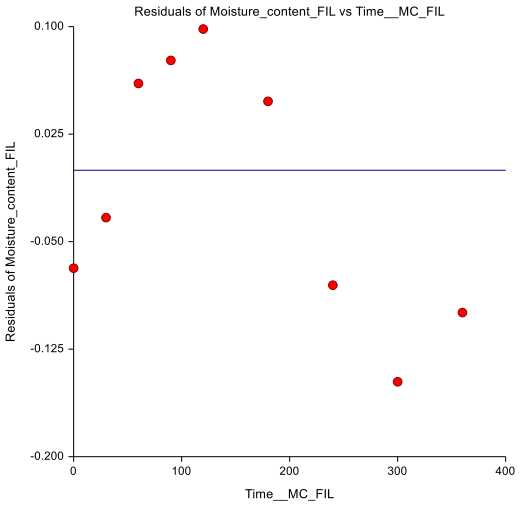

Analysis of Variance Table

Source	DF	Sum of Squares	Mean Square
Mean	1	2.13696	2.13696
Model	2	3.19701	1.59851
Model (Adjusted)	1	1.06005	1.06005
Error	7	0.06544	0.00935
Total (Adjusted)	8	1.12549	
Total	9	3.26245	

Models for Drying Kinetics (17.8.22)

Logarithmic Model Direct Solar

Parameter Estimates for All Groups

Groups	Count	Iter's	R2	A	B	C
All	9	12	0.99530	1.13624	0.00669	-0.13429

Function Plot

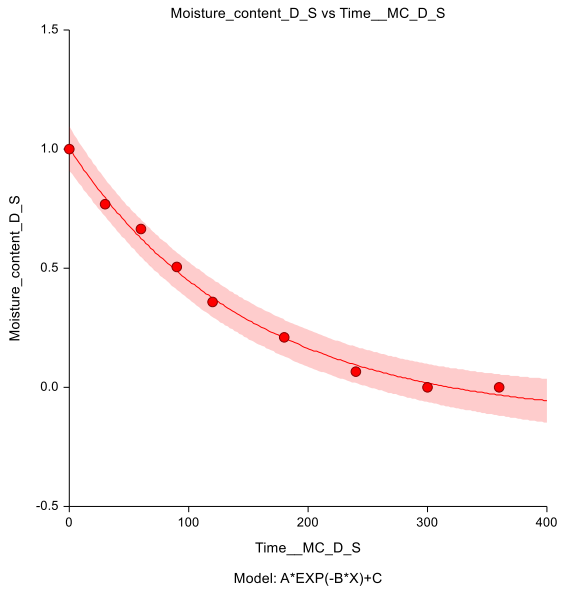

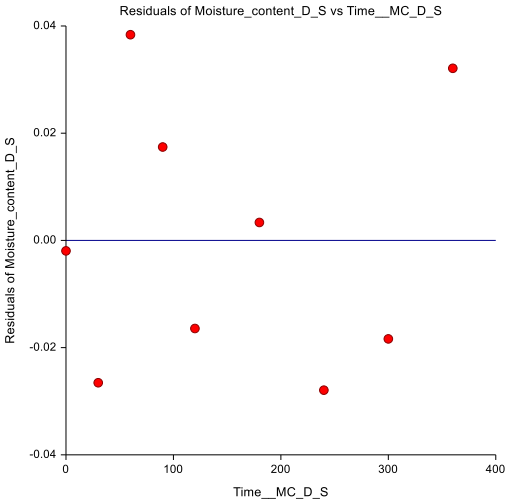

Analysis of Variance Table

Source	DF	Sum of Squares	Mean Square
Mean	1	1.41828	1.41828
Model	3	2.45996	0.81999
Model (Adjusted)	2	1.04168	0.52084
Error	6	0.00491	0.00082
Total (Adjusted)	8	1.04660	
Total	9	2.46487	

Models for Drying Kinetics (17.8.22)

Logarithmic Model ORD

Parameter Estimates for All Groups

Groups	Count	Iter's	R2	A	B	C
All	9	21	0.99616	1.15621	0.00622	-0.15572

Function Plot

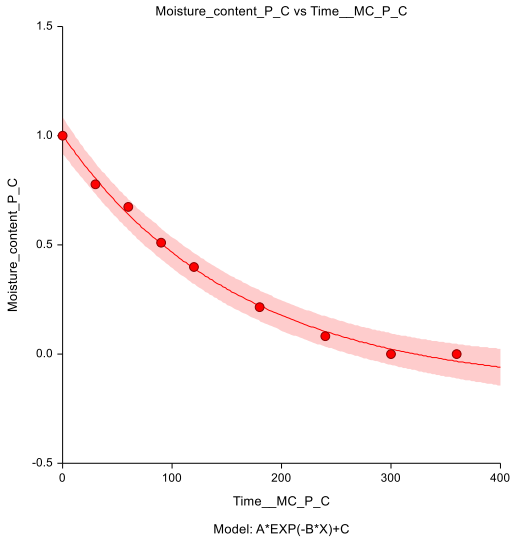

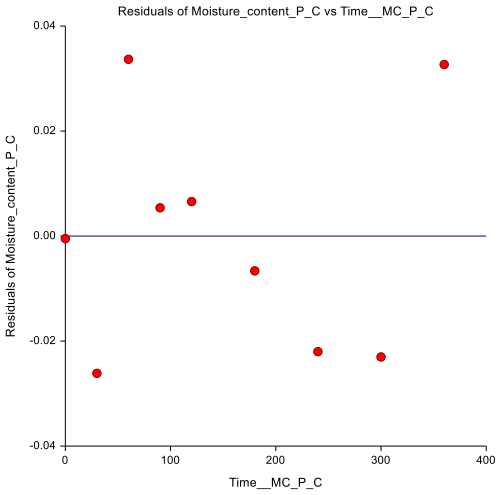

Analysis of Variance Table

Source	DF	Sum of Squares	Mean Square
Mean	1	1.48586	1.48586
Model	3	2.52653	0.84218
Model (Adjusted)	2	1.04067	0.52033
Error	6	0.00402	0.00067
Total (Adjusted)	8	1.04468	
Total	9	2.53054	

Models for Drying Kinetics (17.8.22)

Logarithmic Model CELL

Parameter Estimates for All Groups

Groups	Count	Iter's	R2	A	B	C
All	9	16	0.98716	1.82615	0.00244	-0.81884

Function Plot

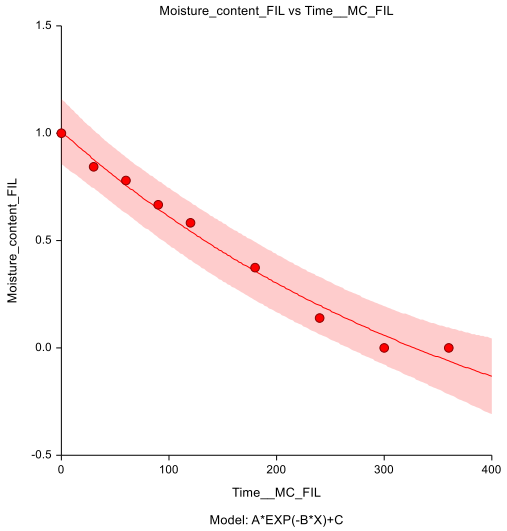

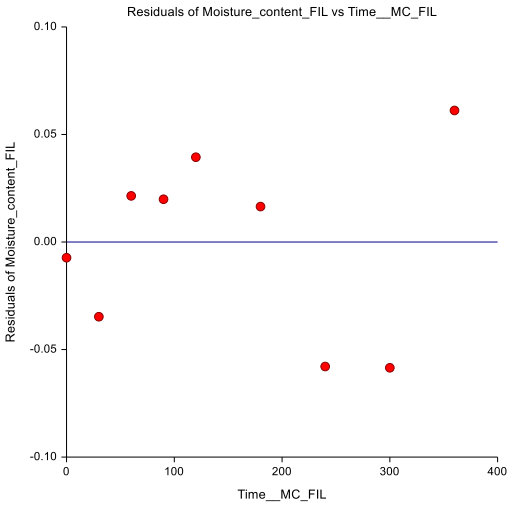

Analysis of Variance Table

Source	DF	Sum of Squares	Mean Square
Mean	1	2.13696	2.13696
Model	3	3.24800	1.08267
Model (Adjusted)	2	1.11103	0.55552
Error	6	0.01445	0.00241
Total (Adjusted)	8	1.12549	
Total	9	3.26245	

Models for Drying Kinetics (17.8.22)

Milidi Model Direct Solar

Parameter Estimates for All Groups

Groups	Count	Iter's	R2	A	B	C
All	9	43	0.99568	0.98739	0.00407	1.13370

Groups	Count	Iter's	R2	D
All	9	43	0.99568	-0.00017

Model Fit: A*EXP(-B*X^C)+D*X

Function Plot

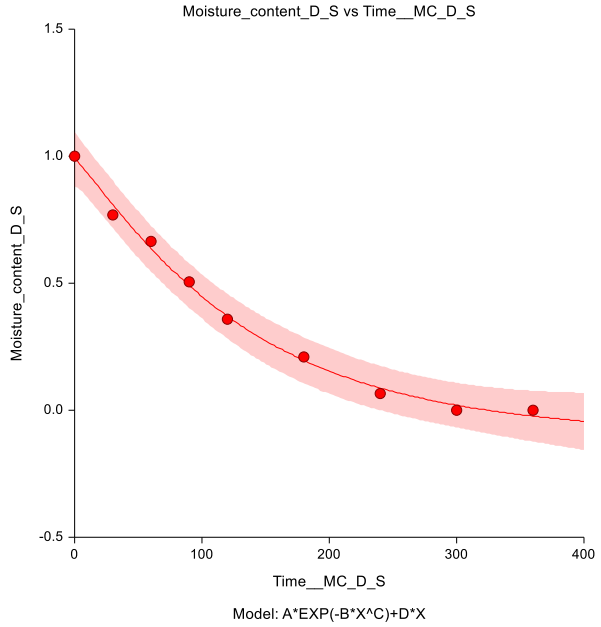

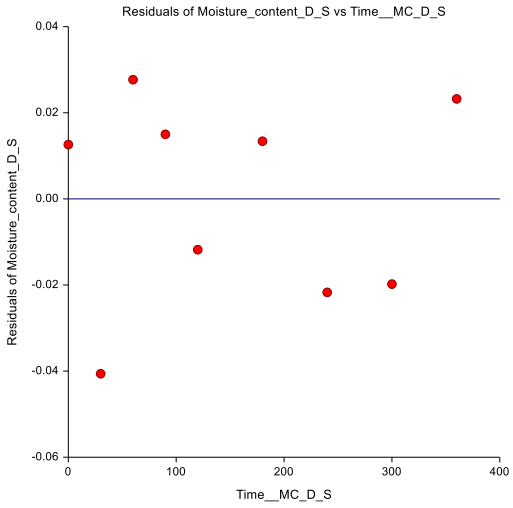

Analysis of Variance Table

Source	DF	Sum of Squares	Mean Square
Mean	1	1.41828	1.41828
Model	4	2.46035	0.61509
Model (Adjusted)	3	1.04207	0.34736
Error	5	0.00452	0.00090
Total (Adjusted)	8	1.04660	
Total	9	2.46487	

Models for Drying Kinetics (17.8.22)

Milidi Model ORD

Parameter Estimates for All Groups

Groups	Count	Iter's	R2	A	B	C
All	9	41	0.99636	0.98736	0.00401	1.12366

Groups	Count	Iter's	R2	D
All	9	41	0.99636	-0.00021

Model Fit: A*EXP(-B*X^C)+D*X

Function Plot

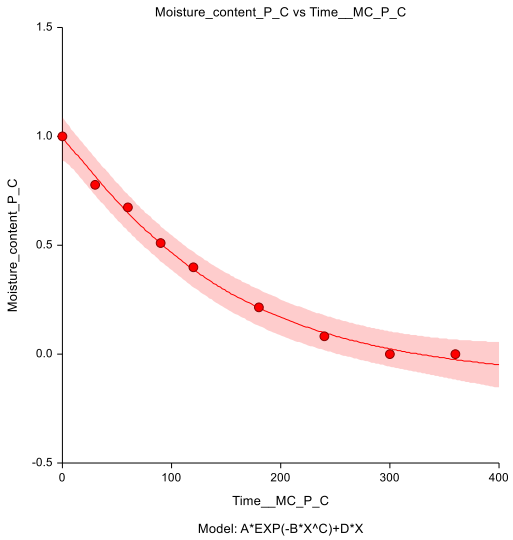

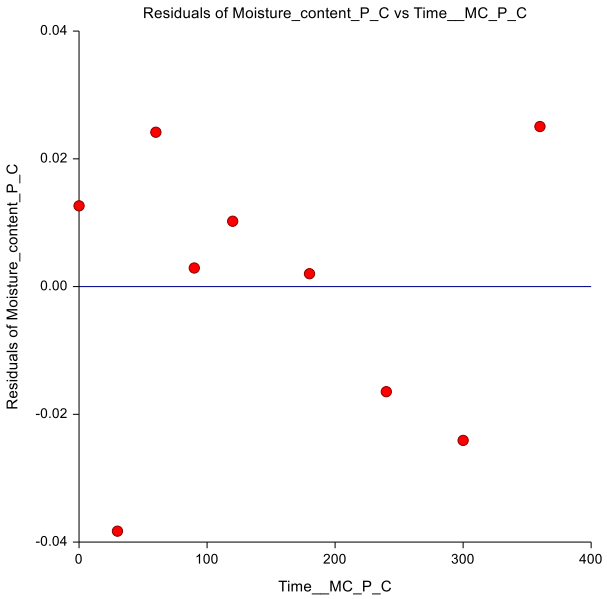

Analysis of Variance Table

Source	DF	Sum of Squares	Mean Square
Mean	1	1.48586	1.48586
Model	4	2.52674	0.63168
Model (Adjusted)	3	1.04088	0.34696
Error	5	0.00381	0.00076
Total (Adjusted)	8	1.04468	
Total 9 2.53054			

Models for Drying Kinetics (17.8.22)

Milidi Model CELL

Parameter Estimates for All Groups

Groups	Count	Iter's	R2	A	B	C
All	9	72	0.99040	0.96092	0.00039	1.48655

Groups	Count	Iter's	R2	D
All	9	72	0.99040	-0.00034

Model Fit: A*EXP(-B*X^C)+D*X

Function Plot

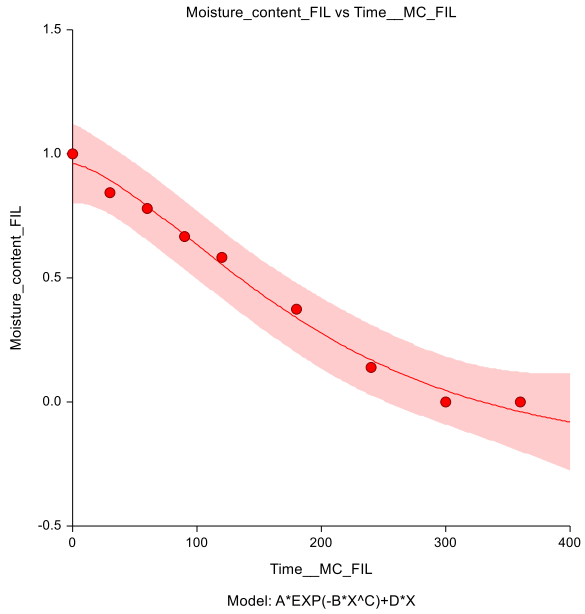

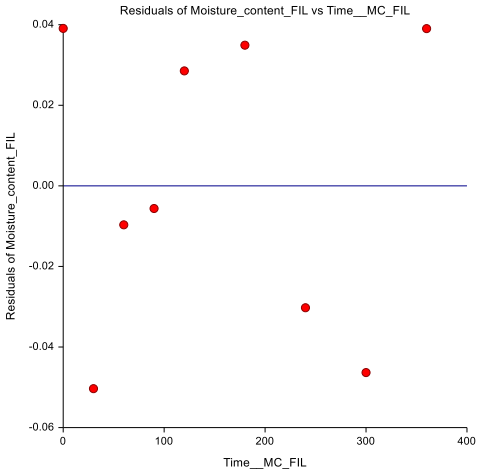

Analysis of Variance Table

Source	DF	Sum of Squares	Mean Square
Mean	1	2.13696	2.13696
Model	4	3.25164	0.81291
Model (Adjusted)	3	1.11468	0.37156
Error	5	0.01081	0.00216
Total (Adjusted)	8	1.12549	
Total	9	3.26245	

Appendix B

Analysis of Variance Report for Anthocyanins (Fresh)

Response Anthocyanins

Analysis of Variance Table

Source Term	DF	Sum of Squares	Mean Square	F-Ratio	Prob Level	Power (Alpha=0.05)
A: Time__A_	7	29.85565	4.265093	20.65	0.000000*	1.000000
B: Treatment__A_	3	6.454263	2.151421	10.42	0.000011*	0.998009
AB	21	3.670118	0.1747675	0.85	0.655135	0.566834
S	64	13.21658	0.2065091			
Total (Adjusted)	95	53.19661				
Total	96					

* Term significant at alpha = 0.05

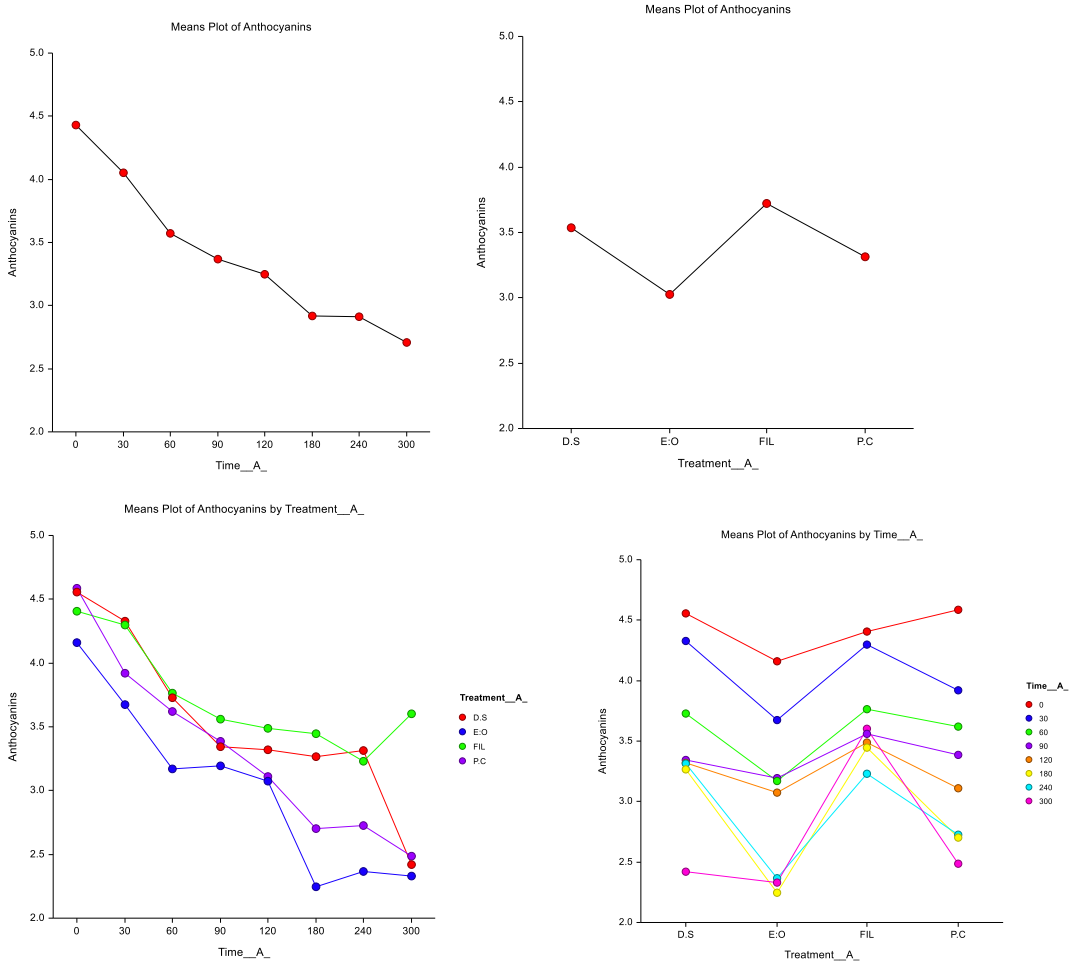

Analysis of Variance Report for Anthocyanins (2 weeks)

Response Anthocyanins__2Wks_

Analysis of Variance Table

Source Term	DF	Sum of Squares	Mean Square	F-Ratio	Prob Level	Power (Alpha=0.05)
A: Time__2Wks_A	7	32.02002	4.574289	6.15	0.000016*	0.998965
B: Treatment__2Wks__A	3	5.974764	1.991588	2.68	0.054461	0.626364
AB	21	6.736311	0.3207767	0.43	0.982786	0.275498
S	64	47.61362	0.7439628			
Total (Adjusted)	95	92.34472				
Total	96					

* Term significant at alpha = 0.05

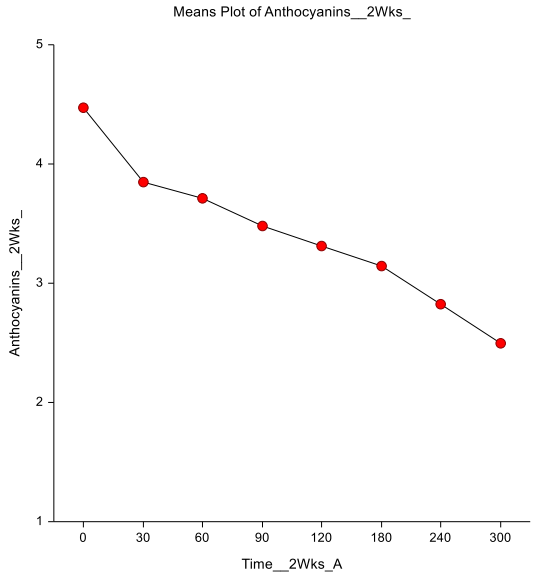

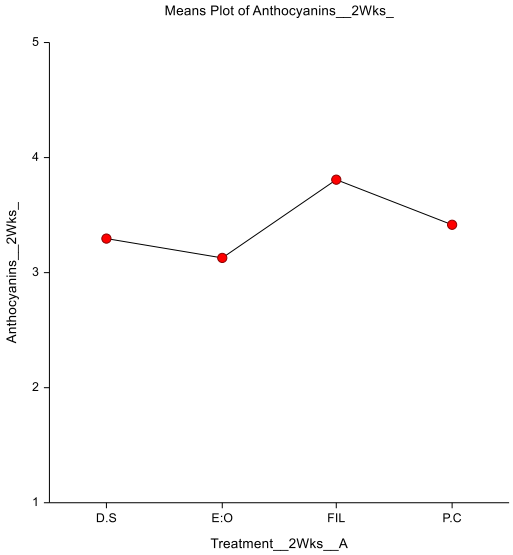

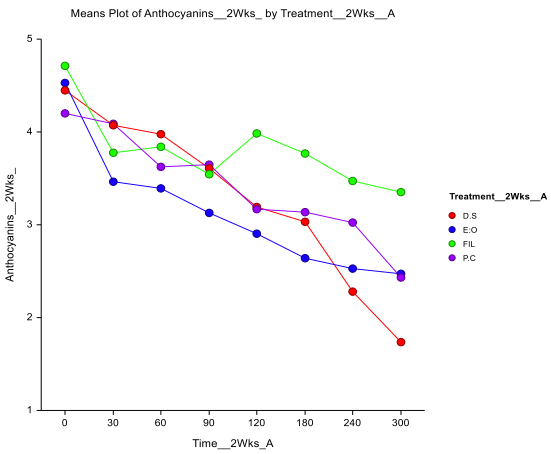

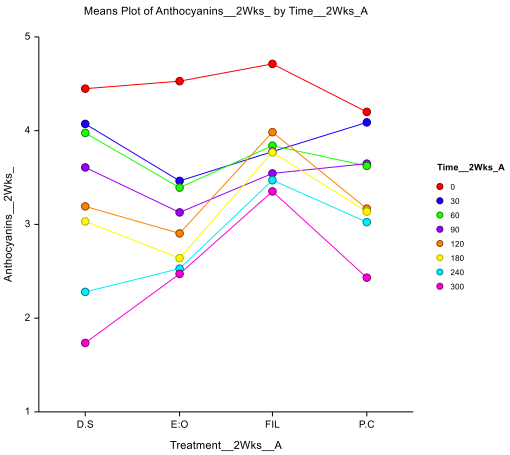

Appendix C

Analysis of Variance Report (Colour)

Response Lightness__2Wks_

Analysis of Variance Table

Source Term	DF	Sum of Squares	Mean Square	F-Ratio	Prob Level	Power (Alpha=0.05)
A: Time__L__2Wks	8	4148.793	518.5991	189.25	0.000000*	1.000000
B: Treatment__2Wks_x	3	575.2172	191.7391	69.97	0.000000*	1.000000
AB	24	197.1757	8.215652	3.00	0.000174*	0.999358
S	72	197.3006	2.740286			
Total (Adjusted)	107	5118.487				
Total	108					

* Term significant at alpha = 0.05

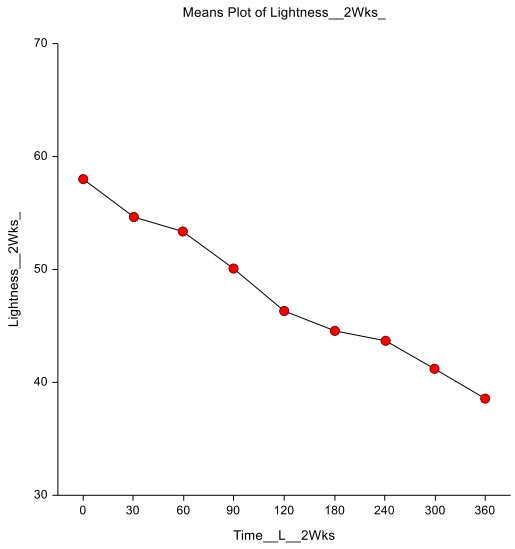

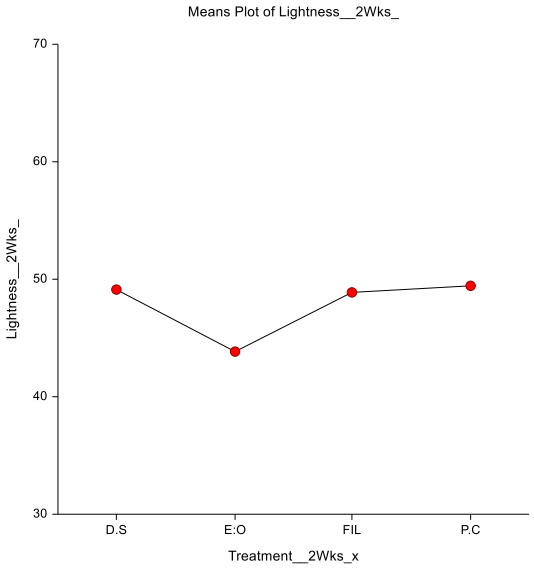

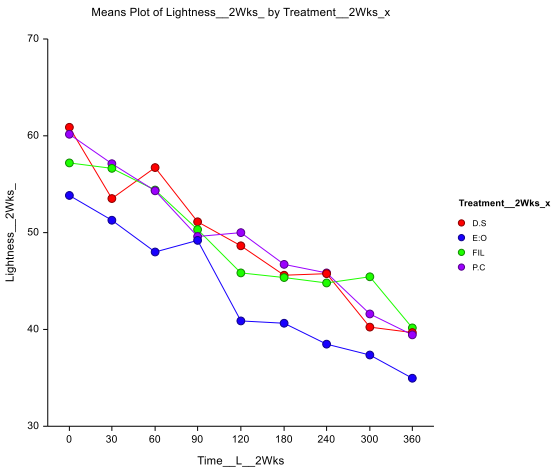

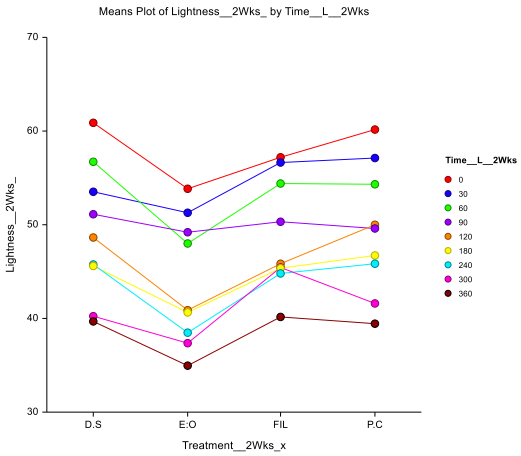

Analysis of Variance Report (Colour)

Response DE__Colour_ (Total colour change)

Analysis of Variance Table

Source Term	DF	Sum of Squares	Mean Square	F-Ratio	Prob Level	Power (Alpha=0.05)
A: Time	8	7764.473	970.5591	346.02	0.000000*	1.000000
B: Treatment	3	423.0156	141.0052	50.27	0.000000*	1.000000
AB	24	245.75	10.23958	3.65	0.000011*	0.999954
S	72	201.9552	2.804934			
Total (Adjusted)	107	8635.194				
Total	108					

* Term significant at alpha = 0.05

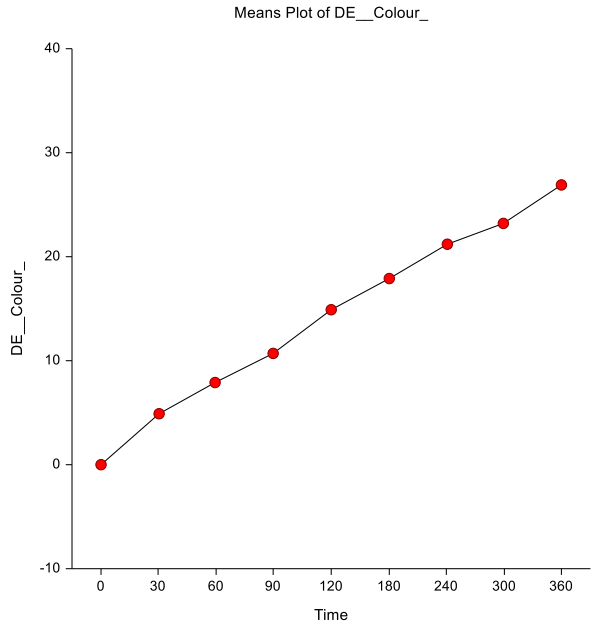

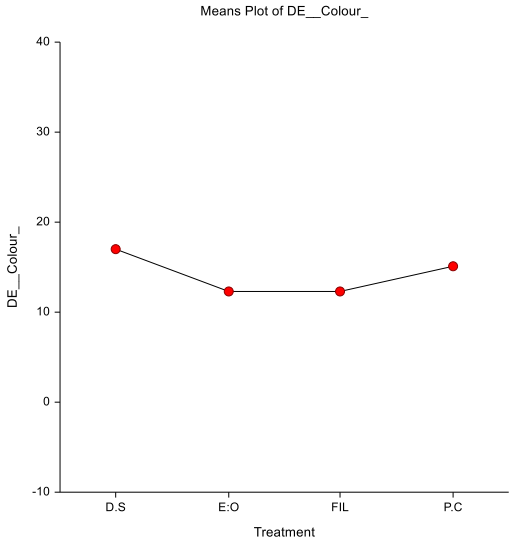

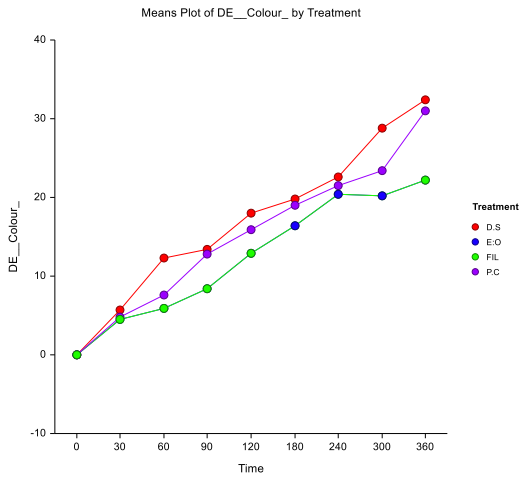

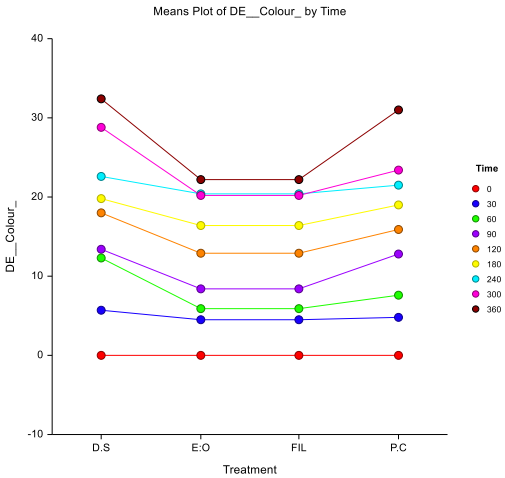

Analysis of Variance Report (Colour)

Response DE_Colour (Total colour change 2 weeks)

Analysis of Variance Table

Source Term	DF	Sum of Squares	Mean Square	F-Ratio	Prob Level	Power (Alpha=0.05)
A: Time_2Wks_	8	3799.759	474.9699	133.01	0.000000*	1.000000
B: Treatment_2Wks_	3	161.3204	53.77348	15.06	0.000000*	0.999964
AB	24	163.1647	6.798528	1.90	0.019247*	0.971271
S	72	257.1071	3.570933			
Total (Adjusted)	107	4381.352				
Total	108					

* Term significant at alpha = 0.05